University of Venda
Creating Future Leaders

UNIVERSITY OF VENDA
LIBRARY
CALL No.
ACC No.

University of Venda

Synthesis, characterization and performance evaluation of groundwater defluoridation capacity of smectite rich clay soils and Mn-modified bentonite clay composites

A master's research submitted to the University of Venda, School of Environmental Sciences, Department of Ecology and Resource Management

By

Mudzielwana Rabelani

11600806

UNIVERSITY OF VENDA
LIBRARY

Supervisor: Prof. Gitari W. M (University of Venda)

Co-supervisor: Prof. Msagati T. A. M (University of South Africa)

2016

© University of Venda

University of Venda
Creating Future Leaders

DECLARATION

I, Rabelani Mudzielwana hereby declare that "**Synthesis, Characterization and performance evaluation of groundwater defluoridation capacity of smectite rich clays soils and Mn-modified bentonite clay composites"** is my own work in design and execution and it has never been submitted for any degree or examination in any other university and that all sources of information herein have been duly, appropriately and acknowledged by means of comprehensive list of references.

Signature: ..... Date 21/04/2016

© University of Venda

University of Venda
Creating Future Leaders

ACKNOWLEDGEMENTS

Firstly I would like to thank the Lord Almighty for giving me wisdom, good health and making everything possible for me. I thank Him for His abundant love and His grace that has always been sufficient to me.

I would like to express my sincere and profound gratitude to my supervisor **Prof Gitari W. M** for his dedicated assistance, invaluable comments, suggestion and constructive criticisms throughout this project. Your contribution made what looked almost impossible at the beginning to be possible at the end.

My sincere gratitude also goes to my co-supervisor **Prof Msagati T. A. M** for his conceptual contribution.

I would also like to express my heartfelt gratitude to my mother **Miss Tshisevhe L**, my uncle, **Mr Tshisevhe T. N** and my siblings for their love, encouragement and moral support. I will not forget my best friend **Nemaguvhuni P** who also gave me encouragement and moral support during the course of this work.

My profound gratitude also goes to Environmental Remediation and Pollution Chemistry Research Group members for the ir invaluable comments to my work during the presentations and stimulating discussions.

I would also like to acknowledge the financial support from WRC Project No. K5/2363/3, NRF Project No. CSUR13092849176, Grant No. 90288, and THRIP Project No. TP12082610644 Research & Innovation Directorate, University of Venda and Sasol Inzalo Foundation.

Lastly, I wish to thank all the stuff members of the **Ecology and Resource Management** Department University of Venda especially the HoD, **Dr. Nelwamondo** and the lab technician **Thandi** for their constant help and extending departmental facilities for my work.

© University of Venda

University of Venda
Creating Future Leaders

ACADEMIC OUTPUTS

PRESENTATIONS AND CONFERENCES

Mudzielwana R, Gitari W.M & Msagati T.A.M. **Physicochemical and mineralogical characterization of smectite rich clay soils: implication for groundwater defluoridation**. 3rd conference on Emerging Frontiers for Sustainable Water" Held in Protea Hotel Wanderers, Johannesburg, South Africa. From 3-5 August 2015.

Mudzielwana R, Gitari W.M & Msagati T.A.M. **Intercalation of Mn^{2+} ions onto bentonite clay: potential application in groundwater defluoridation**. "1st UNIVEN-WSU International Research Conference" Held in ICC, East London, Eastern Cape, South Africa. From 2-4 September 2015.

REPORTS

Gitari W.M, Msagati T.AM, Izuagie A.A, Ngulube T & Rabelani M. **Development and testing of novel metal modified natural clay based adsorbents for groundwater defluoridation: Characterization of Metal modified adsorbents, evaluation and optimization of their F^- adsorption capacity.** 1st -3rd Interim **Reports submitted to the WRC.**

MANUSCRIPTS BEING PREPARED FOR SUBMISSION TO PEER REVIEWED JOURNAL.

Mudzielwana R, Gitari W.M & Msagati T.A.M. **Physicochemical and mineralogical characterization of smectite rich clay soils: implication for groundwater defluoridation**. Submitted to South African Journal of Science for review in 2015.

Mudzielwana R, Gitari W.M & Msagati T.A.M. **Intercalation of Mn^{2+} ions onto bentonite clay: potential application in groundwater defluoridation**. To be submitted to international peer reviewed journal in 2016.

Mudzielwana R, Gitari W.M & Msagati T.A.M. **Surface coating of NaOH activated bentonite with MnO_2 and its potential application on groundwater defluoridation**. To be submitted to an international peer reviewed journal in 2016.

© University of Venda

University of Venda
Creating Future Leaders

DEDICATION

This work is dedicated to my father the late, Mr. Mudzielwana R. J. and my grandmother the late, Mrs. Tshisevhe S.N. To them I say may your souls rest in peace. I will always remember all the support and words of encouragement you gave me all the time.

© University of Venda

University of Venda
Creating Future Leaders

ABSTRACT

Several studies revealed that some of the boreholes within South Africa have F^- concentration above 1.5 mg/L. This study evaluates the use of black smectite rich clay soils from Mukondeni, Mn^{2+} modified bentonite, MnO_2 coated Na-bentonite clay and MnO_2 coated Na-bentonite/smectite rich clay soils composite for defluoridation of groundwater. Mn^{2+} modified bentonite was prepared via ion exchange mechanism and MnO_2 coated Na-bentonite was synthesised by prior activating bentonite using NaOH followed by *in-situ* reduction of $KMnO_4$. The composite was prepared by mixing MnO_2 coated Na-bentonite and smectite rich clay soils at varying ratios followed by moulding into pellets manually. Physicochemical and mineralogical characterization was carried out using XRD, XRF, SEM, BET, FTIR, CEC, and pH_{pzc} techniques. Batch experiments were conducted to evaluate and optimize various operational parameters such as contact time, adsorbent dose, pH and initial adsorbate concentration.

Elemental composition revealed that smectite rich clay soils mainly consist of SiO_2 and Al_2O_3 as major elements; minor components include CaO, Na_2O, MgO and traces of K_2O TiO_2 and MnO. Mineralogical analysis revealed that the clay soils consist of montmorillonite, quartz, albite and anthophyllite. It was observed that 0.8 g/100 mL of smectite rich clay soils removed up to 91.89% from the initial F^- concentration of 3 mg/L at pH of 2 and contact time of 30 min. The experimental data fitted well to Langmuir adsorption isotherm than Freundlich isotherm and followed pseudo second order reaction kinetics. Smectite rich clay soils showed 51.72% F^- removal from field groundwater with 5.4 mg/L initial F^-. Sorption of fluoride occurred via ligand exchange mechanism.

Modification of bentonite clay with Mn^{2+} increased MnO content from 0.09% in raw bentonite to 0.29% in Mn^{2+} modified bentonite clay and further decreased content of Na_2O, CaO and MgO as well as K_2O. Modification of bentonite clay with Mn^{2+} ion lead to the formation of new bonds such as Mn-O, Mn-OH and Mn-H_2O in the bentonite clay surface, this was confirmed using FTIR. Optimum operation conditions for adsorption of fluoride were established to be 30 min contact time 1.0 g/100 mL adsorbent dosage, 3 mg/L adsorbate concentration and pH of 2. Maximum percentage F^- removal of 84.0% was achieved at optimized conditions. The adsorption isotherm data fitted well to Langmuir model showing that the adsorbent is monolayer. Kinetic modelling showed that the data fitted well to pseudo second order than to the pseudo first order indicating that the rate limiting factor is chemisorption.

Coating Na-bentonite with MnO_2 lead to the formation of new minerals such as cryptomelane (KMn_8O_{16}) jacobsite ($Mn_6Fe_4)O_4$ and pyrolusite (MnO_2) which are both the oxides of manganese. Coating increased the percentage composition of Mn in the Na-bentonite and this diluted the percentage of other oxides such as SiO_2, Al_2O_3, MgO and Fe_2O_3. Optimum conditions for fluoride removal were found to be, 30 min contact time at 250 rpm, 1.5 g/100 mL adsorbent dosage, 5 mg/L adsorbate concentration, and pH of 8. Maximum F^- removal of ≈94.66% was achieved under optimum conditions. The adsorption data fitted well to Langmuir adsorption isotherm while the kinetics data fitted well to pseudo second order of reaction kinetics. Intra-

© University of Venda

University of Venda
Creating Future Leaders

particle diffusion model of Weber-Morris indicated that the removal of fluoride by MnO_2 coated Na-bentonite is a highly complex process, involving boundary layer diffusion and intra-particle diffusion as well as equilibrium adsorption. Sorption of fluoride occurred via ligands exchange mechanism at pH below 3 and at pH above 3 it occurred via ion exchange mechanism.

The ratio of MnO_2 coated Na-bentonite clay/smectite rich clay soils for fabricating the composite was established to be 1:3. The optimum calcination temperature was found to be 550 ℃. Mineralogical characterisation of the clay composite showed the presence of quartz, albite, cryptomelane and microcline as the main minerals of the calcined pellets. XRF analysis showed that SiO_2, Al_2O_3, MnO and Fe_2O_3 are the major oxides of the clay composite. Pellets prepared under the established optimum conditions removed ≈63.3% F^- from an initial F^- concentration of 10 mg/L.

Based on the findings of the study smectite rich clay soils, Mn^{2+} bentonite and MnO_2 coated Na-bentonite and the fabricated pellets can be used for defluoridation of groundwater in rural areas and the study further recommended the modification of smectite rich clay to improve its fluoride binding capacity. MnO_2 coated Na-bentonite showed higher adsorption capacity at wider range of pH however the stability test showed that the material is not stable since it released secondary contaminants into the treated water, therefore it is recommended that future work should focus on improving the stability of the mater. The study also recommend that future study should evaluate the use of MnO_2 coated Na-bentonite/smectite rich clay soils composite pellets for fluoride removal in a dynamic flow set-up.

UNIVERSITY OF VENDA
LIBRARY

© University of Venda

University of Venda
Creating Future Leaders

TABLE OF CONTENTS

DECLARATION i
ACKNOWLEDGEMENTS ii
ACADEMIC OUTPUTS iii
DEDICATION iv
ABSTRACT v
Chapter 1: Introduction 1
1.1 Background 1
1.2 Problem statement 3
1.3 Objectives 4
1.3.1 Main objective 4
1.3.2 Specific objectives 4
1.4 Research questions 4
1.5 Hypothesis 5
1.6 Assumption 5
1.7 Significance of the study 5
1.8 Thesis structure 5
References 6
Chapter 2: Literature Review 9
2.1 Introduction 9
2.2 Fluoride in the environment 9
2.3 Occurrence of fluoride in groundwater 9
2.4 Factors affecting the natural Fluoride concentrations in groundwater 10
2.4.1 Geology 10
2.4.2 Climate 11
2.4.3 Chemical composition of groundwater 11
2.5 Health effects of fluoride 12
2.6 Defluoridation methods 13
2.6.1 Adsorption 14
2.6.2 Ion-exchange 15
2.6.3 Precipitation method of defluoridation 16

© University of Venda

University of Venda
Creating Future Leaders

2.6.4 Membrane process 18
2.7 Defluoridation studies in South Africa 19
2.8 Defluoridation at household and community levels 20
2.9 Defluoridation using clay soils 21
2.10 Bentonite clay 22
2.10.1 Physical properties of bentonite clay 23
2.10.2 Chemical properties of bentonite clay 23
2.10.3 Applications of bentonite clay in water treatment 24
2.11 Mukondeni clay 25
2.12 Clay soil's composite adsorbents 25
Reference 26
Chapter 3: Physicochemical characterization of smectite rich clay soils and its implications for groundwater defluoridation 32
3.1 Introduction 33
3.2 Material and Methods 34
3.2.1 Sample collection and preparation 34
3.2.2 Preparation of clay soils 34
3.2.3 Physicochemical and mineralogical characterization 35
3.2.4 Batch defluoridation experiments 35
3.2.5 Regeneration of smectite rich clay soils 36
3.2.6 Method of analysis 36
3.3 Results and discussion 37
3.3.1 Physicochemical and mineralogical characterization 37
3.3.2 Batch adsorption experiments 42
3.3.3 Defluoridation of field water 47
3.4 Adsorption modelling 49
3.5 Adsorption Kinetics 52
3.6 Mechanistic aspect of adsorption of F^- onto smectite rich clay soils 55
3.7 Comparison of fluoride adsorption capacity of smectite rich clay soils with other adsorbents 56
3.8 Conclusions 57

© University of Venda

University of Venda
Creating Future Leaders

References 59

Chapter 4: Intercalation of Mn^{2+} ions onto bentonite clay and its implication for groundwater defluoridation 61

4.1 Introduction 62

4.2 Materials and Methods 63

4.2.1 Sample collection 63

4.2.2 Preparation and synthesis of Mn^{2+} modified bentonite clay 63

4.2.3 Physicochemical and mineralogical characterisation 64

4.2.4 Batch defluoridation experiments 64

4.3 Results and discussion 65

4.3.1 Physicochemical and mineralogical characterisation 65

4.3.2 Batch experiments 71

4.4 Adsorption isotherms 80

4.5 Adsorption kinetics 83

4.6 Mechanistic aspect of F^- adsorption onto Mn^{2+} bentonite clay 87

4.7 Comparison of Mn^{2+} modified bentonite adsorption capacity with other reported adsorbents 88

4.8 Conclusions 88

Chapter 5: Surface coating of NaOH activated bentonite with MnO_2 and its potential application on groundwater defluoridation 92

5.1 Introduction 93

5.2 Material and Methods 94

5.2.1 Sample collection 94

5.2.2 Adsorbent preparation 94

5.2.3 Physiochemical and mineralogical characterization 96

5.2.4 Batch defluoridation experiments 96

5.2.5 Regeneration of MnO_2 coated Na-bentonite clay 97

5.3 Results and discussion 97

5.3.1 Optimizing conditions for activating bentonite with NaOH 97

5.3.2 Optimisation of conditions for coating Na-bentonite with MnO_2 99

5.4 Physicochemical and mineralogical characterization 102

5.4.1 X ray diffraction analysis 102

© University of Venda

University of Venda
Creating Future Leaders

5.4.2 X ray fluorescence 103
5.4.3 Scanning Electron Microscopy 104
5.4.4 Surface area, pore distribution and pore volume 106
5.4.5 FTIR analysis 107
5.4.6 Determination of pH point of zero charge (pH_{pzc}) 108
5.5 Batch defluoridation 109
5.5.1 Effect of contact time 109
5.5.2 Effect of adsorbent dosage 110
5.5.3 Effect of initial adsorbate concentration 111
5.5.4 Effects of pH 112
5.5.5 Effects of Co-Existing ions 113
5.5.6 Regeneration and Reuse of the adsorbent 114
5.5.7 Chemical stability of the adsorbent 115
5.5.8 Defluoridation of Field groundwater 117
5.6 Adsorption isotherms 119
5.7 Adsorption kinetics 122
5.8 Mechanistic aspect 126
5.9 Comparison with other MnO_2 coated adsorbents 126
5.10 Conclusions 127
References 129
Chapter 6: Fabrication of smectite rich clay soil MnO_2 coated bentonite composites and potential application in groundwater defluoridation 131
Abstract 131
6.1 Introduction 132
6.2 Material and Methods 132
6.2.1 Sample collection 132
6.2.2 Adsorbent preparation 133
6.2.3 Physicochemical and mineralogical characterisation 134
6.3 Results and discussion 134
6.3.1 Effect of mixing ratio 134
6.3.2 Effect of calcination temperature 135

© University of Venda

University of Venda
Creating Future Leaders

Chapter 1: Introduction

1.1 Background

Fluorine is the 13th most abundant and highly electronegativity and reactive element in the earth crust. Because it is highly reactive fluorine cannot be found in nature at its elemental state, it exists as fluoride (Daifullah *et al.,* 2007). Fluoride occurs notably as sellaite (MgF_2), fluorospar (CaF_2) cryolite (Na_3AlF_6) and fluoropatite [$3Ca_3(PO_4)_2Ca(FCl_2)$] (Mohapatra *et al.,* 2009; Razbe *et al.,* 2013). The presence of fluoride in groundwater has drawn worldwide attention due to its considerable impact on human physiology. The intake of fluoride into human body from portable water at a level of 1.0 mg/L enhances bone development and prevents dental carries (Rajkumar *et al.,* 2015). The World Health Organisation (WHO) has set maximum fluoride limit of tolerance at 1.5 mg/L (WHO, 2011), while the South African drinking water standard is also set at 1.5 mg/L (DWAF, 1996) but a concentration below that is recommended for children. The assimilation of water containing fluoride concentration above 1.5 mg/L give rise to teeth moulting (dental fluorosis) and higher concentrations lead to major health hazards such as deformation of bones (skeletal fluorosis) (Ncube and Schutte, 2005).

Groundwater may be contaminated by fluoride through anthropogenic and natural sources. Anthropogenic sources include discharges from commercial or domestic activities, and from industry (Velazquez-Jimenez *et al.,* 2015). Natural sources of groundwater contamination with fluoride include leaching of fluoride from fluoride containing rocks such as sallite, fluorapatite, fluorspar and cryolite. Groundwater in many of the parts of the world contains fluoride concentration above the recommended limit. This includes countries like Sir Lanka, India, China, United States of America, South Africa, Argentina and Mexico (Velazquez-Jimenez *et al.,* 2015). Ncube and Schutte (2005) identified areas of high fluoride in groundwater in South Africa and related this to the occurrence of dental fluorosis in most communities using groundwater for domestic purposes. Dental fluorosis was observed in those areas with fluoride levels higher than the recommended limits for drinking water. Main affected communities were the rural areas of Limpopo, North West, Northern Cape, Western Cape, Free State and KwaZulu-Natal provinces. Survey conducted by Odiyo and Makungo (2012) in Siloam Village Limpopo Province revealed that 87% of the households used groundwater and that 85% of these households had family members with mottled teeth. 50% of children between the ages of 11 and 14 in Siloam Primary

UNIVERSITY OF VENDA
LIBRARY

© University of Venda

School also had mottled teeth. There is thus evidence linking negative human health impacts of high fluoride concentrations in groundwater in Siloam Village. Fluorosis is an incurable disease and as such efforts should be directed towards prevention (Craig *et al.,* 2015). Ncube and Schutte (2005) suggested that areas with fluoride concentration above the permissible limit will require defluoridation. They further recommended that proper research must be initiated into investigating cheap and technologically simple processes for small-scale removal of fluoride from fluoride rich groundwater or developing alternative methods of fluoride free water supply in such areas. Various techniques such as precipitation, co-precipitation, ion exchange and adsorption for defluoridation of groundwater have been reviewed by Meenakshi and Maheshwari (2006). Abaire *et al.* (2009) indicated that defluoridation techniques for household use must be feasible and sustainable, this means the technique must rely on locally available material, cost ineffective and have high fluoride adsorption capacity. As such adsorption becomes the suitable method for household defluoridation devices. Various adsorbents such as activated alumina (Maliyekaal *et al.,* 2006), clay soils (Coetzee *et al.,* 2003), cuttlefish bones (Nasr *et al.,* 2011), cow dung (Rajkumar *et al.,* 2015), tea waste (Cai *et al.,* 2015) and metal oxides (Wang *et al.,* 2015) have been evaluated for fluoride removal. Activated alumina has been the most commonly used adsorbent for fluoride removal, but low adsorption capacity, narrow available pH range and aluminium dissolution restrict its application for water treatment (Tang and Zhang, 2016). Recently research works have focused on the use of locally available and low cost clay soils for defluoridation because of their good adsorptive properties such as; larger surface area, higher cation exchange capacity and chemical and mechanical stability (Bhattacharyya *et al.,* 2008). Clay has permanent negative charges, and as such they are poor adsorbent of anionic species due to repulsion forces between the anion and the surface negative charges. To make clay good adsorbent for anion species, negative charges can be neutralized through the adsorption of positively-charged cations. Bentonite clay belongs to the class of alumino-silicate clay group, which comprises of layers of alumino-silicate sheets. It exhibits a high cation exchange capacity and low permeability (Agnello, 2005). Bentonite has a permanent negative charge caused by the isomorphous substitution of Al^{3+} for Si^{4+} in the tetrahedral layer and Mg^{2+} for Al^{3+} in the octahedral layer. These negative charges are balanced by the presence of exchangeable cations (Na^{+}, Ca^{2+} and K^{+}) in the lattice structure, which imparts high cationic exchange to the clay (Bradly and Weils., 2004; Ma *et al.,* 2012). Bentonite modified with high ionic density ions such

© University of Venda

as Fe^{3+}, Al^{3+} and Mg^{2+} has shown improved capacity for anion adsorption. Several studies have been reported on the use of modified bentonite clay for defluoridation of drinking water, this includes Mg^{2+} modified bentonite (Thakre *et al.,* 2010), Fe^{3+} modified bentonite (Gitari *et al.,* 2013) and Al^{3+} modified bentonite (Vhahangwele *et al.,* 2014). Locally available smectite rich clay from Mukondeni has been used for a very long time in making ceramic water filter and it was found to be effective in improving water quality (Tyeryar *et al.,* 2012). Its use in the adsorption of inorganic pollutants has never been evaluated although it is known to be rich in smectite (Dacosta *et al.,* 2013). In recent years, considerable attention has been focused on the study of fluoride removal using composite materials due to their improved adsorption capacity. For example, aluminum-modified hydroapatite (Nie *et al.,* 2012), Fe-Al-Ce composite (Wu *et al*., 2007), La (iii) incorporated carboxylated chitosan composite (Viswanthan and Meenakshi, 2008), Porous 2-line ferrihydrite/bayerite composites (Jia *et al.,* 2015) and Sand-double layered hydroxide composite (Oladoja *et al.,* 2015). In this project, smectite rich clay soils and Mn^{2+} intercalated bentonite were evaluated for defluoridation of groundwater. Further bentonite clay was activated with sodium hydroxide (NaOH) to remove anions naturally occurring and coated with MnO_2. The MnO_2 coated bentonite was then mixed with smectite rich clay soils, the mixture was then moulded manually into pellets, fired to make ceramic pellets that were then evaluated for defluoridation of groundwater.

1.2 Problem statement

Fluorosis is a chronic disease caused by drinking water with fluoride concentration greater than 1.5 mg/L for extended period of time (Coetzee *et al.,* 2003). This disease is manifested by mottled teeth in dental fluorosis and changes in bone structure in skeletal fluorosis. Fluorosis is an incurable disease. Therefore, efforts should be directed towards prevention. In trying to reduce the effect of fluoride, World Health Organization (WHO) has set a standard for fluoride concentration in water at 1.5 mg/L (WHO, 2011).

Groundwater is the most appropriate and widely-used source of drinking water in many rural areas of South Africa. However, the groundwater in many regions of South Africa such as the Northern Cape, Limpopo and North West, has high concentration of fluoride ions. Most of the rural areas of these regions do not have municipal water supply and the communities tend to depend on groundwater from wells and boreholes. This increases the risk of fluorosis

© University of Venda

development in the population that depends on groundwater with high concentration of fluoride. Ncube and Schuttle (2005) indicated that areas which have fluoride concentrations beyond the recommended limits for drinking water will require defluoridation and proper research must be initiated into investigating cheap and technologically simple process for small scale removal of fluoride from fluoride rich groundwater. Bentonite clay and smectite rich clay soils from Mukondeni are cheap and naturally available materials that can be used for small-scale fluoride removal

1.3 Objectives

1.3.1 Main objective

The main objective of the study is to optimize the activation of bentonite clay with NaOH, modify the activated bentonite with MnO_2 and finally blend coated activated bentonite clay with smectite rich clay soils to make clay soil composites.

1.3.2 Specific objectives

- To optimize the activation of bentonite clay with NaOH.
- To evaluate and optimize the conditions of coating the activated bentonite with MnO_2
- To evaluate the physicochemical properties of raw bentonite clay, manganese bentonite and smectite rich clay soils i.e, cation exchange capacity (CEC), surface area, point of zero charge, surface morphology, chemical composition and mineralogy.
- To evaluate the fluoride adsorption capacity of smectite rich clay soils, Mn^{2+} bentonite and MnO_2-modified activated bentonite clay and its smectite rich clay soil composites.
- Evaluate the regeneration potential of the optimized adsorbents using alkaline solutions.

1.4 Research questions

- How to activate bentonite clay with NaOH?
- How to modify activated bentonite clay with MnO_2?
- What are the conditions for fabricating MnO2 coated Na-bentonite/smectite rich clay soil composite?
- What are the physicochemical properties of smectite rich clay soils and Mn modified bentonite clay?
- What is the F^- removal efficiency of smectite rich clay soils, Mn^{2+} bentonite, MnO_2-modified bentonite clay and its composite from groundwater?

© University of Venda

- How to regenerate the adsorbents using alkaline solutions?

1.5 Hypothesis

NaOH-activated MnO_2-modified bentonite clay blended with black smectite rich clay soils from Mukondeni can effectively remove fluoride ions from drinking water.

1.6 Assumption

It is assumed that modified bentonite-smectite rich clay composite will be applied in defluoridation at community and household level in every part of the county.

1.7 Significance of the study

Groundwater is the main source of drinking water in many rural areas of South Africa (Ncube and Schutte, 2005; Gitari *et al.,* 2013; Odiyo and Makungo, 2012). However, this groundwater is rich in fluoride, which is toxic to human health. So far most of the techniques that have been developed to remove fluoride ions from the groundwater cannot be applied in many developing countries, including, South Africa because of financial constraints (Coetzee *et al.,* 2003; Schoeman, 2010). Therefore, the viable option is to look for a low-cost process that can utilize local expertise and locally available and cost-effective fluoride adsorbents.

1.8 Thesis structure

Chapter 1: Introduction

Chapter 2: Literature review

Chapter 3: Physicochemical and Mineralogical characterization of black smectite rich clay soils and its implication for groundwater defluoridation

Chapter 4: Intercalation of Mn^{2+} ions onto bentonite clay and potential application in groundwater defluoridation

Chapter 5: Surface coating of NaOH activated bentonite with MnO_2 and its potential application on groundwater defluoridation

Chapter 6: Fabrication of smectite rich clay soil MnO_2 coated bentonite composites and potential application in groundwater defluoridation

Chapter 7: Conclusions and recommendation.

© University of Venda

University of Venda
Creating Future Leaders

References

Abaire, B., Zewge, F & Endale. M., 2009 Operational experiences on small scale community defluoridation systems. 34th WEDC International Conference, Addis Ababa, Ethiopia.

Agnello, V. N., 2005. Bentonite, Pyrophyllite and talc in the Republic of South Africa. *Department of Minerals and Energy*. Directorate: Mineral Economics, Pretoria.

Bhattachryya, K. G. & Gupta, S. S., 2008. Adsorption of few heavy metals on natural and modified kaolinite and montmorillonite: A review. *Advances in colloid and interface science*. 140, pp.114-131.

Bradley, G. & Weils, D. H., 2004. *Elements of nature*. 5th ed. USA: Blackies and Sons.

Cai, H., Chen, G., Peng, C., Zhang, Z., Dong, Y., Shang, G., Zhu, X., Gao, H. & Wan, X., 2015. Removal of fluoride from drinking water using tea waste loaded with Al/Fe oxides: A novel, safe and efficient biosorbent. *Applied Surface Science,* 328, pp. 34–44.

Coetzee, P. P., Coetzee , L. L., Puka, R & Mubeng, S., 2003. Characterization of selected South African clays for defluoridation of natural water. *Water S.A.* 29(3), pp. 331-338.

Craig, L., Stillings, L. L., Decker, D. L. & Thomas, J. M., 2015. Comparing activated alumina with indigenous laterite and bauxite as potential sorbents for removing fluoride from drinking water in Ghana. *Applied Geochemistry,* 56, pp. 50–66.

Dacosta, F. A. Muzerengi, C. Mhlongo, S. E. & Mukwevho, G. F., 2013. Characterization of clays for making ceramic pots and water filters at Mukondeni village, Limpopo province, South Africa. *ARPN Journal of Engineering and Applied Sciences,* 08 (11), pp.927- 932.

Daifullah, A. A. M., Yakout, S. M & Elreefy, S. A., 2007. Adsorption of fluoride in aqueous solutions using KMnO4-modified activated carbon derived from steam pyrolysis of rice straw. *Journal of Hazardous Materials*, 147, pp. 633–643.

Department of Water Affairs and Forestry (DWAF), South African Water Quality Guidelines for Domestic Use, 1st ed., Department of Water Affairs and Forestry, Pretoria, 1996. Available from: www.dwaf.gov.za

Gitari W. M., Ngulube T, Masindi V., & Gumbo J. R., 2013. Defluoridation of groundwater using Fe^{3+}- modified bentonite clay: Optimization of adsorption condition. *Desalination & water treatment*., pp 1-13.

Jia Y., Zhu B. S., Zhang K. S., Jin Z., Luo T., Yu X. Y., Kong., L. T., & Liu J. H., 2015. Porous 2-line ferrihydrite/byerite composite (LFBC): Fluoride removal performance and mechanism. *Chemical Engineering Journal,* 268, pp. 325-336.

UNIVERSITY OF VENDA
LIBRARY

© University of Venda

Ma, Y., Wang, S. G., Fan, M., Gong, W. X. & Gao, B. Y., 2012. Characteristics and defluoridation performance of granular activated carbons coated with manganese oxides. *Journal of Hazardous Materials*, 168, pp1140–1146.

Maliyekaal, S. M., Sharma, A. K., & Philip, L., 2006. Manganese-oxide-coated alumina: a promising sorbent for defluoridation of water. *Water Res*. 40, pp.3497–3506.

Meenakshi, S. K. & Maheshwari, R. C., 2006. Fluoride in drinking water and its removal. *Journal of Hazardous Matter,* 137(1), pp. 456-463.

Mohapatra, M. Anand, S. Mashra, B. K. & Giles, P., 2009. Review of fluoride removal from drinking water. *Journal of Environmental Management,* 91, pp. 67-77.

Nasr, A. B., Walha, K., Charcosset, C. & Amar, R. B., 2011. Removal of fluoride ions using cuttlefish bones. *Journal of fluoride chemistry,* 132, pp, 57-62.

Ncube, E. J., & Schutte, C. F., 2005. The occurrence of fluoride in South African groundwater: A water quality and health problem. *Water S.A*, 31 (1), pp. 35-40.

Nie, Y. L., Hu, C. & Kong C.P., 2012. Enhanced fluoride adsorption using Al(III) modified calcium hydroxyapatite. *Journal of Hazardous Mater*, 233 (2012) 194–195.

Odiyo J. O., & Makungo, R., 2012. Fluoride concentrations in groundwater and impact on human health in Siloam Village, Limpopo Province, South Africa. *Water S.A*, 38 (5), pp.731-732.

Oladoja, N. A., Liu, Y., Drewes, J. E & Helmreich, B., 2015. Preparation and Characterization of a Reactive Filter for Groundwater Defluoridation. *Chemical Engineering Journal. In press.*

Rajkumar, S., Murugesh, S., Sivasankar, V., Darchen, A., Msagati, T. A. M. & Chaabane, T., 2015. Low-cost fluoride adsorbents prepared from a renewable biowaste: Syntheses, characterization and modeling studies. *Arabian Journal of Chemistry*, pp.1-14.

Razbe, N. Kumar, R. Kumar, P. & Kumar, R., 2013. Various Options for Removal of Fluoride from Drinking Water. *IOSR Journal of Applied Physics*, 3(2), pp. 40-47.

Schoeman, J. J., 2010. Water defluoridation, water denitrification and water desalination in rural areas in South Africa. Proceedings of the third lasted African conference, power and energy systems. Gaborone, Botswana.

Tang, D. & Zhang, G., 2016. Efficient removal of fluoride by hierarchical Ce–Fe bimetal oxides adsorbent: Thermodynamics, kinetics and mechanism. *Chemical Engineering Journal,* 283, pp. 721–729.

© University of Venda

Thakre, D., Rayalu, S., Kawade, R,. Meshram, S., Subrt, J. & Labhsetwar, N., 2010. Magnesium incorporated Bentonite clay for defluoridation of drinking water. *Journal of Hazardous Materials,* 180, pp.122-130.

Tyeryar, M., C. Hackett, D. Harsh & T. Hackett (2012). Establishing a ceramic water filter factory in Limpopo Province, South Africa Public: 104-110.

Velazquez-Jimenez, H. L, Vences-Alvarez, E., Flores-Arciniega, J. L., Flores-Zuniga, H., Jose & Rangel-Mendez, R. 2015. Water defluoridation with special emphasis on adsorbents-containing metal oxides and/or hydroxides: A review. *Separation and Purification Technology,* 150, pp. 292–307.

Vhahangwele, M., Mugera, G. W. & Tholiso, N., 2014. Defluoridation of drinking water using Al^{3+}-modified bentonite clay: optimization of fluoride adsorption conditions. *Toxicol. Environ. Chem.* 96, 1–16.

Viswanathan, N. & Meenakshi, S., 2008. Enhanced fluoride sorption using La (III) incorporated carboxylated chitosan beads, *Journal of Colloid Interface Science.* 322 (2008) 375–383.

Wang, J., Kang, D., Yu, X., Ge, M. & Chen, Y. 2015. Synthesis and characterization of Mg-Fe–La trimetal composite as an adsorbent for fluoride removal. *Chemical Engineering Journal.,* 264, pp. 506–513.

World Health Organization, 2011. *Guideline for drinking water, world health organization.* Geneva.

Wu, X. M., Zhang, Y., Dou, X. M. & Yang, M., 2007. Fluoride removal performance of a novel Fe–Al–Ce tri-metal oxide adsorbent. *Chemosphere*, 69, pp. 1758–1764.

© University of Venda

University of Venda
Creating Future Leaders

Chapter 2: Literature Review

2.1 Introduction

This chapter presents a review of the literature related to fluoride, its health hazards, occurrence of fluoride in the groundwater, methods of removing fluoride from groundwater, South African studies on defluoridation, defluoridation at household and community level, defluoridation using clay soils and physicochemical properties of bentonite clay and smectite rich clay soils.

2.2 Fluoride in the environment

According to Nagendra (2003), fluorine (F_2) is a greenish diatomic gas and it is the 13th most abundant naturally occurring element in the earth's crust and is the lightest member of the halogens. Its compounds make up approximately 0.08 percent of the earth's crust. It is the most electronegative and reactive of all the elements and it is never encountered in its elemental gaseous state except in some industrial processes. According to the Water Quality Association (2005), fluoride is classified as any binary compound of fluorine with another element. Fluoride occurs notably as sellaite (MgF_2), fluorospar (CaF_2) cryolite (Na_3AlF_6) and fluoropatite [$3Ca_3(PO_4)_2Ca(FCl_2)$] (Mohapatra *et al.*, 2009; Razbe *et al.*, 2013).

2.3 Occurrence of fluoride in groundwater

Fluoride occurs in almost all waters from trace to high concentrations (Hemant, 2013). The contamination of groundwater with fluoride may be due to natural or anthropogenic processes. Fluoride is frequently encountered in naturally-occurring minerals and geo-chemical deposits and can enter groundwater through natural processes such as natural weathering and leaching (Thakre *et al.*, 2010; Velazquez-Jimenez *et al.*, 2015). Anthropogenic causes include wastewater from sewage treatment plants, discharge from industries, improper solid waste disposal, agrochemicals and runoff from agricultural fields (Brindha and Elango, 2011). Fluoride concentration in natural waters depends on various factors such as temperature, pH, solubility of fluoride-bearing minerals, anion exchange capacity of aquifer materials (OH^- for F^-) and the nature of geological formations drained by water and contact time of water with a particular formation (Ncube, 2002; Hemant, 2013; Meenakshi and Maheshwari, 2006). The map below shows the regions in South Africa with fluoride concentration greater than 1.5 mg/L.

© University of Venda

University of Venda
Creating Future Leaders

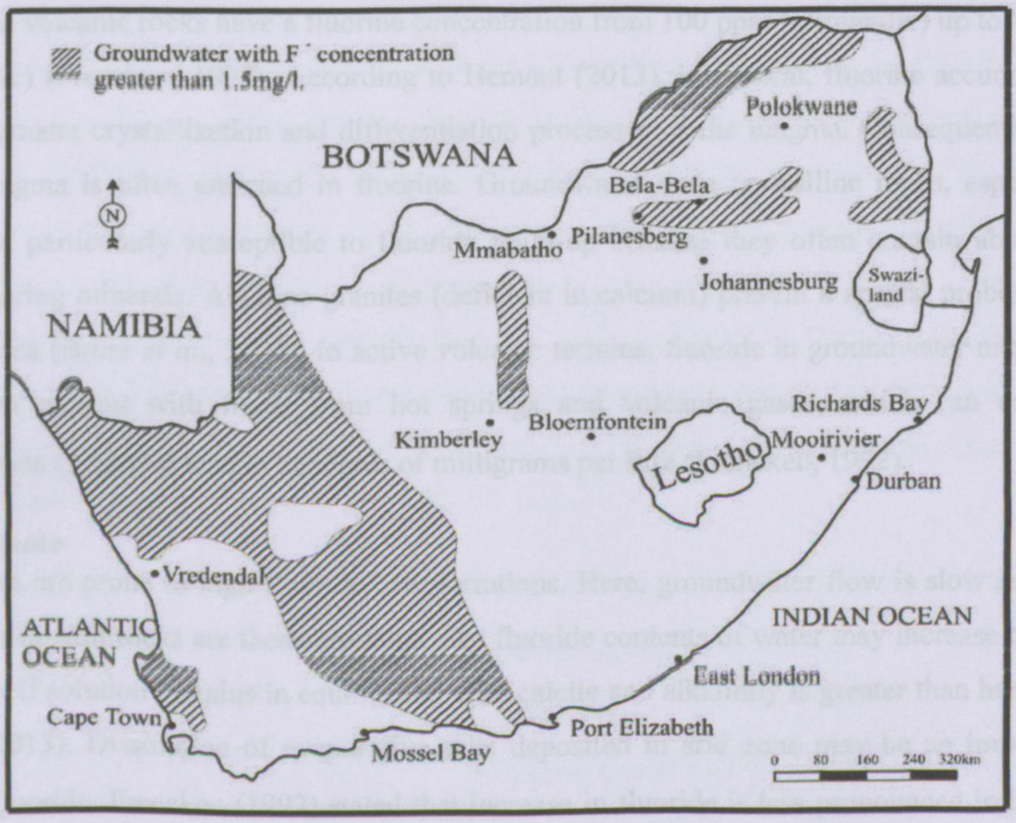

Figure 2.1: South Africa groundwater with fluoride concentrations > 1.5 mg/L (McCaffrey and Willis, 2001)

2.4 Factors affecting the natural Fluoride concentrations in groundwater

2.4.1 Geology

During weathering and circulation of water in rocks and soils, fluoride can be leached out and dissolved in groundwater and thermal gases. The fluoride content of groundwater varies greatly depending on the geological settings and type of rocks. The most common fluoride-bearing minerals are fluorite, apatite and micas. Therefore fluoride problems tend to occur in places where these minerals are most abundant in the host rocks (Brunt *et al.,* 2004). In South Africa, it has been confirmed that the general distribution of fluoride in problem areas is controlled by the geochemistry of the rock in which the groundwater is encountered (McCaffrey and Willis, 2001). Areas of Northern Cape, North West, KwaZulu-Natal and Limpopo are mainly characterized by sedimentary, granite, metamorphic and volcanic rocks, which contain fluoride (Ncube, 2002).

© University of Venda

Igneous and volcanic rocks have a fluorine concentration from 100 ppm (ultramafic) up to >1000 ppm (alkalic) (Frencken, 1992). According to Hemant (2013), in general, fluorine accumulates during magmatic crystallization and differentiation processes of the magma. Consequently, the residual magma is often enriched in fluorine. Groundwater from crystalline rocks, especially granites are particularly susceptible to fluoride build-up because they often contain abundant fluoride-bearing minerals. Alkaline granites (deficient in calcium) present a special problem, as in East Africa (Brunt *et al.*, 2004). In active volcanic terrains, fluoride in groundwater may also derive from mixing with fluids from hot springs and volcanic gases, which can contain concentrations of several tens to hundreds of milligrams per litre (Frencken, 1992).

2.4.2 Climate

Arid regions are prone to high fluoride concentrations. Here, groundwater flow is slow and the reaction times with rocks are therefore long. The fluoride contents of water may increase during evaporation if solution remains in equilibrium with calcite and alkalinity is greater than hardness (Hemant, 2013). Dissolution of evaporative salts deposited in arid zone may be an important source of fluoride. Frencken (1992) stated that increase in fluoride is less pronounced in humid tropics because of high rainfall inputs and their diluting effect on the groundwater.

2.4.3 Chemical composition of groundwater

According to Hemant (2013), high fluoride groundwater is mainly associated with a sodium bicarbonate water-type and relatively low calcium and magnesium concentrations. Ncube (2002) evaluated the correlation of Ca^{2+} and Na^{+} ions with fluoride concentrations. In the study it was reported that high concentrations of Na^{+} increases the solubility of fluoride in water and this lead to increasing concentrations of fluoride in water. Low calcium concentrations increase the solubility of CaF_2 which increases the concentration of fluorides in groundwater. Chae *et al.*, (2007) reported that the thermodynamic relationship between Ca^{2+} and F^{-} ions indicates that fluoride concentration is controlled by equilibrium of fluorite. When the water is saturated with respect to fluorite or is at equilibrium with fluorite, the low calcium concentration leads to higher fluoride concentrations (Nezli *et al.*, 2009). High fluoride concentrations are therefore expected in groundwater from aquifers with low calcium concentrations. In groundwater with a high concentration of calcium, fluoride concentration rarely exceeds 1 mg/L (Rivett *et al.*, 2006).

© University of Venda

2.5 Health effects of fluoride

Fluoride has certain physiological properties of great importance in human health (Muller *et al.*, 1998; Notcutt and Davies, 1999). Fluoride also has beneficial effects on teeth by hardening the enamel and reducing the increase of caries. Although the beneficial effects of fluoride can be demonstrated at low concentrations, it has detrimental effects when concentrations exceed a certain threshold (Li *et al.*, 2001). Optimal concentrations are around 1.0 mg/L. However, chronic ingestion of concentration greater than 1.5 mg/L is linked to fluorosis development (WHO, 2011). The disease is manifested by tooth decay in dental fluorosis and bending of bones in skeletal fluorosis (Wang and Reardon, 2001). The implications of various concentrations of fluoride on human health are listed in the Table 2.1 below.

Table 2.1: The health implication of fluoride content in drinking water (Dissanayake, 1991).

F^- (mg/L)	**Health outcome**
<0.5	Dental caries
0.5-1.5	Optimal dental health
1.5- 4.0	Dental fluorosis
4.0- 10	Dental and skeletal fluorosis
>10.0	Crippling fluorosis

Fluorosis appears to be a public health problem in certain areas of South Africa which requires a great attention at various levels. According to Ncube and Schutte (2005), the majority of dental fluorosis sufferers are black South Africans who live in the rural areas, particularly in Limpopo, Northern Cape, North West and KwaZulu-Natal. These provinces have high populations still living in rural areas and prior to 1994 most of them were using ground and surface water for drinking purposes. The current status of fluoride distribution in South Africa is such that no clear demarcation can be made of areas that have deficient in fluoride requiring fluoridation since some areas have groundwater sources in which fluoride ion concentrations are higher than the recommended limits for drinking water requiring defluoridation. This is an indication that occurrence of low fluoride concentration is not a national problem (Ncube, 2002; Ncube and Schutte, 2005). Many sources of groundwater in the Limpopo, Northern Cape, North West and KwaZulu-Natal provinces are in need of partial defluoridation to the optimum level of fluoride

© University of Venda

University of Venda
Creating Future Leaders

concentration safe for drinking water purposes (Ncube and Schutte, 2005). The map below shows the % morbidity of dental fluorosis in South Africa.

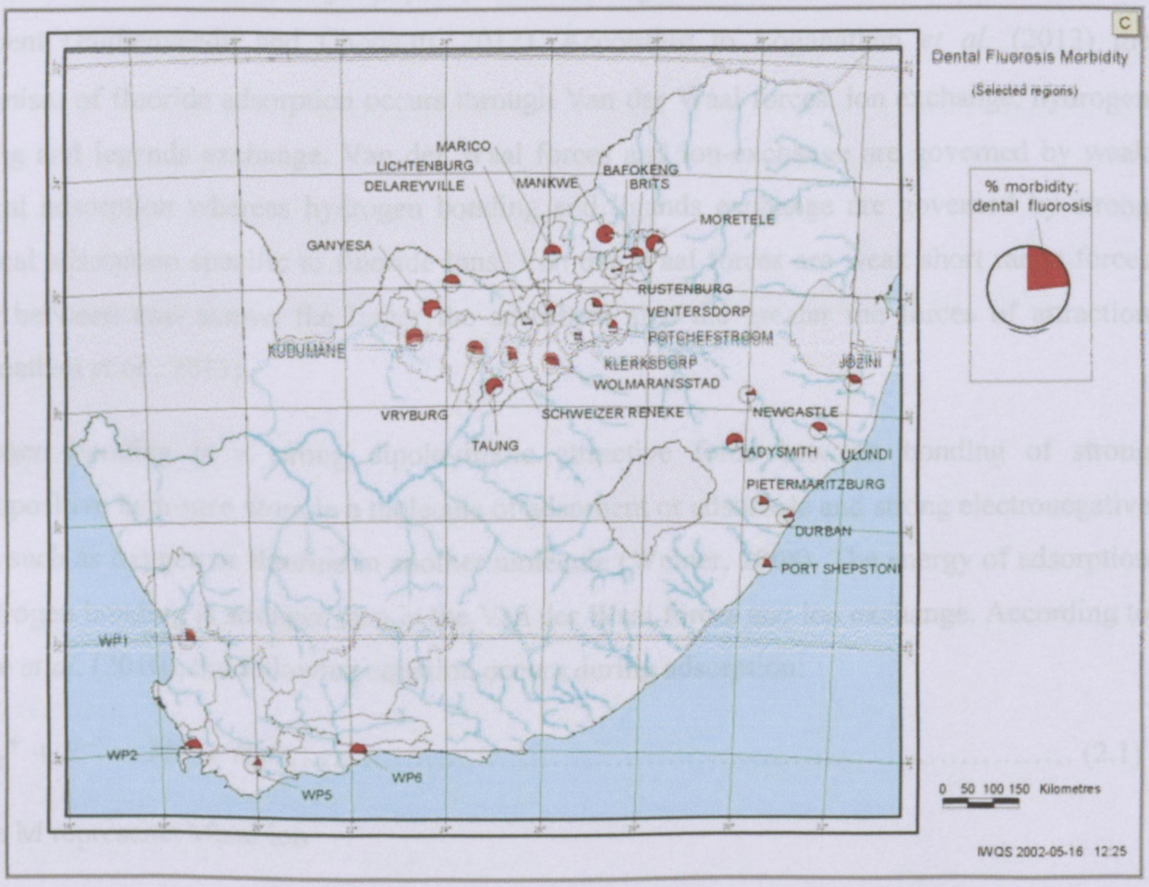

Figure 2.2: The % morbidity of dental fluorosis in South Africa (Ncube and Schutte, 2005).

2.6 Defluoridation methods

Defluoridation is defined as the downward adjustment of level of fluoride in drinking water to the optimal level (Hiremath, 2006). Through chemical reaction, fluoride concentration can be reduced to less than 1.5 mg/L, which is suitable for drinking. This depends on the materials and methods used in defluoridation. Common methods of defluoridation that have been identified in the literature search include adsorption, membrane process, electrocoagulation, ion exchange and precipitation and co-precipitation process (Meenakshi and Maheshwari, 2006).

© University of Venda

UNIVERSITY OF VENDA
LIBRARY

2.6.1 Adsorption

Adsorption involves the passage of contaminated water through an adsorbent bed, where pollutants are removed through physical ion-exchange or surface chemical reaction with adsorbent (Puthenveedu and Chonattu, 2012). According to Loganathan *et al.* (2013) the mechanism of fluoride adsorption occurs through Van der Waal forces, ion exchange, hydrogen bonding and legends exchange. Van der Waal forces and ion-exchange are governed by weak physical adsorption whereas hydrogen bonding and ligands exchange are governed by strong chemical adsorption specific to fluoride ions. Van der Waal forces are weak short range forces acting between two atoms; the larger the adsorbent size the greater the forces of attraction (Loganathan *et al.*, 2013).

Hydrogen bonding is a strong dipole-dipole attractive force between bonding of strong electropositive hydrogen atom in a molecule of adsorbent or adsorbate and strong electronegative atoms such as oxygen or fluorine in another molecule (Weiner, 2008). The energy of adsorption in hydrogen bonding is stronger than in the Van der Waal forces and ion exchange. According to Thakre *et al.* (2010), the following equation occurs during adsorption:

$$MOH_2^+ + F^- \leftrightarrow MF + H_2O \quad \text{(2.1)}$$

Where M represents Metal ion

In the ligands exchange mechanism, the adsorbing anions such as F^- forms a strong covalent chemical bond with metallic cations and adsorbent surface, resulting in the release of potential determining ions such as OH^- previously bonded to metallic cations. Thus, fluoride is said to form an inner sphere complex or specifically adsorbed on the adsorbent surface (Maliyekkal *et al.*, 2006). According to Loganathan *et al.* (2013) the following equation occurs during adsorption:

$$MOH + F^- \leftrightarrow MF + OH^- \quad \text{(2.2)}$$

Where M represents Metallic cation

Several adsorbent materials have been attempted in the past to find out an efficient and economical defluoridating agent. These include activated alumina, activated carbon, fly ash and clay soils. Activated alumina and activated carbon are the commonly used fluoride adsorbents

© University of Venda

(Meenakshi and Maheshwari, 2006). Ghorai and Pant (2005) investigated the use of activated alumina for the adsorption of fluoride and obtained good results, however the fluoride removal from aqueous solution was observed to be strongly dependent on the contact time, pH of the solution and the adsorbent dosage. The use of activated carbon coated with manganese oxide in the adsorption of fluoride was investigated by Ma *et al.* (2009) and it was capable of maintaining a high fluoride adsorption capacity over an acidic pH range. Therefore based on these it can be said that adsorption is dependent on the pH of the solution.

According to Loganathan *et al.* (2013) the adsorption process has the following advantages

Advantages

- Ease of operation
- Treatment is cost-effective.
- The process has high fluoride binding capacity

Limitations

- Frequent adsorbent regeneration required
- Effective mostly at pH < 7 for adsorption.

2.6.2 Ion-exchange

According to Meenakshi and Maheshwari (2006), fluoride can be removed from water supplies with a strongly basic anion-exchange resin containing quaternary ammonium functional groups. Chelating resin and anion exchanger in Cl^- are widely used resins. Ions are adsorbed physically by fully retaining their inner hydration shell and adsorption is due to electrostatic attractions. The ion exchange process is rapid and reversible (Loganathan *et al.*, 2013).

The removal takes place according to the following reaction:

$$MNR_3^+Cl^- + F^- \rightarrow MNR_3^+F^- + Cl^- \quad \text{(2.3)}$$

The fluoride ions replace the chloride ions of the resin. This process continues until all the sites on the resin are occupied. The resin is then backwashed with water that is supersaturated with

© University of Venda

dissolved sodium chloride salt. New chloride ions then replace the fluoride ions, leading to recharge of the resin and starting the process again.

The ion exchange process has the following advantages and disadvantages (Meenakshi and Maheshwari, 2006).

Advantages

- Removes up to 90–95% of the fluoride
- Retains the taste and colour of water.

Disadvantages

- Efficiency is reduced in the presence of other ions like sulphate, carbonate, phosphate and alkalinity.
- Regeneration of resin is a problem because it leads to fluoride rich waste, which has to be treated separately before final disposal.
- The technique is expensive because of the cost of resin, pre-treatment required to maintain the pH, regeneration and waste disposal.
- Treated water has a very low pH and high levels of chloride

2.6.3 Precipitation method of defluoridation

The two major drawbacks of ion-exchange and adsorption techniques are: the flow through system is often difficult to arrange where there is no piped water supply and gradual exhaustion of the active agent is not easily detected. In an attempt to overcome these problems the precipitation techniques have been developed (Larsen and Pearce, 1992). Precipitation methods are based on the addition of chemicals (coagulants and coagulant aids) and the subsequent precipitation of a sparingly soluble fluoride salt as insoluble fluorapatite (Mariappan and Vasudevan, 2002)

Lime and alum are the most commonly used coagulants. Addition of lime leads to precipitation of fluoride as insoluble calcium fluoride and raises the pH value of water to between 11 and 12.

© University of Venda

$$Ca(OH)_2 + 2F^- \rightarrow CaF_2 + 2OH^- \quad (2.4)$$

As lime leaves a residue of 8.0 mg/L fluoride, it is used only in conjunction with alum treatment to ensure the proper fluoride removal (Culp and Stolenberg, 1958). As a first step, precipitation occurs through lime dosing, which is followed by a second step in which alum is added to cause coagulation. When alum is added to water, essentially two reactions occur. In the first reaction, alum reacts with some of the alkalinity to produce insoluble aluminium hydroxide ($Al(OH)_3$). In the second reaction, alum reacts with fluoride ions present in the water. The best fluoride removal is accomplished at pH range of 5.5–7.5 (Potgeiter, 1990). The best example of the application of this technique is the famous Nalgonda technique.

According to Bulusu *et al.* (1979), The Nalgonda Technique involves addition of aluminium salts, lime and bleaching powder followed by rapid mixing, flocculation, sedimentation, filtration and disinfection. Aluminium salt may be added as aluminium sulphate (alum) or aluminium chloride or combination of these two. It is responsible for removal of fluoride from water. The dose of aluminium salt increases with increase in the fluoride and alkalinity levels of the raw water. The selection of either aluminium sulphate or aluminium chloride depends on sulphate and chloride contents of the raw water to avoid exceeding their permissible limits. Lime facilitates formation of dense flocks for rapid settling of insoluble fluoride salts. The dose of lime is empirically $1/20^{th}$ of that of aluminium salt. Bleaching powder is added to the raw water at the rate of 3 mg/L for disinfection. Bulusu *et al.* (1979) stated that Nalgonda Technique was preferable at all levels because of the low price and ease of handling. The technique is highly versatile and is suitable for large communities, fill and draw technique for small communities, fill and draw defluoridation plant for rural water supply and for domestic household defluoridation.

The method has the following advantages and disadvantages (Tewari and Jalili, 1986)

Advantages of Nalgonda technique

- Regeneration of media is not required.
- Can be used to treat water in large quantities for community usage.
- Simplicity of design, construction, operation and maintenance.

© University of Venda

- Highly efficient removal of fluorides from high levels to desirable levels.
- Simultaneous removal of colour, odour, turbidity, bacteria and organic contaminants.
- Little wastage of water and least sludge disposal problems.

Disadvantages of Nalgonda technique

- Desalination may be necessary when the total dissolved solids exceed 1500 mg/L.
- Hardness of the raw water in the range of 200 mg/L to 600 mg/L requires precipitation softening and beyond 600 mg/L becomes a cause for rejection or adoption of desalination.
- Generation of higher quantity of sludge compared to electrochemical defluoridation.
- Large amount of alum needed to remove fluoride.
- Careful pH control of treated water is required.

2.6.4 Membrane process

Membrane process such as reverse osmosis, nanofiltration and electrodialysis are recent developments employed for removal of fluoride ions from drinking water. In reverse osmosis, the hydraulic pressure is exerted on the one side of the semi-permeable membrane, which forces the water across the membrane, leaving the salts behind. The relative size of the pollutants left behind depends on the pressure exerted on the membrane. According to Meenakshi and Maheshwari (2006) nanofiltration is a relatively low pressure process that removes primarily the larger dissolved solids as compared to reverse osmosis. In electrodialysis, the membranes allow the ions to pass but not the water. The driving force is an electric current which carries the ions through the membranes. The removal of fluoride in the reverse osmosis process has been reported to vary from 45 to 90% as the pH of the water was raised from 5.5 to 7 (Meenakshi and Maheshwari, 2006).

This method has the following advantages and disadvantages (Meenakshi and Maheshwari, 2006):

© University of Venda

Advantages

- The process is highly effective for fluoride removal. Membranes also provide an effective barrier to suspended solids, all inorganic pollutants, organic micro pollutants, pesticides and microorganisms.
- The process permits the treatment and disinfection of water in one step.
- No chemicals are required and very little maintenance is needed.
- Life of membrane is sufficiently long, therefore the problem of regeneration or replacement is encountered less frequently.
- It works under a wide pH range.
- No interference by other ions is observed.

Disadvantages

- It removes all the ions present in water, though some minerals are essential for proper growth, remineralisation is required after treatment.
- The process is expensive in comparison to other options.
- The water becomes acidic and needs pH correction.
- Much water is wasted as brine.
- Disposal of brine is a problem.

2.7 Defluoridation studies in South Africa

Several studies have been done in South Africa on high fluoride concentration in groundwater. Detailed studies were done in the Bushveld and Pilansberg region (Bond, 1947; McCaffrey and Willis, 2001). These two areas were seen as areas deserving investigation because of endemic dental fluorosis. Fluoride concentration in rivers flowing through Kruger National Park were determined by Raubenheimer *et al.* (1999), all five rivers (Olifant, Luvuvhu, Letaba, Sabie and Crocodile rivers) had high concentration of fluoride ion during the latter part of the dry season.

© University of Venda

Fluoride in drinking water of South Africa received great attention back in the mid-1980 following study done by Schoeman (1985). Most of these studies were concerned with the removal of fluoride using activated alumina as an adsorbent (Schoeman, 1985; Schoeman and Steyn, 2000). Activated alumina reduced fluoride ions from 8 mg/L to less than 1.5 mg/L which is the required concentration of fluoride ions in the drinking water. However, the constraints associated with the use of activated alumina for defluoridation such as the alkalinity of treated water and its reduced adsorption capacity has led to the evaluation of other fluoride adsorbents by many South African scholars (Schoeman, 2010). The main challenge here was to find adsorbent that is readily available and at low cost.

2.8 Defluoridation at household and community levels

According to Abaire *et al.* (2009) defluoridation techniques for household must be feasible and sustainable, this means the technique must be using locally available material, cost ineffective and have high fluoride adsorption capacity. Defluoridation techniques such as ion exchange, and membrane process are not feasible and sustainable for household and community levels since they are expensive and they do not use locally available material.

Nalgonda technique of water defluoridation has been developed in India for community level defluoridation, this method involve the addition of alum and lime to water followed by settling and filtration. The method was found to be effective in treating high fluoride water; however it needs daily operations and requires a well-trained operator (Pranati and Devaraj, 2011).

Adsorption technique is widely used for defluoridation of water at household and community level. The use of adsorption started in the ancient times with the use of mud pots (Piddennavar and Krishnappa, 2013). The raw pots are subjected to heat treatment as in case of brick production. The pots were being used as fluoride adsorbent for household purposes; the problem with the mud pots is their adsorption capacity which is poor. The adsorption is said to be dependent on the soil used to produce the pot with the pots made from aluminium containing soil having good adsorption capacity. Adsorption rate and capacity of fluoride is also said to be dependent on the firing temperature. Clay pots fired at approximately 600 °C are most effective; a temperature above 700 °C causes a decline in fluoride adsorption (Hauge *et al.*, 1994; Piddennavar and Krishnappa, 2013).

© University of Venda

Fluoride removal using activated alumina has been one of the widely-used fluoride adsorption techniques for rural areas of developing countries (Daw, 2004). The main disadvantage of activated alumina was its poor adsorption capacity and narrow pH range. Activated alumina-based treatment devices also accumulate bacteria during the long run process (Maliyekkal *et al.*, 2006). This approach was not feasible in developing countries especially in rural areas. Clay based adsorbents have been paid more attention in recent investigations due to their high binding affinity of fluoride and they are available in large quantities at lower or no cost (Mohapatra *et al.*, 2009). Moreover clays can be modified using acid, base and metal oxides to increase their fluoride binding affinity. This makes bentonite clays and smectite rich clay soils from Mukondeni to be a promising adsorbent for defluoridation at household and community level.

2.9 Defluoridation using clay soils

According to Coetzee *et al.* (2003) clays are potentially good adsorbent of fluoride ions since they contains crystalline minerals such as kaolinite, smectite and amorphous minerals such as allophane and other metal oxides and hydroxides which could adsorb anions. The structure of the clay plays a critical role in determining the key charges on the surface of the clay and the type of exchange that will occur with ions in the solution (Puka, 2004). The more the positive the clay surface is, the better the sorption will be for negative charged ions.

Many studies have reported on the fluoride adsorption of capacities of clay soils and their potential use as adsorbent. A comprehensive study on the adsorption of fluoride onto clay minerals and soils was published in 1967 (Bower and Hatcher, 1967). The results showed that, fluoride adsorption capacity vary depending on the soil and clay minerals in particular aluminium hydroxide. It was also found that fluoride adsorption by clay soils is followed by the release of OH^- ions.

After the above study was been published, more fluoride adsorption studies using clay soils were been published throughout the world. Fired clay chips in Ethiopia (Moges *et al.*, 1996), illite-geothite soils in China (Wang and Reardon, 2001), the study on selected South African clays (Coetzee *et al.*, 2003), the use of chemically modified bentonite clay (Kamble *et al.*, 2009), magnesium incorporated bentonite clay (Thakre *et al.*, 2010), red mud (Lv *et al.*, 2012) and Fe^{3+} modified bentonite in South Africa (Gitari *et al.*, 2013) and Al^{3+} bentonite clay Vhahangwele *et al.*, 2014).

© University of Venda

2.10 Bentonite clay

Bentonite is alumina silicate clay made up of sodium and calcium montmorillonite (Agnello, 2005). According to Patterson and Murray (1983) bentonites are clays rich in smectite regardless of their mode of origin. Bentonite clay is valued for its properties such as crystal shape and size, cation exchange capacity, hydration and swelling, thixotrophy, bonding capacity, impermeability, plasticity and tendency to react with organic molecules (Highley, 1972; Odom, 1984).

The formation of bentonite predominantly takes place in aqueous environmental conditions during or after deposition of volcanic ash (Dixon and Weed, 1989; Langmuir, 1997). In addition to montmorillonite as the main mineral, bentonite may also contain feldspar, biotite, kaolinite, illite, cristablite, pyroxene, zircon and crystalline quartz. This may also depend on physiochemical properties of parent weathered material (Sparks, 1997).

Bentonite belongs to the 2:1 clay family composed of two tetrahedral coordinated sheets of silicon surrounding octahedrally coordinated sheet of aluminium ions (WHO, 2005). Clays play an important role in the environment by taking up cations and anions through adsorption or ion exchange, thus, clays invariably contain exchangeable cations and anions held to the surface. Predominant ions found on the clay surface are; Ca^{2+}, Mg^{2+}, NH_4^+, Na^+, and SO_4^{2-}, Cl^-, PO_4^{3-}, NO_3^- (Bhattachryya and Gupta, 2008). These ions can be exchanged with other ions relatively easily without affecting clay mineral structure. Figure 2.3 shows the structure of bentonite clay.

© University of Venda

University of Venda
Creating Future Leaders

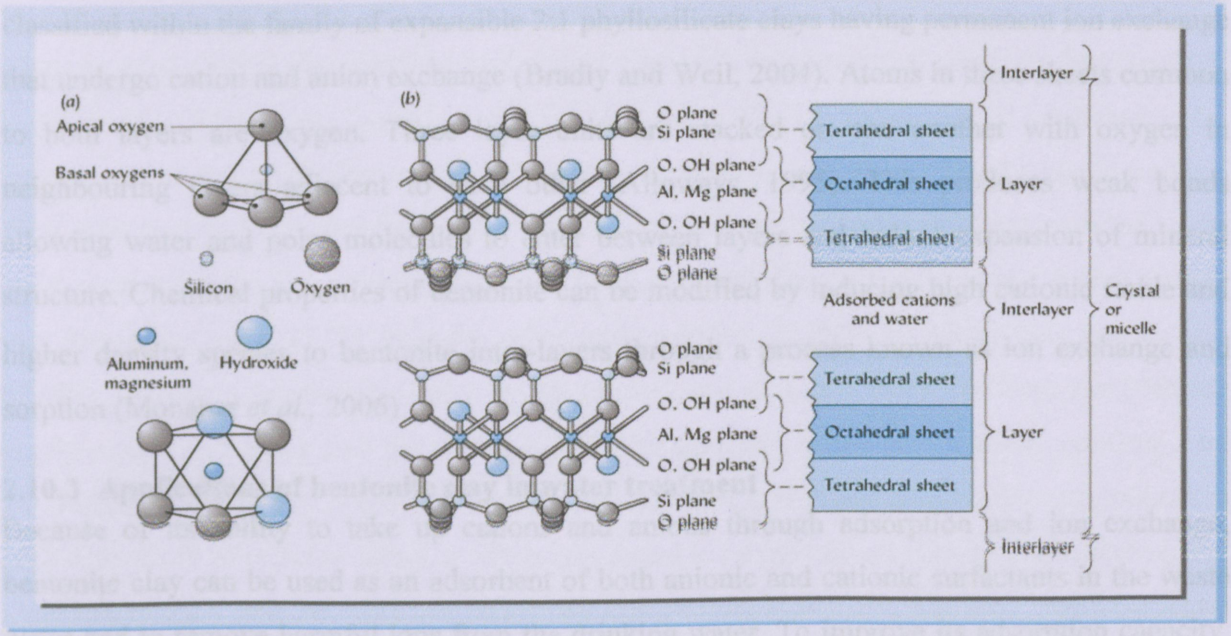

Figure 2.3: Structure of bentonite (Agnello, 2005)

2.10.1 Physical properties of bentonite clay

Bentonite is white, pale green or blue and with exposure, darkens in time to yellow, red or brown (Besq *et al.,* 2003). It consists of aggregates of flat platelets, has high specific surface area, high plasticity and can expand several times from its original volume when placed in water (Agnello, 2005). Nevertheless, bentonite clay has a high water holding capacity which enables it to swell 30 times its original size hence allowing water to retain within its materials for a long period of time, thus promoting high chemical reactions between solution and bentonite clay (Bradly and Weil, 2004). The physical state of bentonite may be changed with increasing water content from a hydrous solid to hydrated material, semi rigid plastic, gel and suspension respectively (Onal, 2006). Bohn *et al.* (1979) indicated that these physical properties enable bentonite clay to scavenge polar pollutants and firmly hold them on clay fractions through weak Van der Waal force or chemical bonding.

2.10.2 Chemical properties of bentonite clay

Chemical properties of the surface of clay mineral are strongly dependent on their mineral structure. The basic unit of montmorillonite crystals is an extended layer composed of an octahedral alumina sheets (O) between the two tetrahedral silica sheets (T) forming TOT unit (Bhattachryya and Gupta, 2008). The stacks of TOT layers produce crystals. As such they are

© University of Venda

classified within the family of expansible 2:1 phyllosilicate clays having permanent ion exchange that undergo cation and anion exchange (Bradly and Weil, 2004). Atoms in these sheets common to both layers are oxygen. Three layer units are stacked on one another with oxygen in neighbouring layers adjacent to each other (Alloways, 1995). This produces weak bonds allowing water and polar molecules to enter between layers and induce expansion of mineral structure. Chemical properties of bentonite can be modified by inducing high cationic stable and higher density species to bentonite inter-layers through a process known as ion exchange and sorption (Monahar *et al.,* 2006)

2.10.3 Applications of bentonite clay in water treatment

Because of its ability to take up cations and anions through adsorption and ion exchange, bentonite clay can be used as an adsorbent of both anionic and cationic surfactants in the waste water and to remove harmful ions from the drinking water. To improve its adsorption capacity, bentonite clay can be modified by other exogenous species (Ramesh *et al.,* 2007). Modification of bentonite clay can be done through intercalation and pillaring and by activating bentonite clay with acidic or basic solution (Bhattacharyya and Gupta, 2008). Acid activation of bentonite clay appears to be most commonly used modification techniques because it is said to be simple and low cost process (Toor *et al.,* 2014).

Thakre *et al.* (2010) investigated the use of magnesium incorporated bentonite clay for defluoridation of drinking water and concluded that chemical modification of bentonite clay with magnesium result in significant enhancement in its fluoride removal efficiency at wide range of pH (3-10). The maximum fluoride adsorption capacity was found to be 2.26 mg/g at the initial fluoride concentration of 5.52 mg/L.

Gitari *et al.* (2013) evaluated the removal of fluoride from borehole water using raw and Fe^{3+} modified bentonite clay and observed that both raw and modified bentonite clays could remove fluoride from borehole water, however, at different degrees of efficiency. Fe^{3+} modified bentonite clay was found to be more effective than the raw bentonite clay. The degree of fluoride removal was highly dependent on the pH of the solution.

© University of Venda

2.11 Mukondeni clay

Dacosta *et al.* (2013) characterized Mukondeni clay soils and found that there are three types of clays found in Mukondeni, namely red, black and green. The red colour can be attributed to the presence of slightly high iron oxide and the black colour is attributed to high organic matters. They also analysed the smectite content of the clay soils and it was found that smectite is the main content in all types of clay soils found in Mukondeni. Smectite content in red clay sample was the lowest with 37.7% than the other two varieties, 55.08% for black clay sample and 55.69% for green clay sample. High smectite in black and green indicates that these materials are highly plastic and sticky than the red clay soils. The plasticity of the clay was also confirmed by the plasticity index (PI) of the clay samples. PI of black and green clay sample was relatively high than the PI of red clay samples. Silica was found to be the highest component in Mukondeni clay soils ranging from 58.01% to 61.01% with the average of 62.01%. The trace elements found in Mukondeni clay soils were also determined and it was found that clay soil contains Zn, Cr, V and Ni was constantly high in the soil.

Mukondeni clay soils fall into smectite group with high swelling and shrinking potential. Smectite is generally sticky with high plasticity and strength in both dry and wet state (Onal, 2006). Mukondeni clay soils are mainly used for making clay pots and ceramic filters. The main property that supports its use for making clay pots and ceramic filters is its plasticity. According to Dies (2003), plasticity of the clay and the cohesive forces between the clay allows the ceramist to form different shapes of ceramic pots that remain even after fired.

2.12 Clay soil's composite adsorbents

In recent years, considerable attention has been focused on the study of fluoride removal using composite materials. For example, aluminum modified hydroapatite (Nie *et al.,* 2012), Fe-Al-Ce composite (Wu *et al.,* 2007) and La (iii) incorporated carboxylated chitosan composite (Viswanthan and Meenakshi, 2008) all these composite adsorbent materials have shown very promising result for fluoride removal from aqueous solution. In this study a composite adsorbent will be prepared by blending MnO_2-coated modified bentonite clay with Mukondeni black clay soils and later tested for defluoridation.

© University of Venda

University of Venda
Creating Future Leaders

Reference

Abaire. B., Zewge. F & Endale. M., 2009 Operational experiences on small scale community defluoridation systems. 34th WEDC International Conference, Addis Ababa, Ethiopia.

Agnello, V. N., 2005. Bentonite, Pyrophyllite and talc in the Republic of South Africa. *Department of Minerals and Energy*. Directorate: Mineral Economics, Pretoria.

Alloways, B. J., 1995. *Heavy metals in soil*. 2nd ed. London: Blackie academic and professional.

Besq, A. Malfoy, C. Pantet, A. Monnet, P. & Righi, D., 2003. Physicochemical characterisation and flow properties of some bentonite muds. *Applied Clay Science,* 23, pp. 275-286.

Bhattachryya, K. G. & Gupta, S. S., 2008. Adsorption of few heavy metals on natural and modified kaolinite and montmorillonite: A review. *Advances in colloid and interface science*. 140, pp. 114-131.

Bohn, H. L. Mcneal, B. L. & O'connor, G., 1975. Soil chemistry. *A Wiley-interscience publication*. New York: John Wiley and Sons.

Bond D. S., 1947. A geochemical survey of the underground water supplies of the union of South Africa. *Dept of mines, geological survey memoir*. p.203.

Bower, C. A., Hatcher, J. T., 1967. Adsorption of fluoride by soils and minerals. *Journal of Soil Science,* 3, pp.151–154.

Bradley G. & Weils, D. H., 2004. *Elements of nature*. 5th ed. USA: Blackies and Sons.

Brindha, K, &Elango, L., 2011. Fluoride in groundwater: causes and mitigation measures. In Monroy, S. D. (ed). *Fluoride properties, application, and Environmental Management* , pp.111-136.

Brunt, R. Vasak, L, & Griffioen, J., 2004. Fluoride in groundwater: probability of occurrence of excessive concentration on global scale. Igrac. Report nr. Sp 2004-2.

Bulusu, K. R. Sundaresan, B. B. Pathak, B. N. Nawlakhe W. G, Kulkarni D. N. & Thergaonkar, V. P., 1979. Fluorides in water, defluoridation methods and their limitations. *J. Institute Engineers (India) – Environmental Engineering Division*. 60, pp.1-25.

Chae, G. T, Yun, S. T, Mayer, B, Kim, K. H, Kim, S. Y, Kwon J. S, Kim, K & Koh, Y. K., 2007. Fluorine geochemistry in bedrock groundwater of South Korea. *Sci. Total Environ.* 385 272–283.

Coetzee P. P., Coetzee, L. L. & Mubeng, S., 2003. Characterization of selected South African clays for defluoridation of natural water. *Water S.A.* 29(3), pp.331-338.

Culp, R. & Stolenberg, H., 1958. Fluoride reduction at La Crosse. *Journal of American Water Works Association,* 50(3), pp.423–431.

UNIVERSITY OF VENDA
LIBRARY

© University of Venda

Dacosta, F. A. Muzerengi, C. Mhlongo, S. E. & Mukwevho, G. F., 2013. Characterization of clays for making ceramic pots and water filters at Mukondeni village, Limpopo province, South Africa. *ARPN Journal of Engineering and Applied Sciences,* 08 (11), pp. 927- 932.

Daw. R. K, 2004. Experiences with domestic defluoridation in India. 30th WEDC International Conference, Vientiane, Lao PDR.

Dies, R. W., 2003. Development of Ceramic Water filters for Nepal. M.Sc. Thesis. Department of Civil and Environmental Engineering. Massachusetts Institute of Technology. pp. 170.

Dissanayake, C. B., 1991. The fluoride problem in the groundwater of Sri Lanka– environmental management and health. *Int. Journal of Environmental Studies*, 19, pp.195–203.

Dixon, J. B. & Weed, S. B., 1989. *Mineral in soil environment*. USA: Soil Science Society of America.

Frencken, J. E., 1992. Endemic Fluorosis in developing countries, causes, effects and possible solutions. Netherlands: NIPG-TNO, Leiden, Publication number 91.082.

Ghorai, S. & Pant, K. K., 2005 Investigations on the column performance of fluoride adsorption by activated alumina in a fixed-bed, *Chem. Eng. J.* 98, pp.165–173

Gitari W. M., Ngulube T, Masindi V., & Gumbo J. R., 2013. Defluoridation of groundwater using Fe^{3+}- modified bentonite clay: Optimization of adsorption condition. *Desalination & water treatment*., pp 1-13.

Hauge, S., O¨sterberg, R., Bjorvatn, K., Selvig, K.A., 1994. Defluoridation of drinking water with pottery: effect of firing temperature. *Scandinavian journal of dental research,* 102, pp.329–333.

Hemant, W. K., 2013. Fluoride contaminated water and its implication on human health- A review. *International journal of chem tech research,* 5(5), pp. 502-511.

Highley, D. E., 1972. *Fuller's Earth*. London: Mineral Resources Consultative Committee.

Hiremath, S. S., 2006. *Textbook of preventive and community dentistry*. Elsevier India: Bengalore.

Kamble, S. Dixit, P. Rayalu, S. S. & Labhsetwar, N. K., 2009. Defluoridation of drinking water using chemically modified bentonite clay. *Desalination and water treatment journal,* 249, pp.687-693.

Langmuir, D. 1997. *Aqueous environmental geochemistry*. New Jersy: Prentice of Hall, Inc. Upper Saddle river.

© University of Venda

Larsen, M. J. & Pearce, E. I. F., 1992. Partial defluoridation of drinking water using fluorapatite precipitation. *Caries Res*. 26, pp. 22-28.

Li, Y. H., Wang, S., Cao, A. Zhao, D. Zhang, X. Xu, C. Luan, Z. Ruan, D. Liang, J. Wu, D. & Wei, B., 2001. Adsorption of fluoride from water by amorphous alumina supported on carbon nanotubes.*Chem. Phys. Lett*., 350, pp.412–416.

Loganathan, P., Vigneswaran, S., Kandasamy, J., & Naidu, R., 2013. Review: Defluoridation of drinking water using adsorption processes. *Journal of Hazardous Materials,* 248 (249) pp.1–19.

Lv, G., Wu, L., Liao, L., Zhang, Y. & Zhaohui, Y., 2012. Preparation and characterization of red mud sintered porous materials for water defluoridation. *Journal of Applied Clay Science,* pp.1-7

Ma, Y. Wang, S. G, Fan, M. Gong, W. X. & Gao, B. Y., 2009. Characteristics and defluoridation performance of granular activated carbons coated with manganese oxides. *Journal of Hazardous Materials,* 168, pp.1140–1146.

Maliyekkal, S. M., Sharma, A. K. & Philip, L., 2006. Manganese-oxide-coated alumina: a promising sorbent for defluoridation of water. *Water Res*. 40, pp. 3497–3506.

Mariappan, P. & Vasudevan, T., 2002. *Domestic defluoridation techniques and sector approach for fluorosis mitigation*. [online] Available at: www.twadboard.gov.in. (Accessed 4 March 2015).

McCaffery, L. P. & Willis, J. P., 2001. Distribution of fluoride rich groundwater in the eastern and Mogwase regions of the northern and western provinces. *WRC Report no*. 52/1/01.

Meenakshi, S. K. & Maheshwari, R. C., 2006. Fluoride in drinking water and its removal. *Journal of Hazardous Matter,* 137(1), pp. 456-463.

Moges, G., Zewge, F. & Socher, M., 1996. Preliminary investigations on the defluoridation of water using fired clay chips. *J. Afr. Earth Sci.* 21(4), pp. 479-482.

Mohapatra, M. Anand, S. Mashra, B. K. & Giles, P., 2009. Review of fluoride removal from drinking water. *Journal of Environmental Management,* 91, pp. 67-77.

Monahar, D. M. Noeline, B. F. & Anirudhan, T. S., 2006. Adsorption performance Al-pillared bentonite clay for the removal of cobalt (II) from aqueous phase. *Applied Clay Science,* 31, pp.194-206.

Muller, W. J. Heath, R. G. M & Villet, M. H., 1998. Finding the optimum: Fluoridation of portable water in South Africa. *Water SA,* 24(1), pp.21-27.

Nagendra Rao, C. R., 2003. "Fluoride and Environment - A Review". In Martin J. B, Madha Suresh V, & Vasantha Kumaran, T., eds. *Proceedings of the Third International Conference on*

© University of Venda

Environment and Health. Chennai, India 15-17 December 2003. Department of Geography, University of Madras and Faculty of Environmental Studies, York University. pp. 386 – 399: Chennai.

Ncube, E. J., & Schutte, C. F., 2005. The occurrence of fluoride in South African groundwater: A water quality and health problem. *Water S.A*, 31 (1), pp. 35-40.

Ncube, E. J., 2002. The Distribution of Fluoride in South African Groundwater and the Impact thereof on Dental Health. M.Sc. dissertation submitted to the University of Pretoria.

Nezli, I. E., Achour, S., Djidel, M & Attalah, S., 2009. Presence and origin of fluoride in the complex terminal water of Ouargla Basin (Northern Sahara of Algeria). *Am. J. Appl. Sci.* **6** (5) 876–881.

Nie, Y. L. Hu, C. & Kong C.P., 2012. Enhanced fluoride adsorption using Al(III) modified calcium hydroxyapatite. *Journal of Hazardous Mater*. 233 (2012) 194–195.

Notcutt, G. & Davies, F., 1999. Bio monitoring of volcanogenic fluoride, furnas caldera, sao Miguel, Azores. *Journal of volcan. and geoth,* . 92, pp.209-214.

Odom, I. E., 1984. *Smectite clay minerals: properties and uses*. London: Philos. Trans. R. Soc. Ser. A 311, pp. 391–409.

Onal, M., 2006. *Physicochemical properties of bentonite: overview*. Turkey: Ankara.

Patterson, S. H. & Murray, H. H., 1983. Clays. In: S. J. Lefond, ed. *Industrial Minerals and Rocks*. New York: Am. Inst. Mining Engineers. pp.519–585.

Piddennavar, R. & Krishnappa, P., 2013. Review on defluoridation techniques of water. *The International Journal of Engineering and Science,* 2(3), pp.86-94.

Potgeiter, J. H., 1990. An experimental assessment of the efficiency of different defluoridation methods, *Chem. SA,* pp.317–318.

Pranati. E. & Devaraj. C. G., 2011. Water defluoridation: Field studies in India. *Indian journal of dental advancements.* 3(2), pp. 526-533.

Puka, L. R., 2004. Fluoride Adsorption Modelling and the Characterization of Clays for Defluoridation of Natural Waters. MSc dissertation, Faculty of Science, Rand Afrikaans University.

Puthenveedu, S. P. & Chonattu, J., 2012. Defluoridation of water using biosorbents. *Water Quality Division, Centre for Water Resources Development and Management,* 4(4), pp. 245-251. India: Kozhikode.

© University of Venda

Ramesh, A. Hasegawa, H. & Ueda, K., 2007. Adsorption of inorganic and organic arsenic from aqueous solution by polymeric Al/Fe modified montmorillonite. *Separation and Purification Technology,* 56, pp.90-100.

Raubenheimer, E. J, Okonska, E. T. Dauth, J. Dreyes, M. J. Lourens, C. Bruwer, C. A. & De Vos, V., 1990. Fluoride concentration in the rivers in Kruger National Park. *S. African Journal of Wildlife Resource,* pp.127-129

Razbe, N. Kumar, R. Kumar, P. & Kumar, R., 2013. Various Options for Removal of Fluoride from Drinking Water. *IOSR Journal of Applied Physics*, 3(2), pp. 40-47.

Rivett, M., Drewes, J., Barrett, M., Chilton, S., Appleyard, S., Dieter, H. H., Wauchope, D & Fastner J., 2006. Chapter b4. Chemicals: health relevance transport and attenuation. In: Schmoll O, Howard G, Chilton J & Chorus J (eds) Protecting Groundwater for Health: Managing the Quality of Drinking Water Sources. WHO Drinking Water Quality Series, IWA publishing, London.

Schoeman, J. J., 1985. An evaluation of the activated alumina process for fluoride removal from drinking water and some factors influencing its performance. *Water SA,* 11(1), pp.25-31.

Schoeman, J. J, & Steyn, A., 2000. Defluoridation, denitrification and desalination of water using ion exchange and reverse osmosis technology. *WRC Report*, 124/00

Schoeman, J. J., 2010. Water defluoridation, water denitrification and water desalination in rural areas in South Africa. Proceedings of the third lasted African conference, power and energy systems. Gaborone, Botswana.

Spark, D. L., 1997. *Environmental soil chemistry*. 2nd ed. Amsterdam: Academic Press.

Teweri, A. & Jalili, V. P., 1986. Fluoride and dental caries. *Journal of India dental association*, 58 (7), pp.251-256.

Thakre, D., Rayalu, S., Kawade, R,. Meshram, S., Subrt, J. & Labhsetwar, N., 2010. Magnesium incorporated Bentonite clay for defluoridation of drinking water. *Journal of Hazardous Materials,* 180, pp. 122-130.

Toor M., Jin B., Dai S., Vimonoses V., 2014. Activating natural bentonite as a cost effective adsorbent for removal of Congo red in waste water, *J. industrial & engineering chemistry*, 1979, pp. 1-9.

Velazquez-Jimenez, H. L, Vences-Alvarez, E., Flores-Arciniega, J. L., Flores-Zuniga, H., Jose Rangel-Mendez, R. 2015. Water defluoridation with special emphasis on adsorbents-containing metal oxides and/or hydroxides: A review. *Separation and Purification Technology,* 150, pp. 292–307.

© University of Venda

Vhahangwele, M., Mugera, G. W., Tholiso, N., 2014. Defluoridation of drinking water using Al^{3+}-modified bentonite clay: optimization of fluoride adsorption conditions. *Toxicol. Environ. Chem*. 96, 1–16.

Viswanathan, N., Meenakshi, S., 2008. Enhanced fluoride sorption using La (III) incorporated carboxylated chitosan beads, *Journal of Colloid Interface Science.* 322 (2008) 375–383.

Wang, Y. & Reardon, E. J., (2001) Activation and regeneration of a soil sorbent for defluoridation of drinking water. *Appl. Geochem,* 16, pp. 531-539.

Water Quality Association, 2005. Technical application bulleting fluoride. USA: National Headquarters and Laboratory.

Weiner, E. R., 2008. Applications of Environmental Aquatic Chemistry, CRC Press, Taylor and Francis Group, Florida.

Word Health Organization, 2005. *Bentonite, kaolinite and selected clay minerals (Environmental Health Criteria; 231)*. Geneva.

World Health Organzation, 2011. *Guideline for drinking water, world health organization.* Geneva

Wu, X. M., Zhang, Y., Dou, X. M. & Yang, M., 2007. Fluoride removal performance of a novel Fe–Al–Ce tri-metal oxide adsorbent. *Chemosphere*, 69, pp. 1758–1764.

© University of Venda

University of Venda
Creating Future Leaders

Chapter 3: Physicochemical characterization of smectite rich clay soils and its implications for groundwater defluoridation

Abstract

Groundwater is a widely used and affordable source of drinking water in most of the rural areas of South Africa. Several studies have indicated that groundwater in some of the boreholes has fluoride concentration above the recommended levels by World Health Organization (1.5 mg/L). Low concentration of fluoride (<1.5 mg/L) reduces dental caries especially in children. If it is above the permissible limits (>1.5 mg/L), fluoride can lead to dental fluorosis and still higher concentrations lead to skeletal fluorosis. The present work evaluates the application of smectite rich clay soils from Mukondeni in defluoridation of groundwater. The clay soils were characterized for mineralogy using x-ray diffraction (XRD) and elemental composition using x-ray fluorescence (XRF) and morphology using Scanning Electron Microscopy (SEM). Surface area and pore volume was determined by Brunauer Emmet Teller (BET) method using micrometrics TriStar II. Cation exchange capacity and pH_{pzc} of the soils were also evaluated using standard laboratory methods. Batch experiments were conducted to evaluate and optimize various operational parameters such as contact time, adsorbent dose, pH and initial adsorbate concentration. It was observed that 0.8 g/100 mL of smectite rich clay soils removed up to 91.89% from the initial F^- concentration of 3 mg/L at pH of 2 and contact time of 30 min. The experimental data fitted well to Langmuir adsorption isotherm than Freundlich isotherm and followed pseudo second order reaction kinetics. Smectite rich clay soils showed 51.72% F^- removal from field groundwater with 5.4 mg/L initial F^-. Sorption of fluoride occurred via ligand exchange mechanism. The study shows that smectite rich clay soils from Mukondeni have a potential for application in defluoridation of groundwater and it recommends chemical modification to improve its defluoridaton capacity.

Key words: *Adsorption, batch experiments, characterisation, defluoridation, groundwater, Smectite rich clay soils.*

© University of Venda

3.1 Introduction

Groundwater is the most affordable and widely used natural resource for many of the rural areas in South Africa. Its chemical nature is one of the most important criteria that determines its usefulness for a specific need and as such not all groundwater is fit for drinking (Nagendra, 2003). The presence of elements such as fluoride in high concentration in drinking water is a serious concern from the health point of view. The presence of fluoride in drinking water, within permissible limits is beneficial for the production and maintenance of healthy bones and teeth, while excessive intake of fluoride causes dental or skeletal fluorosis (Susheela, 2001). The South African government and the World Health Organisation set a permissible limit of fluoride in groundwater to be 1.5 mg/L (DWAF, 1996, WHO, 2011).

Fluorosis is an incurable disease caused by drinking water with fluoride concentration of greater than 1.5 mg/L for extended period of time and therefore efforts must be made to prevent it by providing water with fluoride concentration below 1.5 mg/L. Ncube and Schutte (2005) indicated that areas which have fluoride concentrations beyond the recommended limits for drinking water will require defluoridation. Meenakshi and Maheshwari (2006), reported various treatment methods for defluoridation, this includes adsorption method, ion exchange, membrane technique and precipitation method. Among all the methods of defluoridation which have been reported, adsorption has been considered as the effective and applicable method for defluoridation of groundwater in rural areas because of it uses materials which are readily available and inexpensive. Different materials such as clay soils (Coetzee *et al.*, 2003), activated alumina (Ghorai and Pant, 2004), activated carbon (Ma *et al.*, 2009) and other low cost material have been tested for defluoridation of groundwater. Among the tested adsorbents activated alumina is widely used because it is inexpensive and it has high defluoridation capacity (Meenakshi and Maheshwari, 2006). Recently more studies have focused on the use of clay soils for defluoridation due to their good adsorptive properties such as large specific surface area, chemical and mechanical stability, layered structure and high cation exchange capacity. Several studies that have reported the use of clay soils for defluoridation have been published and this includes study on illite-geothite soils in China (Wang and Reardon, 2001) the study on selected South African clays (Coetzee *et al.*, 2003), the use of chemically modified bentonite clay (Kamble *et al.*, 2009), magnesium incorporated bentonite clay (Thakre *et al.*, 2010), Fe^{3+} modified bentonite in South Africa (Gitari *et al.*, 2013) and Al^{3+} modified bentonite

© University of Venda

University of Venda
Creating Future Leaders

(Vhahangwele *et al.,* 2014). Smectite rich clay from Mukondeni has been used for a very long time in making ceramic water filter and it was found to be effective in improving water quality (Tyeryar *et al.,* 2012). Its use in the adsorption of inorganic pollutants has never been evaluated although it is known to be rich in smectite (Dacosta *et al.,* 2013). The present work evaluated the physicochemical properties of the black mukondeni smectite rich clay soil and its potential application in defluoridation of groundwater using batch experiments. Optimum operating conditions such as, contact time, adsorbent dosage, initial adsorbate concentration and initial pH were evaluated and optimized. The regeneration and re-usability of smectite rich clay soils as well as the effects of co-existing ions on defluoridation efficiency was also evaluated. Lastly the mechanism of fluoride adsorption on the clay soils was elucidated.

3.2 Material and Methods

3.2.1 Sample collection and preparation

Smectite rich clay soil was collected from Mukondeni Village, Vhembe district in South Africa. Field water was collected from community borehole in Siloam, Vhembe district in South Africa All reagents and TISAB-III were obtained from Rochelle Chemicals & Lab Equipment CC, South Africa Ltd and they were of analytical grade. A stock solution containing 1000 mg/L fluoride was prepared by dissolving 2.21 g NaF in 1 L of MILLIQ water (18.2 MΩ/cm) and fluoride solutions for batch experiments were prepared from fresh stock fluoride solution by appropriate dilution.

3.2.2 Preparation of clay soils

Clay soils were washed by mixing the soil with MILLIQ water (18.2 MΩ/cm) at a ratio of 1:5 in a 1 L beaker, the mixture was stirred for 5 min, and the procedure was repeated twice. After stirring, mixtures were agitated for 15 min using Stuart Reciprocating shaker and then centrifuged for 10 min at 5 000 rpm. Samples were then dried in an oven for 12 hrs at 105 °C. Soil samples were then milled to pass through < 250 µm sieve.

© University of Venda

University of Venda
Creating Future Leaders

3.2.3 Physicochemical and mineralogical characterization

Mineralogical and chemical composition of the clay soils were determined using X-ray diffraction (XRD) (PANalytical X'Pert pro power) and X-ray fluorescence (XRF) (Thermo Fisher ARL9400 XP+ Sequential XRF with WinXRF software) respectively. Surface morphology was determined using Scanning electron microscopy (SEM) (Leo1450 SEM, voltage is 10Kv, working distance 14mm). Surface area and pore volume was determined by Brunauer Emmet Teller (BET) method using micrometrics TriStar II. Functional groups and surface chemistry was determined using Fourier transform infrared spectroscopy (FTIR). Cation exchange capacity was determined using ammonium acetate buffer at pH 5.4 and 7.4 as described by Gitari et al., (2013) and The concentration of exchangeable cation was determined using flame atomic absorption spectrum (FAAS) (600 PerkinElmer). The surface charge and point of zero charge (PZC) was determined using solid addition method as described by Kumar *et al.* (2011).

3.2.4 Batch defluoridation experiments

Batch experiments were carried out to evaluate the effect of contact time, effect of initial adsorbate concentration, effect of adsorbent dosage and the effect of pH on fluoride adsorption. 100 mL of a known F^- concentration was pipetted onto 250 mL plastic bottle and known mass of the smectite rich clay was suspended to the mixtures and then agitated for 30 min, on a table shaker to attain equilibrium except on the effect of contact time where time was varied. After agitation samples were then filtered using 0.45 µm pore filter membrane. Filtrates were analysed for residual fluoride using ion selective electrode calibrated with four standards containing 1 mL of total ionic strength buffer (TISAB III) per 10 mL of solution. Same ratio was maintained for the sample. TISAB was added to decomplex F^- from Al^{3+}, Fe^{3+} and Si^{4+} complex and to maintain pH at between 5.2 and 5.5 optimum for the F^- selective electrode. To evaluate the effect of contact time, the contact time was varied from 5 to 270 min. Effect of adsorbent dosage was evaluated by varying the adsorbent dosage from 0.1 to 2 g. To evaluate the effect of adsorbate concentration, the initial concentration was varied from 3 to 15 mg/L and to evaluate the effect of initial pH, the pH of the solution was adjusted from 2 to 12 using 0.1 M NaOH and 0.1 M HCl. The effect of competing ions was investigated by spiking a 3 mg/L F^- solution with 5 mg/L of SO_4^{2-}, Cl^-, CO_3^{2-} and NO_3^- separately, blank experiment was set for control with initial F^- concentration of 3 mg/L. Mixtures were agitated for 30 min. All experiments were carried out at

© University of Venda

room temperature. Equation 3.1 and 3.2 were used to calculate the percentage of removal and adsorption capacity respectively.

$$\%\, removal = \left(\frac{C_o - C_e}{C_o}\right) \times 100 \quad (3.1)$$

Where: C_o is initial fluoride ion concentration and C_e is equilibrium fluoride ion concentration in mg/L.

$$Q = \left(\frac{C_o - C_e}{m}\right) \times v \quad (3.2)$$

Where: C_i = initial F^- concentration (mg/L), C_e = F^- concentrations at equilibrium (mg/L),

V = Volume of solution (L) and m = Weight of the adsorbent (g)

3.2.5 Regeneration of smectite rich clay soils

Regeneration of the adsorbent was carried out as follows; 0.8 g of fluoride loaded clay was agitated with 100 mL of 0.1 M NaOH for 30 min on a table shaker. After agitation, the adsorbent was filtered through 0.45 µm pore membrane filter and the filtrate was diluted to 100 mL and then analysed for desorbed fluoride. The collected adsorbent on filter paper was washed with MILLIQ water and then dried at 110 °C for 3 hrs. Regenerated adsorbent was then re-used for defluoridation up to 5 times.

3.2.6 Method of analysis

The fluoride concentration in the treated water sample was measured using ion selective electrode 9609 BNWP Orion (USA) attached to Thermo Scientific Orion Star A215 ISE/pH meter. Similar ion meter coupled with pH electrode was used for measuring pH of the treated samples. Metrohm 850 professional IC was used to measure other anionic species concentrations. All experiments were conducted in triplicate for better accuracy and the mean values were reported.

© University of Venda

3.3 Results and discussion

3.3.1 Physicochemical and mineralogical characterization

3.3.1.1 X-ray diffraction analysis

XRD analyses were carried out to identify the mineral phase of the adsorbent. As shown in figure 3.1, the smectite rich clay soil is mainly composed of montmorillonite, quartz, albite and anthophyllite. The Quantitative results further confirms the presence of smectite (60.34%) as the major mineral and the presence of quartz (20.21%) and plagioclase (20.39%) as minor minerals.

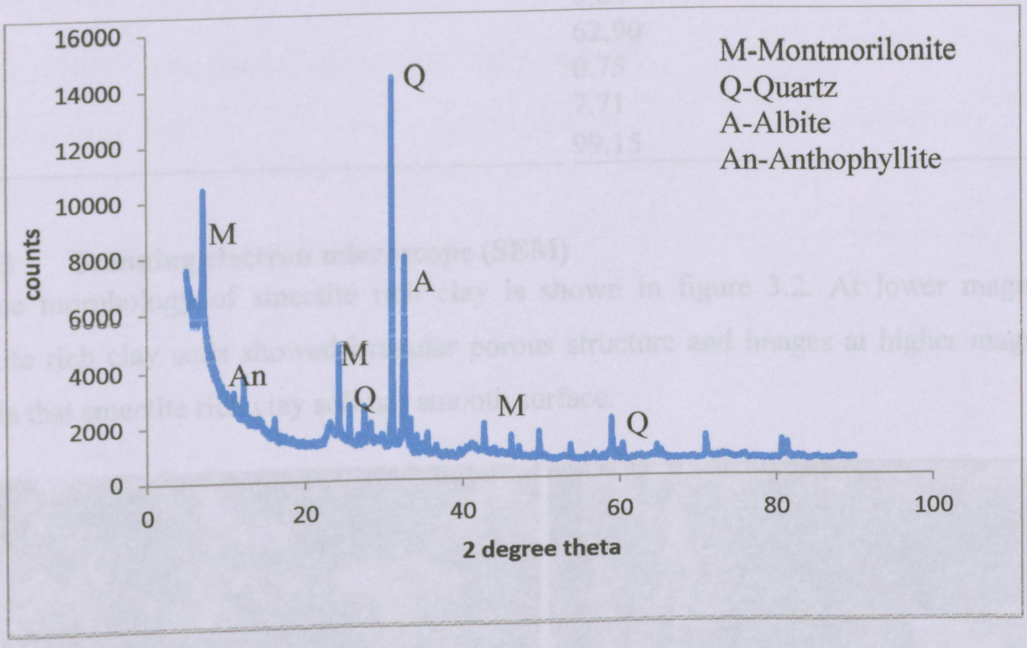

Figure 3.1: XRD spectra of the smectite clay soils.

3.3.1.2 X-ray fluorescence analysis

Table 3.1 presents the major elemental composition of smectite rich clay soils. The analysis reveals that silica (SiO_2) is the main component averaging 62.90% followed by Al_2O_3 with an average of 14.35%. High concentration of SiO_2 and Al_2O_3 reveal that the clay soil is an alumino-silicate material.

© University of Venda

University of Venda
Creating Future Leaders

Table 3.1: Elemental composition of the clay soils

Major elements	% composition
Al_2O_3	14.35
CaO	1.79
Cr_2O_3	0.02
Fe_2O_3	5.45
K_2O	0.93
MgO	2.79
MnO	0.08
Na_2O	2.52
P_2O_5	0.04
SiO_2	62.90
TiO_2	0.75
L.O.I	7.71
Total	99.15

3.3.1.3 Scanning electron microscope (SEM)

Surface morphology of smectite rich clay is shown in figure 3.2. At lower magnifications, smectite rich clay soils showed irregular porous structure and images at higher magnifications reveals that smectite rich clay soil has smooth surface.



Figure 3.2: Surface morphology of smectite rich clay.

UNIVERSITY OF VENDA
LIBRARY

© University of Venda

3.3.1.4 Surface area and pore volume

The surface area and pore size of the clay are the significant properties that influence the sorption of ions by the clay. Surface area, pore volume and pore size of smectite rich clay soil was determined using BET method and the results are summarized in Table 3.2. Figure 3.3 shows the distribution of pores of smectite rich clay soils, it was observed that the greatest amount of pores lies between 17.34 and 157.22 Å (1.73 nm and 15.72 nm) with the average of pore diameter of 70.457 Å (7.04 nm). This suggests that smectite rich clay contains significant amount of small pores ranging from microporous to mesoporous.

Table 3.2: BET surface area, pore volume and pore width.

Surface area (m^2/g)	Pore volume (cm^3/g)	Pore width (nm)
20.3437	0.03027	7.04

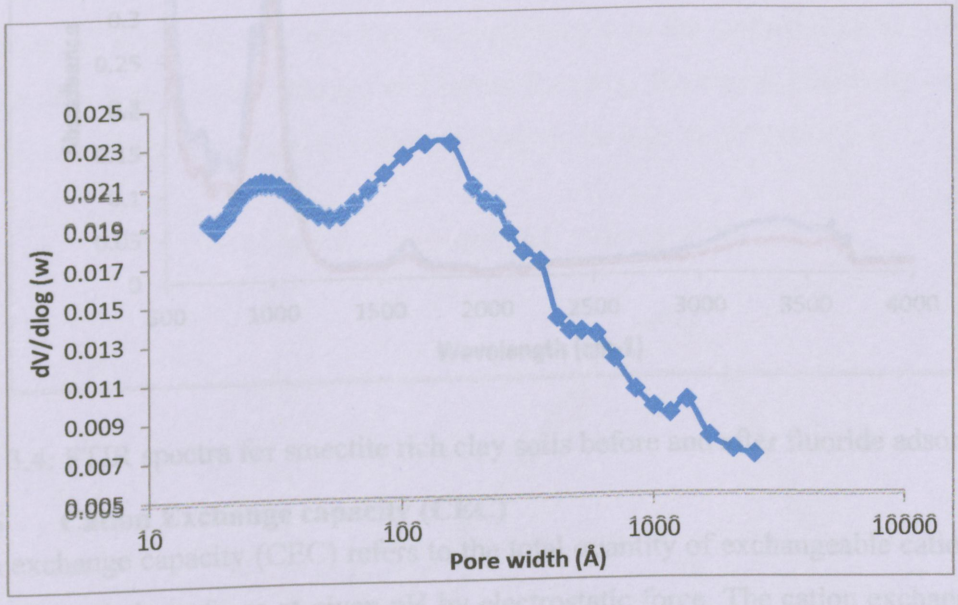

Figure 3.3: Pore distribution of smectite rich clay soils.

3.3.1.5 FTIR

FTIR spectra analysis were carried out in order to understand the surface chemistry and functional groups of smectite rich clay soils and also to help in understanding of adsorption mechanism. Figure 3.4 shows the FTIR spectrum of raw and fluoride loaded smectite clay soil. The analysis shows three main absorption regions of smectite rich clay soils i.e., 3000-3800 cm^{-1}, 1300-1800 cm^{-1} and 500-1200 cm^{-1} the same absorbance bands were observed by Toor *et al.*

© University of Venda

(2014) in montmorillonite clay. A notable difference was observed in those regions in raw smectite clay soils and F^- loaded smectite clay soils. The absorption band at 3694.38 cm^{-1} may be due to stretching and vibration of structural OH^- group and the broad band at 3620.51 cm^{-1} may be attributed to the stretching and vibration of structural hydroxyl groups and water. In the lower frequencies, strong band at 996.06 was observed and it may be due to the stretching and vibration of Si-O groups in the clay mineral. IR peak at 910 may be attributed to stretching and vibration of Al-OH-Al. After F^- sorption there was a decrease in the intensity of absorbance in all the peaks. This confirms that the fluoride adsorption in smectite rich clay soils was mainly through interaction with OH groups and also direct interaction with the metal surface.

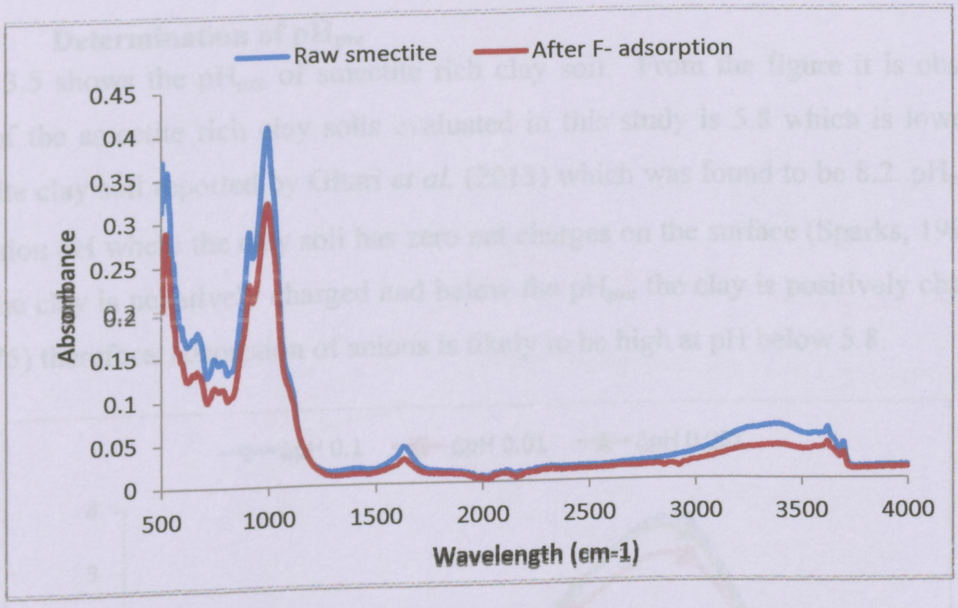

Figure 3.4: FTIR spectra for smectite rich clay soils before and after fluoride adsorption.

3.3.1.6 Cation Exchange capacity (CEC)

Cation exchange capacity (CEC) refers to the total quantity of exchangeable cations that the soil can retain on their surfaces at given pH by electrostatic force. The cation exchange capacity for smectite rich clay was identified by measuring the concentrations of Na^+, K^+, Mg^{2+} and Ca^{2+} in mg/L released in solution and the concentrations were then converted to milli-equivalent per 100 g (meq/100g). Table 3.3 shows the CEC of smectite rich clay soils at pH 5.4 and 7.4. The CEC for smectite rich clay soils was found to be 74.23 (meq/100 g) at pH 5.4 and it increased to 79.93 (meq/100 g) at pH 7.4. From the results it can be said that CEC is not dependent on pH since there is no significant difference in the concentration of cations at different pH. The results

© University of Venda

University of Venda
Creating Future Leaders

correlate with the results by Gitari *et al.* (2013) who also concluded that CEC is independent of pH. It can also be concluded that the clay soils have moderate CEC.

Table 3.3: CEC of smectite rich clay soils at pH 5.4 and 7.4

	Na^+	K^+	Mg^{2+}	Ca^{2+}	CEC (meq/100 g)
pH 5	10.15	3.3	34.6	26.18	74.23
pH 7	7.57	4.2	38.8	29.3	79.93

3.3.1.7 Determination of pH_{pzc}

Figure 3.5 shows the pH_{pzc} of smectite rich clay soil. From the figure it is observed that the pH_{pzc} of the smectite rich clay soils evaluated in this study is 5.8 which is lower than that of bentonite clay soil reported by Gitari *et al.* (2013) which was found to be 8.2. pH_{pzc} refers to the suspension pH where the clay soil has zero net charges on the surface (Sparks, 1997). Above the pH_{pzc} the clay is negatively charged and below the pH_{pzc} the clay is positively charged (Bohn *et al.*, 1975) therefore, adsorption of anions is likely to be high at pH below 5.8.

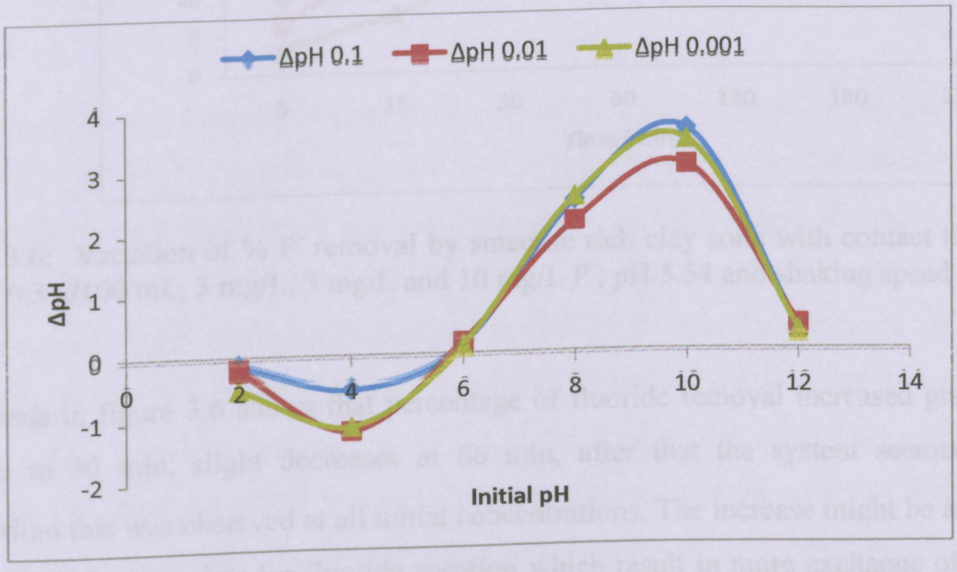

Figure 3.5: Variation of initial pH with ΔpH (0.1, 0.01 and 0,001 M KCl, dosage of 0.5 g/50 mL and shaking time of 48 hrs).

© University of Venda

University of Venda
Creating Future Leaders

3.3.2 Batch adsorption experiments

Batch experiments were carried out to evaluate the effects of contact time, adsorbent dosage, initial concentration, pH and co-existing ions in the adsorption of fluoride onto smectite rich clay soils.

3.3.2.1 Effect of contact time

The effect of contact time in adsorption of fluoride was evaluated at various initial concentrations ranging from 3 mg/L to 10 mg/L and adsorbent dosage of 0.3 g/100mL. Contact time was varied from 5 to 270 min at 250 rpm shaking speed. Figure 3.6 shows the plot of percentage fluoride removal with time.

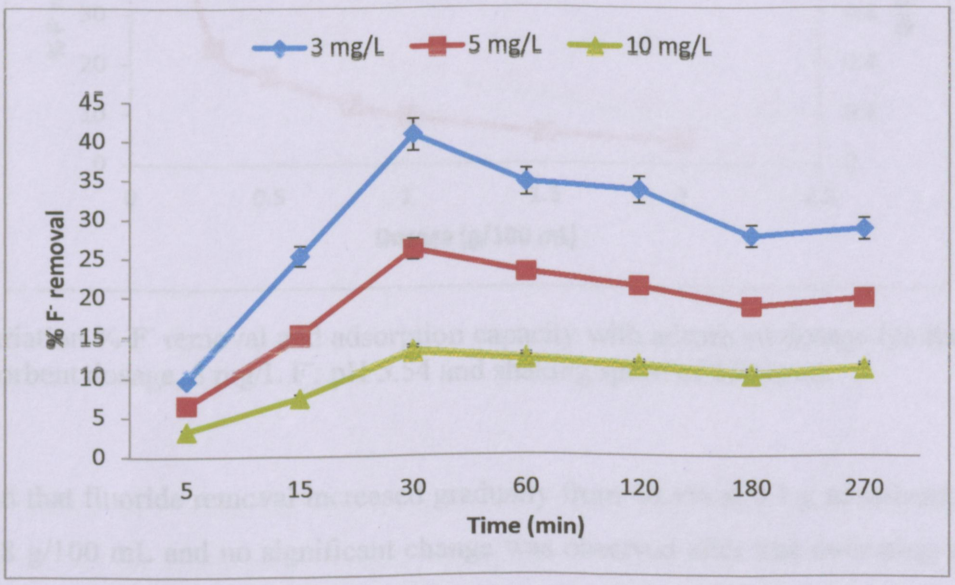

Figure 3.6: Variation of % F^- removal by smectite rich clay soils with contact time (adsorbent dosage 0.3 g/100 mL, 3 mg/L, 5 mg/L and 10 mg/L F^-, pH 5.54 and shaking speed of 250 rpm).

The trends in figure 3.6 shows that percentage of fluoride removal increased gradually from 5 min up to 30 min, slight decreases at 60 min, after that the system seemed to approach equilibrium this was observed at all initial concentrations. The increase might be attributed to the availability of active sites for fluoride sorption which result in more exchange of OH^- ions and the decrease might be an indication that the active sites were getting saturated as the interaction continued with the system reaching equilibrium. The % fluoride removal was observed to decrease with increase in initial fluoride concentration. Optimum fluoride uptake was observed at 30 min and this contact time was applied in subsequent experiments.

© University of Venda

University of Venda
Creating Future Leaders

3.3.2.2 Effect of adsorbent dosage

The effect of adsorbent dosage was evaluated by varying the amount of clay from 0.1 to 2.0 g/ 100 mL. The initial fluoride of 3 mg/L was used. The mixtures were agitated for 30 min at 250 rpm shaking speed. The results were reported as percentage fluoride removal in figure 3.7.

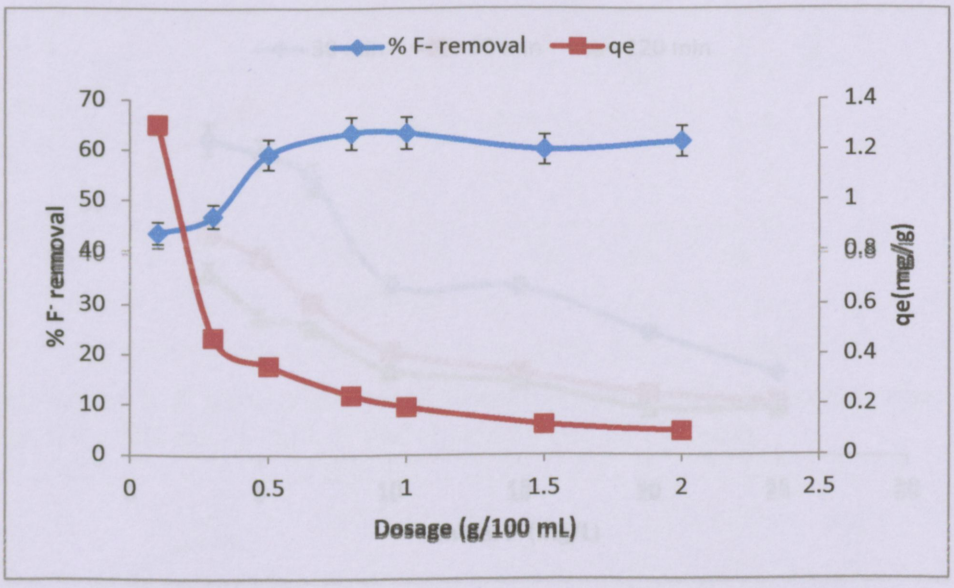

Figure 3.7: Variation % F^- removal and adsorption capacity with adsorbent dosage (contact time of 30 min, adsorbent dosage, 3 mg/L F^-, pH 5.54 and shaking speed of 250 rpm).

It was observed that fluoride removal increased gradually from 46.5% at 0.1 g adsorbent dosage to 62.2% at 0.8 g/100 mL and no significant change was observed after that indicating that the system had reached equilibrium and that increased adsorbent dosage did not have any further effect on adsorption of fluoride. The increase is due to an enhancement in the number of adsorption active sites available for adsorption of F^- as the adsorbent mass increased (Thakre *et al.*, 2010). Adsorption capacity on the other hand decreased with increase in adsorbent dosage. Similar results have been reported by Kamble *et al.* (2009) with chemically modified bentonite for which they have cited two reasons: (i) better utilization of the available active sites at low adsorbent dose in comparison to high adsorbent dose where too many sites are available for limited quantity of adsorbate, (ii) reduced driving force for adsorption as high adsorbent dose causes lower equilibrium fluoride concentration. 0.8 g/100 mL was then chosen as the optimum adsorbent dosage and was applied in subsequent experiments.

UNIVERSITY OF VENDA
LIBRARY

© University of Venda

3.3.2.3 Effect of initial adsorbate concentration

Effect of adsorbate concentration was evaluated by varying initial concentration from 3 mg/L to 15 mg/L at 30, 60 and 120 min contact time at 250 rpm shaking speed and 0.8 g/100 mL. Results were reported in terms of percentage removal in figure 3.8.

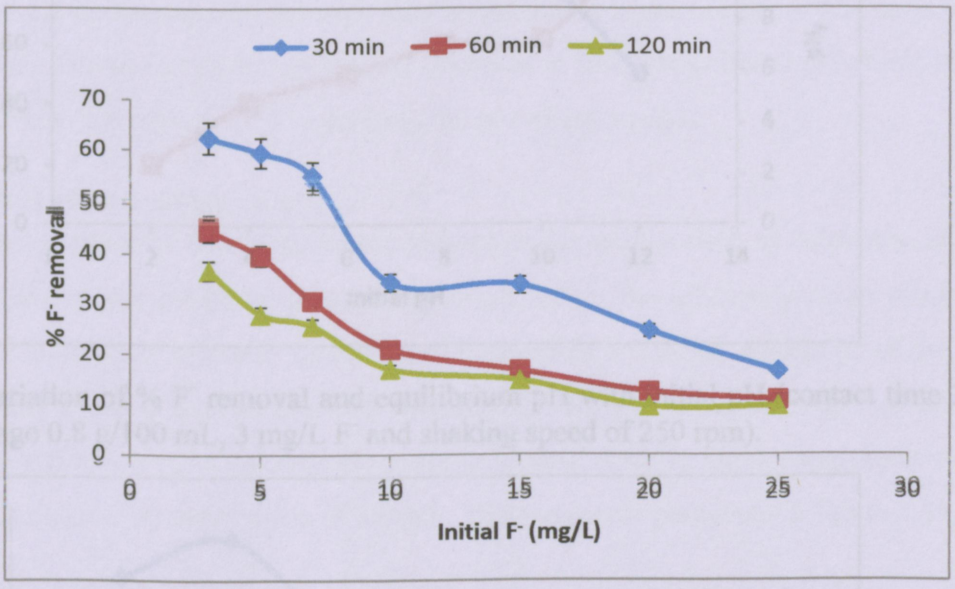

Figure 3.8: Variation of % F^- removal with initial concentration at various contact time (adsorbent dosage 0.8 g/100 mL, pH 5.54 and shaking speed of 250 rpm).

It is observed that the % F^- removal decreased with an increase in initial concentration, same trend was observed for the three contact times. According to Thakre *et al.* (2010), the decrease in fluoride adsorption is due to the availability of more fluoride ions in solution at higher fluoride concentration, which also indicates that the fluoride binding capacity of smectite rich clay soil was getting exhausted. Initial adsorbate concentration of 3 mg/L was chosen to be the optimum concentration for subsequent experiments.

3.3.2.4 Effect of initial pH

Effect of initial pH was evaluated by varying the initial pH of the solution from 2 to 12 using 0.1 M NaOH and 0.1 M HCl. The results are presented in figure 3.9 in terms of percentage fluoride removal and figure 3.10 shows the change in pH during adsorption.

© University of Venda

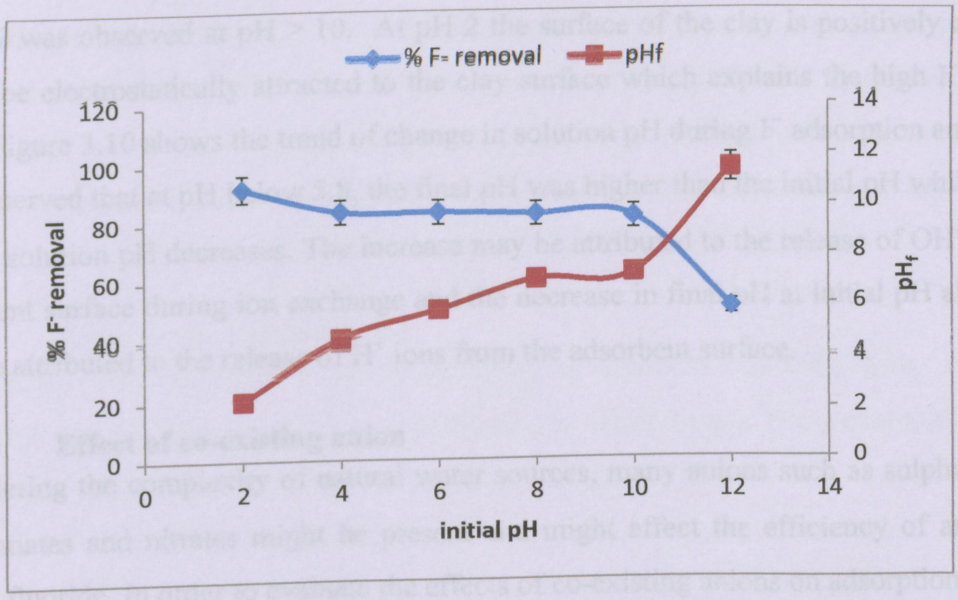

Figure 3.9: Variation of % F^- removal and equilibrium pH with initial pH (contact time 30 min, adsorbent dosage 0.8 g/100 mL, 3 mg/L F^- and shaking speed of 250 rpm).

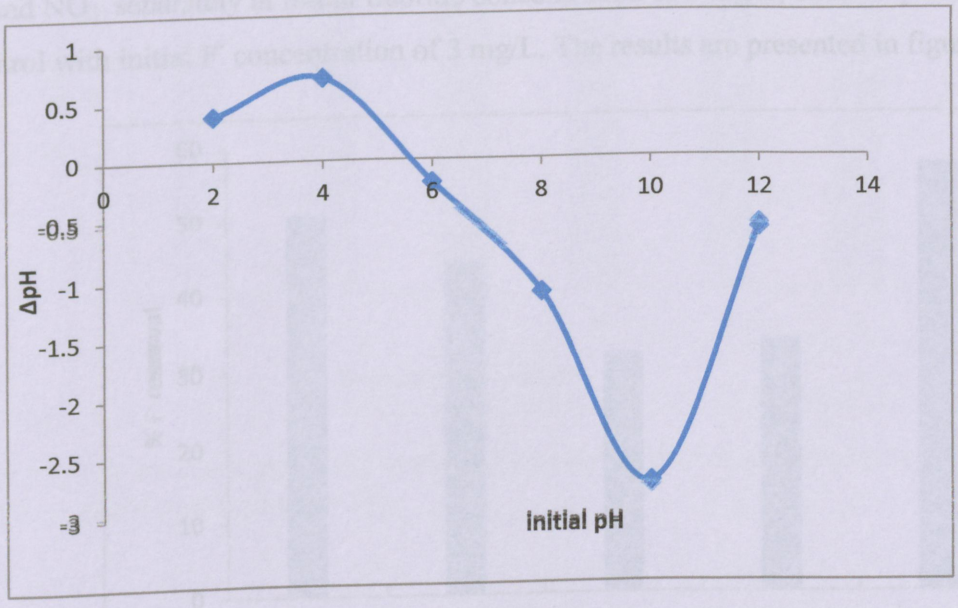

Figure 3.10: Variation of ΔpH with initial pH during F^- adsorption onto smectite rich clay soils.

pH of the medium is one of the important parameters that influence fluoride removal efficiency significantly and helps in the understanding of fluoride uptake mechanism of the adsorbent (Loganathan *et al.*, 2013). From the results presented in figure 3.9 it is evident that smectite rich clay showed significantly high fluoride removal efficient over a wide range of pH, from 2 to 10. The optimal pH was at acidic pH of 2 with fluoride removal of about 91.89%. Decline by

© University of Venda

University of Venda

31.33% was observed at pH > 10. At pH 2 the surface of the clay is positively charged and F^- would be electrostatically attracted to the clay surface which explains the high F^- adsorption at pH 2. Figure 3.10 shows the trend of change in solution pH during F^- adsorption and initial pH. It was observed that at pH below 5.8, the final pH was higher than the initial pH while at pH above 5.8 the solution pH decreases. The increase may be attributed to the release of OH^- ions from the adsorbent surface during ion exchange and the decrease in final pH at initial pH above the pH_{pzc} may be attributed to the release of H^+ ions from the adsorbent surface.

3.3.2.5 Effect of co-existing anion

Considering the complexity of natural water sources, many anions such as sulphates, chlorides, bicarbonates and nitrates might be present and might affect the efficiency of an adsorbent to adsorb fluoride. In order to evaluate the effects of co-existing anions on adsorption of fluoride by smectite rich clay soils, defluoridation was conducted in the presence of 5 mg/L of SO_4^{2-}, Cl^-, CO_3^{2-} and NO_3^- separately at initial fluoride concentration of 3 mg/L, blank experiment was done for control with initial F^- concentration of 3 mg/L. The results are presented in figure 3.11.

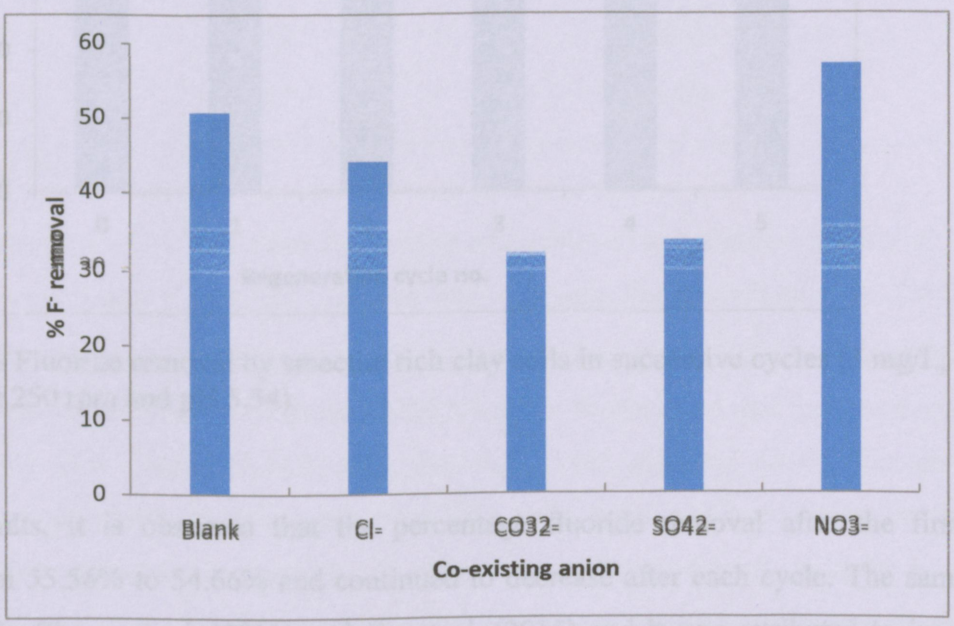

Figure 3.11: Effects of co-existing anions on fluoride removal by smectite rich clay soils (3 mg/L F^-, 0.8 g/100 mL adsorbent dosage, 30 min contact time at 250 rpm).

From the results it is observed that presence of NO_3^- increased the percentage of fluoride removal to 57%. This may be due to an increase in the ionic strength of the solution or a

© University of Venda

weakening of lateral repulsion between adsorbed fluoride ions. However, the presence of Cl^-, SO_4^{2-} and CO_3^{2-} decreased the fluoride adsorption to 44%, 33.33% and 31.66% respectively; this may be due to the fact that these ions compete with fluoride ions for the surface functional groups on adsorbent surface and thereby decreasing the fluoride removal. Fluoride removal in the presence of anions increased in the order of $CO_3^{2-}>SO_4^{2-}>Cl^->NO_3^-$.

3.3.2.6 Regeneration of adsorbent

To evaluate the regeneration and recyclability of smectite rich clay soils, five successive adsorption and desorption cycles were performed at initial 3 mg/L F^- concentration, pH 5.54 and contact time of 30 min. The results are presented in figure 3.12.

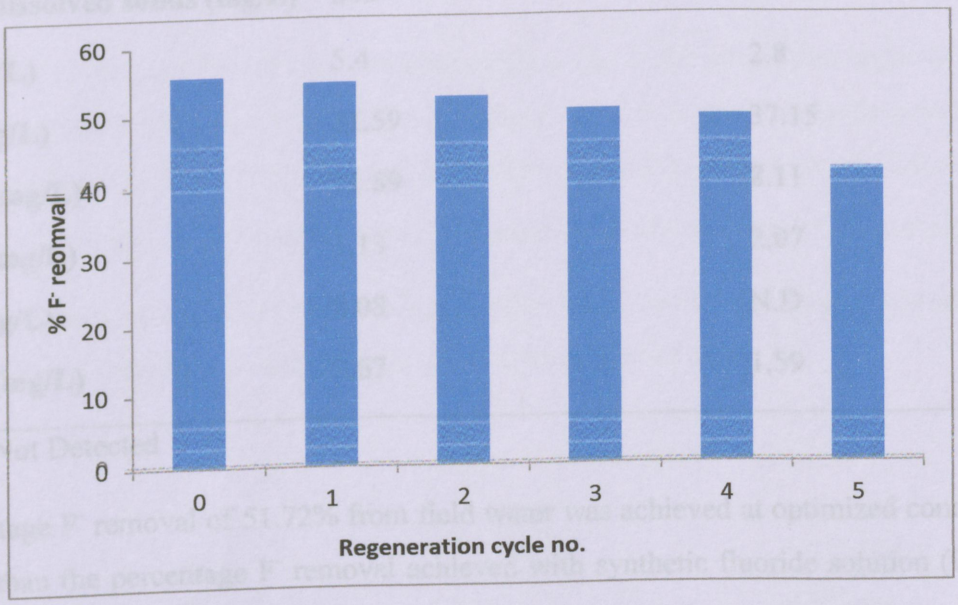

Figure 3.12: % Fluoride removal by smectite rich clay soils in successive cycles (3 mg/L, 30 min contact time at 250 rpm and pH 5.54).

From the results, it is observed that the percentage fluoride removal after the first cycle decreased from 55.56% to 54.66% and continued to decrease after each cycle. The same trend was reported in Zhang *et al.* (2011) and Jia *et al.* (2015) and it was attributed to inadequate regeneration of the adsorbent.

3.3.3 Defluoridation of field water

The efficiency of smectite rich clay soils on fluoride removal was tested by using field groundwater collected from Siloam borehole at the established optimum conditions of pH,

© University of Venda

University of Venda
Towards Future Excellence

contact time, and adsorbent dosage. The experiment was conducted at optimized pH (pH 2). Table 3.4 shows physicochemical parameters of the field water before and after treatment.

Table 3.4: Physicochemical parameters of field water before and after treatment

Parameters	Before treatment	After treatment (initial pH adjusted to 2)
pH	7.8	2.68
Conductivity (µS/cm)	192.0	140.0
Total dissolved solids (mg/L)	203	135.2
F^- (mg/L)	5.4	2.8
Cl^- (mg/L)	31.59	37.15
SO_4^{2-} (mg/L)	11.89	8.11
NO_3^- (mg/L)	1.13	2.07
Br^- (mg/L)	2.08	N.D
PO_4^{3-} (mg/L)	2.67	1.59

N.D= Not Detected

Percentage F^- removal of 51.72% from field water was achieved at optimized conditions. This is lower than the percentage F^- removal achieved with synthetic fluoride solution (91.89%) at the same conditions. This may have been due to the presence of competing anions such as Br^-, PO_4^{3-} and SO_4^{2-} present in the field water. From Table 3.4 it can be observed that the concentration of these co-existing ions decreased indicating that they were adsorbed during the adsorption process. The results shows that smectite rich clay soils from mukondeni can be used for defluoridation for groundwater containing F^- concentration below 3 mg/L in order to achieve recommended limit of 1.5 mg/L. However the fact that it removed high percentage at lower pH may be the limitation in its application since it will require the acidification of water before treatment.

© University of Venda

University of Venda
Creating Future Leaders

3.4 Adsorption modelling

Langmuir and Freundlich equations are generally used to describe the equilibrium relationship between adsorbate concentration and amount of adsorbate adsorbed on the surface of the surface of the adsorbent. Langmuir adsorption isotherm is the most applicable isotherm commonly applied in solid/liquid system to describe saturated monolayers sorption (Sun *et al.*, 2011). It assumes that the adsorbent surface is uniform, i.e., all the adsorption sites are equivalent and adsorption molecules do not interact (Zhang *et al.*, 2011). The linear equation of Langmuir adsorption is expressed by equation 3.3 as follows:

$$\frac{C_e}{Q_e} = \frac{1}{Q_m b} + \frac{C_e}{Q_m} \qquad (3.3)$$

Where, C_e is the equilibrium concentration (mg/L), Q_e is the adsorption capacity (mg/g), Q_m is theoretical maximum adsorption capacity (mg/g) and b is the Langmuir constant related to enthalpy of adsorption (L/mg). Q_m and b are determined from the slope and intercept of the plot of $\frac{C_e}{Q_e} Vs\ C_e$. Figure 3.13 shows the plot of Langmuir isotherm. The Langmuir plots at different contacts time gave a straight line and higher correlation coefficient value suggesting a better fit. The values of Langmuir parameters Q_m and b are reported in Table 3.5.

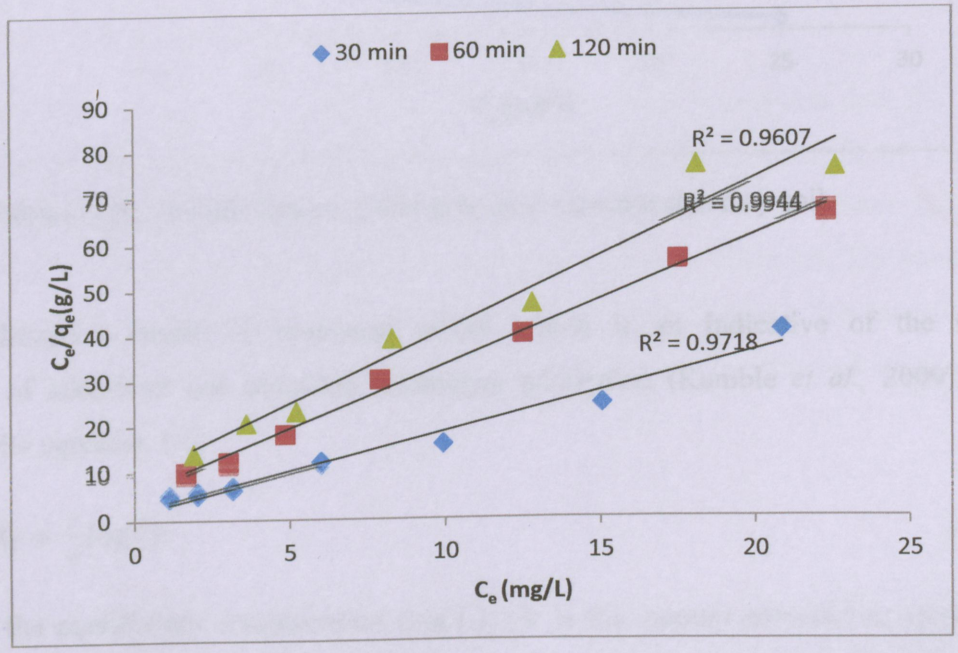

Figure 3.13: Langmuir isotherm (contact time 30 min, 60 min, 120 min, adsorbent dosage 0.8 g/100 mL and shaking speed of 250 rpm).

© University of Venda

University of Venda

In order to predict the adsorption efficiency of the process, the dimensionless equilibrium parameter (R_L) was calculated using the equation 3.4:

$$R_L = \frac{1}{1+bC_o} \quad (3.4)$$

Where C_o is the initial concentration and b is the Langmuir constant. The value of R_L less than 1 generally indicate favourable adsorption and greater than 1 indicate unfavourable adsorption. Calculated R_L values at various contact times in figure 3.14 lie within the range 0 – 1 indicating adsorption process was favourable at room temperature for all the adsorbate concentrations tested.

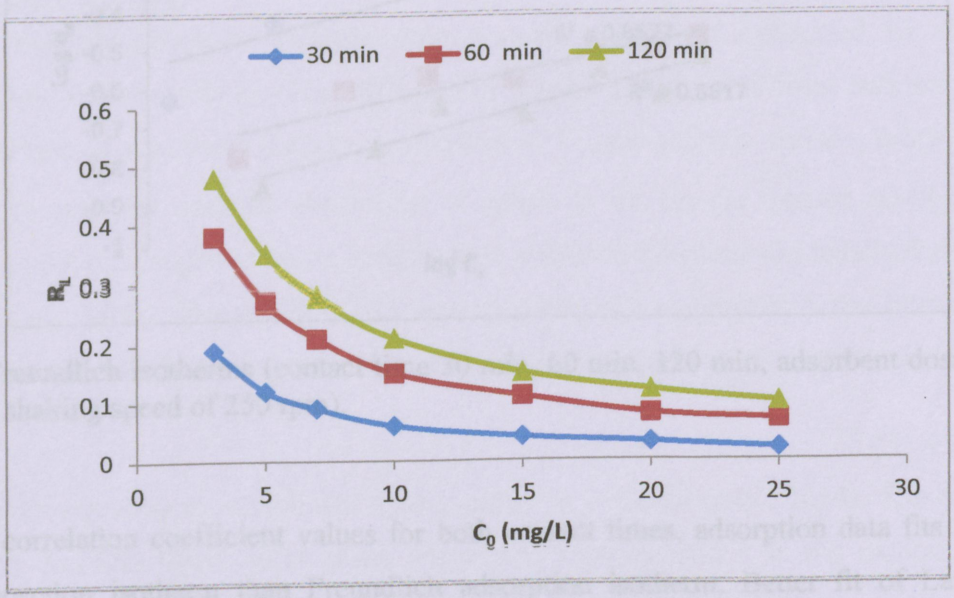

Figure 3.14: Values of R_L, for adsorption of fluoride onto smectite rich clay soil.

Freundlich adsorption model is empirical model which is an indicative of the surface heterogeneity of adsorbent and considers multilayer adsorption (Kamble *et al.*, 2009). It is expressed by the equation 3.5:

$$\log Q_e = \log K_f + \frac{1}{n}\log Ce \quad (3.5)$$

Where, Ce is the equilibrium concentration (mg/L), Qe is the amount adsorbed at equilibrium (mg/g), K_f is the Freundlich constant related to adsorption capacity and represents the strength of adsorptive bonds and $1/n$ is the adsorption intensity. When $0 < 1/n < 1$, the adsorption is

© University of Venda

University of Venda

favourable; when $1/n = 1$, the adsorption is irreversible; and when $1/n > 1$, the adsorption is unfavourable. The value of K_f and $1/n$ are obtained from the slope and intercepts of a linear plot of log Q_e vs log C_e. Figure 3.15 shows Freundlich isotherm. Values of K_f and $1/n$ are reported in Table 3.5.

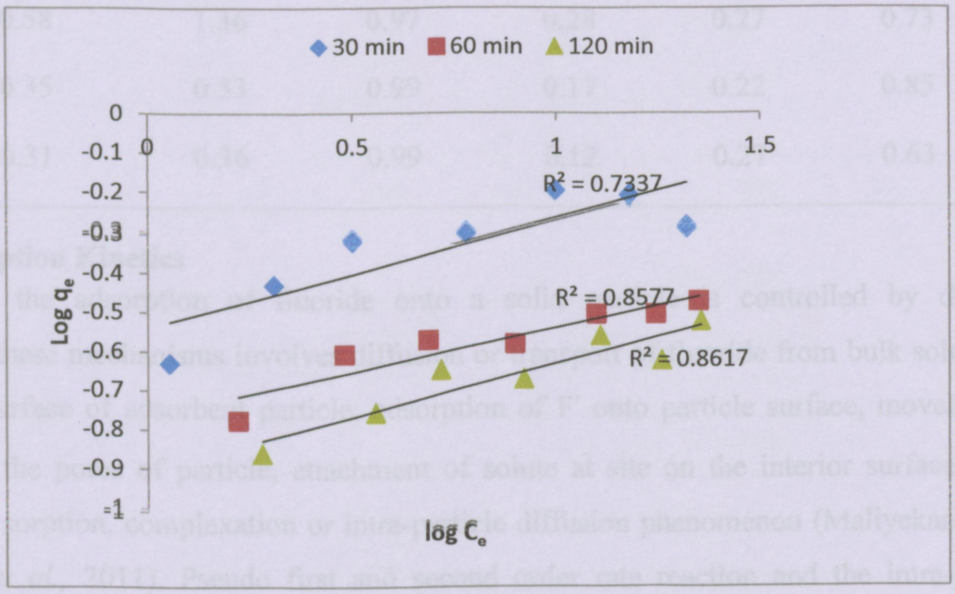

Figure 3.15: Freundlich isotherms (contact time 30 min, 60 min, 120 min, adsorbent dosage 0.8 g/100 mL and shaking speed of 250 rpm).

Based on the correlation coefficient values for both contact times, adsorption data fits well to Langmuir adsorption isotherm than Freundlich adsorption isotherm. Better fit of Langmuir isotherm model suggests monolayer uniform adsorption on the surface of adsorbent. Calculated model constants for Langmuir and Freundlich isotherms are shown in Table 3.5. The value of R_L, dimensionless equilibrium parameter and the value of $1/n$ Freundlich adsorption intensity were both between 0 and 1, which indicate that the adsorption of F^- onto smectite rich clay soil was favourable.

© University of Venda

University of Venda

Table 3.5: Values of Langmuir and Freundlich isotherm models (contact time 30 min, adsorbent dosage 0.8 g/100 mL and shaking speed of 250 rpm).

	Langmuir isotherm			Freundlich isotherm		
	Q_m (mg/g)	b (L/mg)	R^2	K_f (mg/g)	1/n	R^2
30 min	0.58	1.36	0.97	0.28	0.27	0.73
60 min	0.35	0.53	0.99	0.17	0.22	0.85
120 min	0.31	0.36	0.99	0.12	0.27	0.63

3.5 Adsorption Kinetics

Theoretically, the adsorption of fluoride onto a solid particle is controlled by different mechanisms, these mechanisms involves diffusion or transport of fluoride from bulk solution to the exterior surface of adsorbent particle, adsorption of F^- onto particle surface, movement of solute within the pores of particle, attachment of solute at site on the interior surface of the adsorbent via sorption, complexation or intra-particle diffusion phenomenon (Maliyekaal *et al.*, 2006; Chen *et al.*, 2011). Pseudo first and second order rate reaction and the intra-particle diffusion models are widely used to elucidate the adsorption mechanisms and the rate limiting factors.

Pseudo first order equation is represented by equation 3.6 (Oladoja *et al.*, 2014). The model is widely used to describe liquid–solid phase adsorption systems, and it is the earliest known kinetic model describing the adsorption rate based on the adsorption capacity

$$\log(q_e - q_t) = \log(q_e) - \frac{k_{ad}t}{2.303} \tag{3.6}$$

Pseudo second order is represented by the linear equation 3.7 and it is used to describe chemisorption, as well as cation exchange reactions.

$$\frac{t}{q_t} = \frac{1}{K_{2ads}q_e^2} + \frac{1}{q_e}t \tag{3.7}$$

Where q_e and q_t (both in mg/g) are the amount adsorbed per unit mass at a time, t (in min). K_{ad} (min^{-1}) and K_{2ads} ($g.mg^{-1}/min$) are first and second order rate constant ($g.mg^{-1}/min$). The value of K_{ad} is determined from the slope and intercepts of log ($q_e - q_t$) vs t (min) and the value of K_{2ads} is determined from the slope and intercepts of t/q_t vs t. Figure 3.16 and 3.17 shows plots of pseudo

© University of Venda

University of Venda

first and second order respectively. The plots of pseudo second order yielded straight lines and higher correlation coefficient at both concentrations. The plots of pseudo first order did not give straight lines, this shows that adsorption of fluoride onto smectite rich clay soils followed pseudo second order and it occurred through chemisorption. Model constants for pseudo first and second order are presented in Table 3.6.

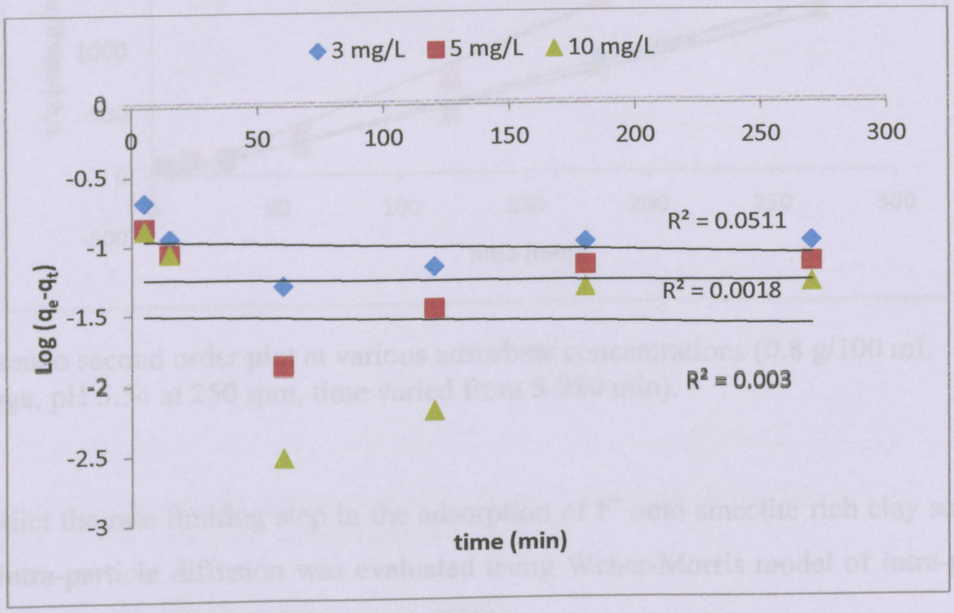

Figure 3.16: Pseudo first order plot at various adsorbate concentrations (0.8 g/100 mL adsorbent dosage, pH 5.54 at 250 rpm, time varied from 5-280 min).

© University of Venda

University of Venda
Creating Future Leaders

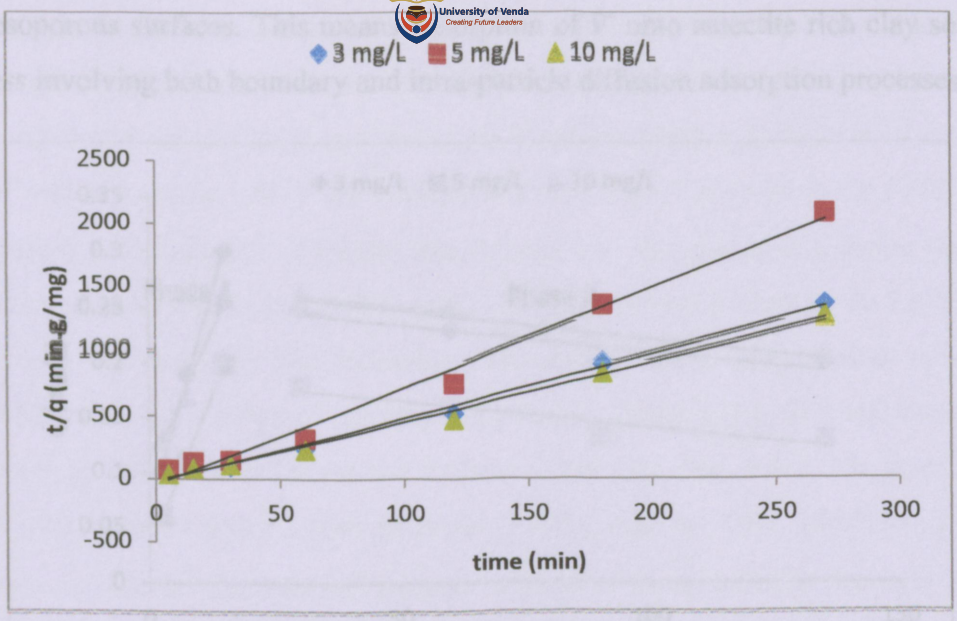

Figure 3.17: Pseudo second order plot at various adsorbate concentrations (0.8 g/100 mL adsorbent dosage, pH 5.54 at 250 rpm, time varied from 5-280 min).

In order to predict the rate limiting step in the adsorption of F^- onto smectite rich clay soils, the possibility of intra-particle diffusion was evaluated using Weber-Morris model of intra-particle diffusion expressed by equation 3.8 (Chen *et al.*, 2011).

$$q_t = K_i t^{0.5} \qquad (3.8)$$

Where q_t is the amount adsorbed ($mg.g^{-1}$) at a given time t (min), K_i ($mg\ g^{-1}\ min^{-1}$) is the intra particle diffusion rate constant and is determined from the slope of $t^{0.5}$ vs q_t. Figure 3.18 shows the plot of the amount of fluoride adsorbed and $t^{0.5}$. The intercept did not pass through the origin at each of the evaluated concentrations and the data showed a bilinear plot, with the initial portion (phase 1) indicating the boundary layer diffusion and the other represents the intra-particle diffusion (phase 2) and the values of K_{i1} and K_{i2} (intra-particle diffusion co-efficient rate constant for phase 1 and phase 2 respectively) obtained from the plot are shown in Table 3.6. At both initial concentrations, the K_{i1} value is higher than the K_{i2} value, suggesting that the initial sorption step is rapid than the final step (phase 2), which may be due to difference in the rate of mass transfer in the initial and final stages of adsorption (Jia *et al.*, 2015). This observation is connected to a mechanism consisting of an external mass transfer followed by diffusion into

© University of Venda

micro- and mesoporous surfaces. This means adsorption of F^- onto smectite rich clay soils is a complex process involving both boundary and intra-particle diffusion adsorption processes.

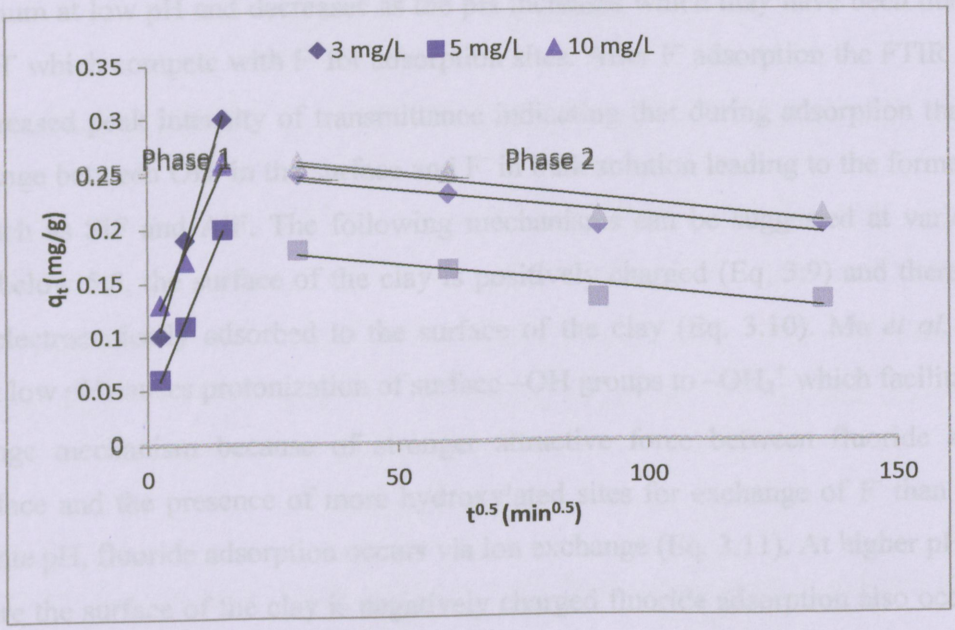

Figure 3.18: Plot for intra-particle diffusion at various concentrations (0.8 g/100 mL, pH 5.54 and shaking speed of 250 rpm time varied from 5-280 min).

Table 3.6: Calculated adsorption kinetics model values.

		Pseudo first order		**Pseudo second order**			**Intra-particle diffusion**	
	$q_{e(exp)}$ (mg/g)	K_{ad} (min^{-1})	R^2	K_{2ad} ($g.mg^{-1}$ min^{-1})	$q_{e(cal)}$ (mg/g)	R^2	K_{i1}	K_{i2}
3 mg/L	0.19	$1.15x10^{-3}$	0.05	0.986	0.23	0.99	0.015	-0.005
5 mg/L	0.13	$2.3x10^{-4}$	0.001	1.13	0.2	0.98	0.01	-0.005
10 mg/L	0.21	$6.9x10^{-4}$	0.003	1.12	0.21	0.99	0.011	-0.005

3.6 Mechanistic aspect of adsorption of F^- onto smectite rich clay soils

Mechanism of fluoride adsorption onto smectite rich clay was evaluated by comparing the FTIR spectra of smectite rich clay soils before and after adsorption (Fig 3.4). FTIR spectra showed that the clay soils surface is mainly characterised by Si-OH and Al-OH groups which may be easily modified by changing the pH of the medium. pH_{pzc} determination showed that at pH 5.8

© University of Venda

University of Venda

(Fig.3.5) the surface has neutral charge, below pHzpc surface is positively charged and above that it is negatively charged. Figure 3.9 showed that the adsorption of F^- onto smectite rich clay soil was optimum at low pH and decreases as the pH increases which may have been due to the increase in OH^- which compete with F^- for adsorption sites. After F^- adsorption the FTIR spectra showed a decreased peak intensity of transmittance indicating that during adsorption that there was ion exchange between OH^- in the surface and F^- in bulk solution leading to the formation of new bonds such as SiF and AlF. The following mechanisms can be suggested at various pH levels; at pH below 5.8, the surface of the clay is positively charged (Eq. 3.9) and therefore F^- ions will be electrostatically adsorbed to the surface of the clay (Eq. 3.10). Ma *et al.* (2012) suggested that low pH causes protonization of surface –OH groups to $–OH_2^+$ which facilitates the ligand exchange mechanism because of stronger attractive force between fluoride and the adsorbent surface and the presence of more hydroxylated sites for exchange of F^- than at high pH. At moderate pH, fluoride adsorption occurs via ion exchange (Eq. 3.11). At higher pH above the pH_{pzc} where the surface of the clay is negatively charged fluoride adsorption also occurs via ion exchange (Eq. 3.12).

$$\equiv M(OH)_2 + H^+ \leftrightarrow \equiv MOH_3^+ \quad (3.9)$$

$$\equiv MOH + H_3O^+ + F^- \leftrightarrow \equiv MOH_2^+ - F^- + H_2O \quad (3.10)$$

$$\equiv MOH + F^- \leftrightarrow MF + OH^- \quad (3.11)$$

$$\equiv M(OH)_2^- + 2F^- \leftrightarrow MF_2 + 2OH^- \quad (3.12)$$

Where ≡M represent Si and Al in the adsorbent surface.

3.7 Comparison of fluoride adsorption capacity of smectite rich clay soils with other adsorbents

Comparison of adsorption capacity of smectite rich clay soils with adsorption capacities of other developed adsorbents is presented in Table 3.7. From Table 3.7 it is observed that smectite rich clay soil has lower adsorption capacities compared to other fluoride adsorbents developed. Therefore its surface modification will be essential to improve its adsorption capacity.

© University of Venda

University of Venda

Table 3.7: Comparison of different adsorption capacities of different adsorbents for fluoride.

Adsorbent	Adsorption capacity (mg/g)	Experimental conditions	Reference
Al/Fe granular ceramic adsorbent	1.79	pH 6, 10 mg/L F^-	Chen *et al.*, (2011)
Fe^{3+} zeolite	2.31	pH 6.94, 10 mg/L F^-	Sun *et al.*, (2011)
Red mud	0.6	pH 3-4. 20 mg/L F^-	Lv *et al.*, (2012)
La^{3+} Bentonite/chitosan beads	2.31	pH 5, 10 mg/L F^-	Yi *et al.*, (2014)
Smectite rich clay soils	0.34	pH 2, 3 mg/L F^-	Present study

3.8 Conclusions

This study assessed the use of smectite rich clay soils from Mukondeni in defluoridation of groundwater, the following major conclusion were made:

- Mineralogy of the clay is mainly smectite with traces of quartz
- X-ray fluorescence analysis showed that the main components in the clay soils are SiO_2 Al_2O_3, minor components include CaO, Na_2O, MgO and traces of K_2O TiO_2 and MnO
- SEM showed that the morphology of smectite rich clay soils is smooth and is porous in nature
- BET showed that the adsorbent has a surface area of about 20.34 m^2/g and average pore diameter of 7.045 nm hence its mesoporous in nature
- Optimum conditions for F^- adsorption were evaluated and found to be 30 min contact time at 250 rpm shaking speed on a table shaker, adsorbent dosage of 0.8 g /100 mL, 3 mg/L adsorbate concentration and pH of 2. Fluoride removal at optimum conditions was ≈91.89% for 3 mg/L initial concentration.
- Regeneration study revealed that smectite rich clay soils can be successfully regenerated using 0.1 M NaOH
- Adsorption isotherms showed that the data fits well to Langmuir isotherm than to Freundlich isotherm suggesting that adsorption of fluoride occurred on a monolayer surface

© University of Venda

- Kinetic modelling showed that the data fitted to pseudo second order than to pseudo second order suggesting that the adsorption occurs via chemisorption.
- The data did not fit well to intra-particle diffusion model of Weber-Morris and showed bilinear plot which showed that the adsorption of fluoride onto smectite rich clay soils is a complex process
- Ligands exchange and ion exchange mechanism of F^- adsorption was suggested to be the main mechanism taking place during the adsorption process
- Field water defluoridation experimental results showed that smectite rich clay soil is a potential candidate material for defluoridation of groundwater.

© University of Venda

University of Venda
Creating Future Leaders

References

Bohn, H. L. Mcneal, B. L. & O'connor, G., 1975. Soil chemistry. *A Wiley-interscience publication*. New York: John Wiley and Sons.

Chen, N., Zhang, Z., Feng C., Li M., Zhu D., Sugiura N., 2011. Studies on fluoride adsorption of iron-impregnated granular ceramics from aqueous solution., *Journal of material and physics*, 125,pp 293-298.

Coetzee P. P., Coetzee , L. L. & Mubeng, S., 2003. Characterization of selected South African clays for defluoridation of natural water. *Water S.A.* 29(3), pp.331-338

Dacosta, F. A. Muzerengi, C. Mhlongo, S. E. & Mukwevho, G. F., 2013. Characterization of clays for making ceramic pots and water filters at Mukondeni village, Limpopo province, South Africa. *ARPN Journal of Engineering and Applied Sciences,* 08 (11), pp. 927- 932.

Department of Water Affairs and Forestry (DWAF). 1996. South African Water Quality Guidelines for Domestic Use, 1st ed., Department of Water Affairs and Forestry, Pretoria. Available from: www.dwaf.gov.za.

Ghorai, S., & Pant, K. K., Investigations on the column performance of fluoride adsorption by activated alumina in a fixed-bed, Chem. Eng. J. 98 (2004) 165–173.

Gitari W. M., Ngulube T, Masindi V., & Gumbo J. R., 2013. Defluoridation of groundwater using Fe^{3+}- modified bentonite clay: Optimization of adsorption condition. *Desalination & water treatment*., pp. 1-13.

Jia Y., Zhu B. S., Zhang K. S., Jin Z., Luo T., Yu X. Y., Kong., L. T., & Liu J. H., 2015. Porous 2-line ferrihydrite/byerite composite (LFBC): Fluoride removal performance and mechanism. *Chemical Engineering Journal,* 268, pp. 325-336.

Kamble, S. Dixit, P. Rayalu, S. S. & Labhsetwar, N. K., 2009. Defluoridation of drinking water using chemically modified bentonite clay. *Desalination and water treatment journal,* 249, pp.687-693.

Loganathan, P., Vigneswaran, S., Kandasamy, J., & Naidu, R., 2013. Review: Defluoridation of drinking water using adsorption processes. Journal of Hazardous Materials, 248 (249) pp.1–19.

Lv, G., Wu, L., Liao, L., Zhang, Y., Zhaohui, Y,. 2012. Preparation and characterization of red mud sintered porous materials for water defluoridation. *Journal of Applied Clay Science,* pp.1-7
Ma, Y. Wang, S. G, Fan, M. Gong, W. X. & Gao, B. Y., 2009. Characteristics and defluoridation performance of granular activated carbons coated with manganese oxides. *Journal of Hazardous Materials,* 168, pp.1140–1146.

Maliyekkal, S. M., Sharma, A. K., Philip, L., 2006. Manganese-oxide-coated alumina: a promising sorbent for defluoridation of water. *Water Resources*. 40, pp.3497–3506.

Meenakshi, S. K. & Maheshwari, R. C., 2006. Fluoride in drinking water and its removal. *Journal of Hazardous Matter,* 137(1), pp. 456-463

© University of Venda

University of Venda

Nagendra Rao, C. R., 2003. "Fluoride and Environment - A Review". In Martin J. B, Madha Suresh V, & Vasantha Kumaran, T., eds. *Proceedings of the Third International Conference on Environment and Health.* Chennai, India 15-17 December 2003. Department of Geography, University of Madras and Faculty of Environmental Studies, York University. pp. 386 – 399: Chennai.

Ncube, E. J., & Schutte, C. F., 2005. The occurrence of fluoride in South African groundwater: A water quality and health problem. *Water S.A*, 31 (1), pp. 35-40.

Oladoja N. A., Helmreich B., (2014) Batch defluoridation appraisal of aluminium oxide infused diatomaceous earth. *Chemical Engineering Journal*. 258: 51–61

Spark, D. L., 1997. *Environmental soil chemistry*. 2nd ed. Amsterdam: Academic Press.

Sun, Y., Fang, Q. Dong, J., Cheng X, & Xu, J., 2011. Removal of fluoride from drinking water by natural stilbite zeolite modified with Fe (III). *Desalination*, 277, pp. 121–127.

Susheela A. K., (2001) Treatise on Fluorosis, Fluorosis Research and Rural Development Foundation, India.

Thakre, D., Rayalu, S., Kawade, R,. Meshram, S., Subrt, J. & Labhsetwar, N., 2010. Magnesium incorporated Bentonite clay for defluoridation of drinking water. *Journal of Hazardous Materials,* 180, pp.122-130.

Toor M., Jin B., Dai S., Vimonoses V., 2014. Activating natural bentonite as a cost effective adsorbent for removal of Congo red in waste water, *J. industrial & engineering chemistry*, 1979, pp. 1-9.

Tyeryar, M., C. Hackett, D. Harsh and T. Hackett (2012). Establishing a ceramic water filter factory in Limpopo Province, South Africa. Public: 104-110.

Vhahangwele, M., Mugera, G. W., Tholiso, N., 2014. Defluoridation of drinking water using Al^{3+}-modified bentonite clay: optimization of fluoride adsorption conditions. Toxicol. Environ. Chem. 96, 1–16.

Wang, Y. & Reardon, E. J., (2001) Activation and regeneration of a soil sorbent for defluoridation of drinking water. *Appl. Geochem,* 16, pp. 531-539.

World Health Organzation, 2011. *Guideline for drinking water, world health organization.* Geneva.

Yi, Z., Ying, X., Hao, C., Bingjie, L., Xiang, G., Dongfeng, W. & Peng L. 2014. La(III)-loaded bentonite/chitosan beads for defluoridation from aqueous solution. *Journal of rare earths, vol. 32(5)*. pp.458-466.

Zhang, Z., Tan, Y. & Zhong, M., 2011. Defluoridation of wastewater by calcium chloride modified natural zeolite. *Desalination*, 276, pp. 246–252.

© University of Venda

University of Venda
Creating Future Leaders

Chapter 4: Intercalation of Mn^{2+} ions onto bentonite clay and its implication for groundwater defluoridation

Abstract

Fluorosis is a chronic disease caused by drinking water with fluoride concentration greater than 1.5 mg/L for extended periods of time. The disease is manifested by tooth decay in dental fluorosis and deformation of bones in skeletal fluorosis. World Health Organization (WHO) has set fluoride limits in drinking water at 1.5 mg/L. Most rural areas of South Africa depend on groundwater as source of drinking water, however groundwater in some of the boreholes has concentration of fluoride above the permissible limit and will require defluoridation. The present work aims at evaluating the use of Mn^{2+} intercalated bentonite clay for defluoridation of groundwater. Clay was characterized for mineralogy using x-ray diffraction (XRD) and elemental composition using x-ray fluorescence (XRF) and morphology using Scanning Electron Microscopy (SEM), Surface chemistry and functional groups using FTIR, surface area and pore structure using Brunauer Emmet Teller (BET) and BJH. pH point of zero charge (pH_{pzc}) and Cation Exchange Capacity (CEC) were determined using standard laboratory methods. Batch experiments were conducted to evaluate and optimize various operational parameters such as contact time, adsorbent dose, pH and initial adsorbate concentration. Optimum operation conditions for adsorption of fluoride were established to be 30 min contact time 1.0 g/100 mL adsorbent dosage, 3 mg/L adsorbate concentration and pH of 2. Maximum percentage F^- removal of 84.0% was achieved at optimized conditions. Regeneration using 0.1 M NaOH alkaline solution showed that Mn^{2+} can be regenerated up to 5 successive cycles. Assessment of chemical species leaching from the adsorbent at various pH levels showed that Mn^{2+} bentonite is safe for use in defluoridation and does not release secondary pollutants. The adsorption isotherm data fitted well to Langmuir model showing that the adsorbent is monolayer. Kinetic modelling showed that the data fitted well to pseudo second order than to the pseudo first order indicating that the rate limiting factor is chemisorption. Mn^{2+} intercalated bentonite clay removed ≈55.89% of fluoride from field water. The study shows that Mn^{2+} intercalated bentonite clay has potential for application in defluoridation of groundwater.

Key words: *Batch Experiments, fluorosis, bentonite clay, defluoridation, kinetics, isotherms.*

© University of Venda

University of Venda
Creating Future Leaders

4.1 Introduction

Fluoride in drinking water may have beneficial or harmful effects on human health depending on its concentration. Optimal concentration of fluoride in drinking water set by World Health Organization is at 1.5 mg/L (WHO, 2011). A concentration higher than this can lead to fluorosis. The disease is manifested by mottled teeth in dental fluorosis and deformation of bones in skeletal fluorosis (Coetzee *et al.*, 2003). Groundwater in many regions contains fluoride concentration greater than 1.5 mg/L and will therefore require defluoridation. Various techniques such as precipitation, co-precipitation, ion exchange and adsorption for defluoridation of groundwater have been reviewed by Meenakshi and Maheshwari (2006). Among these techniques, adsorption is widely used because of its viability and sustainability since it uses locally available and cost effective materials. It involves the passage of high fluoride water through an adsorbent bed, where fluoride is removed by physical ion-exchange or surface chemical reaction with adsorbent. In the previous chapter black smectite clay soils was used for fluoride removal. The clay showed low adsorption capacity of 0.34 mg/g at acidic initial pH of 2 and that limit its application for defluoridation of groundwater for drinking purpose. There is therefore need to develop a high adsorption capacity fluoride adsorbents based on locally available clay materials and that can operate at wide range pH. Thakre *et al.* (2010) reported that magnesium incorporated bentonite works effectively over a wide range of pH and showed a maximum fluoride removal capacity of 2.26 mg/g at an initial fluoride concentration of 5 mg/L, which is much better than the unmodified bentonite. Gitari *et al.* (2013) reported that Fe^{3+} modified bentonite exhibit ≈ 100% of fluoride removal from drinking water over a pH range of 2-10 at initial 10 mg/L F^- concentration while the unprocessed bentonite clay showed release of fluoride over the same range of pH. Vhahangwele *et al.* (2014) reported that Al^{3+} bentonite clay achieved maximum adsorption capacity of 5.7 mg/g from initial F^- concentration of 60 mg/L at pH 2. The objectives of the present work are as follows: (1) Physicochemical characterization of raw and Mn^{2+} modified bentonite, (2) to optimize the loading of Mn^{2+} onto raw bentonite inter-layers, and lastly (3) to evaluate the effect of various operating parameters (contact time, adsorbent dosage, adsorbate concentration and pH) on the adsorption capacity of F^- by Mn^{2+} modified bentonite clay.

© University of Venda

University of Venda
Creating Future Leaders

4.2 Materials and Methods

4.2.1 Sample collection

Bentonite clay used in this project was collected from ECCA pty (Ltd) in Cape Town. Field water was collected from a community borehole in Siloam, Vhembe district in South Africa. All reagents and total ionic strength adjustment buffer (TISAB-III) were obtained from Rochelle Chemicals & Lab Equipment CC, South Africa Ltd. A stock solution containing 1000 mg/L fluoride was prepared by dissolving 2.21 g analytical grade sodium fluoride in 1 L of ultra-pure water (18.2 MΩ/cm) and fluoride solutions for batch experiments were prepared from fresh stock fluoride solution by appropriate dilution. Mn^{2+} stock solution containing 1000 mg/L was prepared by dissolving 2.29 g of analytical grade manganese chloride in 1 L of ultra-pure water.

4.2.2 Preparation and synthesis of Mn^{2+} modified bentonite clay

Raw bentonite clay was washed by mixing with ultra-pure water at a ratio of 1:5 in a 1000 mL beaker, the mixture was stirred for 5 min, and the procedure was repeated twice. After stirring, mixtures were agitated for 15 min using Stuart reciprocating shaker and then centrifuged for 10 min at 5 000 rpm. Samples were then dried in an oven for 12 hrs at 110 °C. Clay samples were then milled to pass through <250 µm sieve. Intercalation of Mn^{2+} ions onto bentonite clay was done according to the procedure developed in preliminary work conducted in 2014 (Mudzielwana, 2014). Optimum conditions (i.e., contact time, adsorbate concentration, adsorbent dosage, and pH) for modifying bentonite clay with Mn^{2+} ion were evaluated using batch experiments. The obtained conditions were: 60 min contact time, 4 g/100 mL adsorbent dosage, 50 mg/L Mn^{2+} adsorbate concentration and initial pH of 8. To synthesize Mn^{2+} modified bentonite, 200 mL of 50 mg/L Mn^{2+} solution was mixed with 8 g of raw bentonite to make up S/L ratio of 4 g/100 mL, the pH of the mixture was then adjusted to 8 using 0.1 M NaOH and 0.1 M HCl. The mixture was put on a 1 L Erlenmeyer flask in order to avoid spillage during agitation. The mixture was agitated for 60 min at 250 rpm on a table shaker and filtered. The solid residue left on the filter paper was dried for 12 hrs at a temperature of 105 °C in the oven. The modified clay was then milled to pass through <250 µm sieve. The experiments were repeated five times to generate enough Mn^{2+} modified bentonite for subsequent experiments.

© University of Venda

University of Venda

4.2.3 Physicochemical and mineralogical characterisation

Mineralogical and chemical composition of Mn^{2+} bentonite clay was evaluated using XRD and XRF techniques respectively. Surface morphology was determined using Scanning electron microscopy (SEM) (Leo1450 SEM, at 10Kv, working distance 14mm). Surface area and pore volume was determined by Brunauer Emmet Teller (BET) method using micrometrics TriStar II. Functional groups were evaluated using FTIR. Cation exchange capacity was determined using ammonium acetate buffer at pH 5.4 and 7.4 as described by Gitari et al., (2013) and The concentration of exchangeable cation was determined using flame atomic absorption spectrum (FAAS) (600 PerkinElmer). The surface charge and point of zero charge (PZC) was determined using solid addition method as described by Kumar *et al.* (2011). Properties were compared to those of raw bentonite clay soils.

4.2.4 Batch defluoridation experiments

Batch experiments were carried out to evaluate the effects of contact time, effect of adsorbent dosage, adsorbate initial concentration and the effect of pH on fluoride adsorption. The fluoride concentration in the treated samples was measured using an ion selective electrode 9609 BNWP Orion (USA) attached to Thermo Scientific Orion Star ISE/pH/EC meter. Similar ion meter coupled with pH and EC electrode was used for measuring pH and EC of the treated samples. For residual fluoride, ion selective electrode was calibrated with four standards containing 1 mL of total ionic strength buffer (TISAB III) per 10 mL of solution. Same ratio was maintained for the sample. TISAB was added to decomplex F^- from Al^{3+}, Fe^{3+} and Si^{4+} fluorocomplexes and to maintain pH at between 5.2 and 5.5. All experiments were conducted in triplicate for better accuracy and the mean values were reported. Equation 4.1 and 4.2 were used to calculate the percentage removal and adsorption capacity respectively.

$$\%\, removal = \left(\frac{C_o - C_e}{C_o}\right) \times 100 \qquad (4.1)$$

Where: Co is initial fluoride ion concentration and Ce is equilibrium fluoride ion concentration.

$$Q = \left(\frac{C_o - C_e}{m}\right) \times v \qquad (4.2)$$

Where: C_i = initial F^- concentration (mg/L), C_e = F^- concentrations at equilibrium (mg/L),

V = Volume of solution (L) and m = Weight of the adsorbent (g)

© University of Venda

University of Venda
Creating Future Leaders

4.3 Results and discussion

4.3.1 Physicochemical and mineralogical characterisation

4.3.1.1 X-ray diffraction analysis

X- ray diffraction spectra of raw and Mn^{2+} modified bentonite clay is presented in figure 4.1. Analysis confirms the presence of montmorillonite and quartz as the major minerals and muscovite as one of the trace minerals of bentonite clay. No change in mineralogy of bentonite clay observed after modification with Mn^{2+} ions.

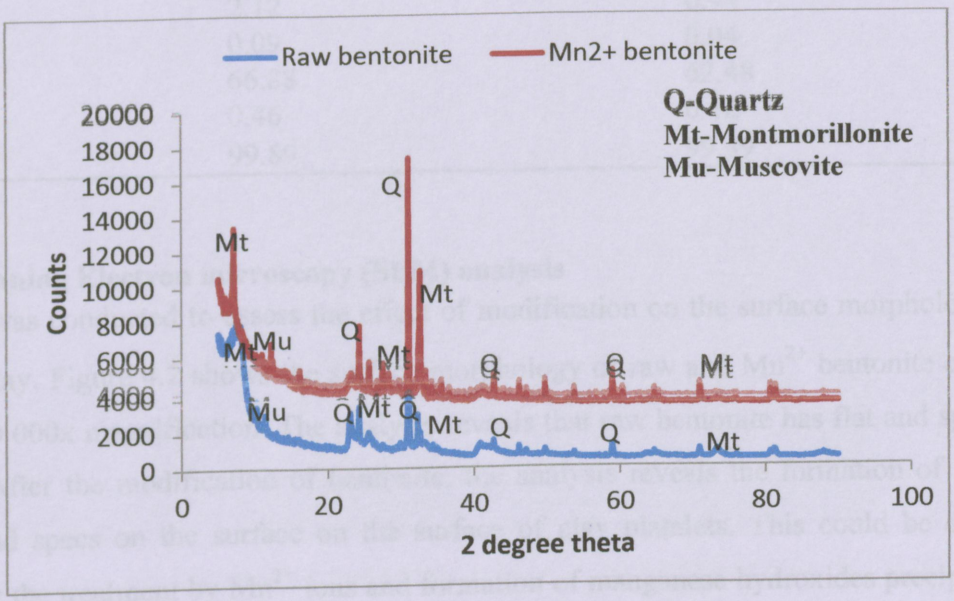

Figure 4.1: X-ray diffraction spectra for raw and Mn^{2+} bentonite.

4.3.1.2 X-ray fluorescence analysis

The results for major chemical components are reported as percentage oxide in Table 4.1. The analysis reveals that silica (SiO_2) is the main component of bentonite clay while Al_2O_3 is the main minor component. High concentration of SiO_2 and Al_2O_3 reveal that bentonite clay is an alumino-silicate material. Manganese oxide is higher in Mn^{2+} bentonite (0.29%) than in raw bentonite (0.09 %). The relatively high concentrations of MgO, Na_2O, CaO, and K_2O indicates that Mg^{2+}, Na^+, Ca^{2+}, and K^+ are the main exchangeable cations and main charge balancing cations in the clay interlayers. This is confirmed by the subsequent decrease of the content of these chemical species in the Mn^{2+} modified bentonite clay.

© University of Venda

Table 4.1: Chemical composition of raw and Mn modified bentonite clay

Oxide	Raw bentonite (W/W %)	Mn^{2+} bentonite (W/W %)
Al_2O_3	15.30	15.84
CaO	0.88	1.50
Cr_2O_3	0.01	0.00
Fe_2O_3	3.41	3.18
K_2O	0.98	0.39
MgO	3.20	3.06
MnO	0.06	0.29
Na_2O	2.12	0.94
P_2O_5	0.09	0.04
SiO_2	66.88	62.48
TiO_2	0.46	0.12
Sum Of Conc.	99.89	99.49

4.3.1.3 Scanning Electron microscopy (SEM) analysis

SEM analysis was conducted to assess the effect of modification on the surface morphology of the bentonite clay. Figure 4.2 shows the surface morphology of raw and Mn^{2+} bentonite clay at 20 000x and 40 000x magnification. The analysis reveals that raw bentonite has flat and spongy like material. After the modification of bentonite, the analysis reveals the formation of larger agglomerate and specs on the surface on the surface of clay platelets. This could be due to swelling during the treatment by Mn^{2+} ions and formation of manganese hydroxides precipitates on the clay surface.

© University of Venda

University of Venda
Creating Future Leaders

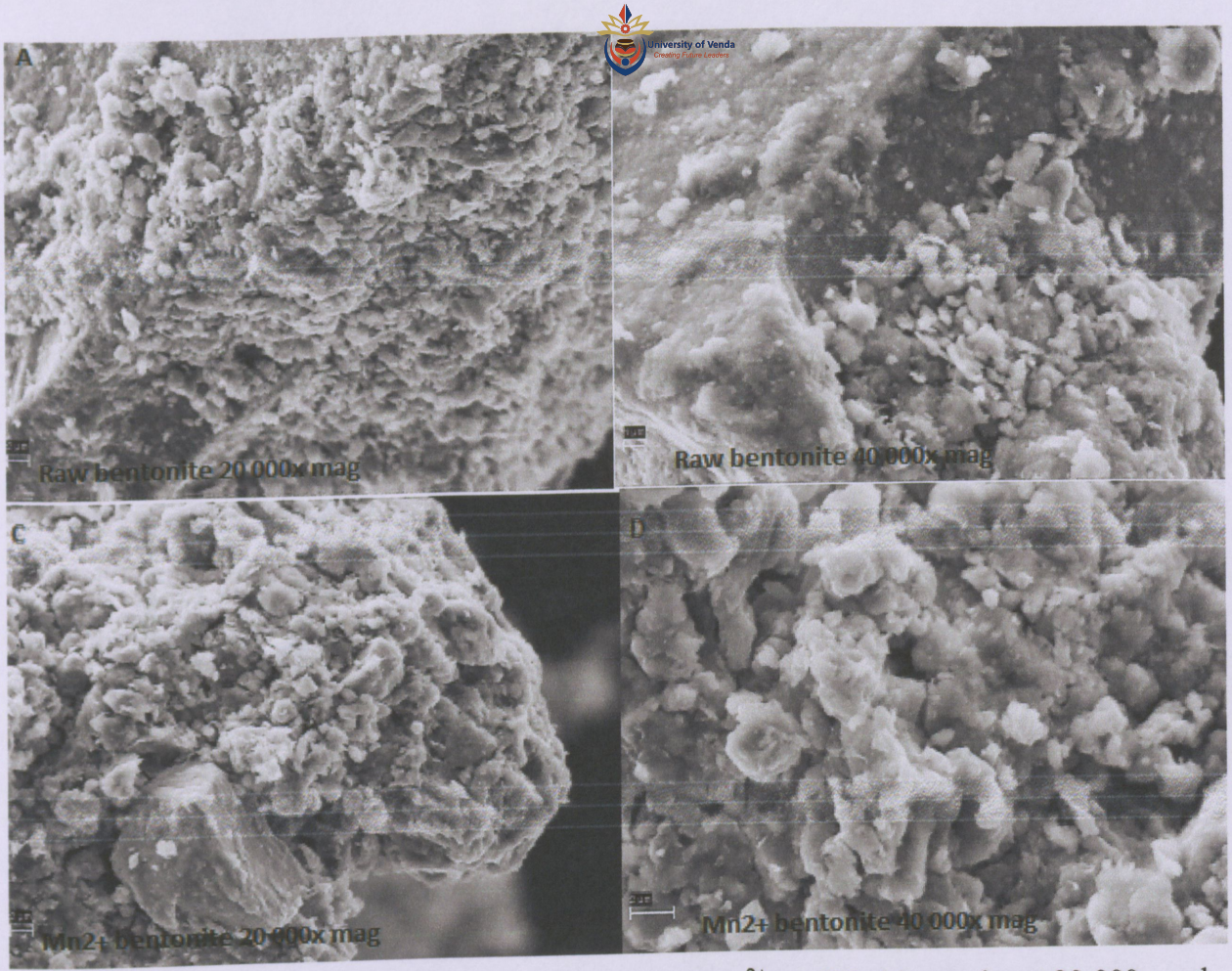

Figure 4.2: Surficial morphology of raw bentonite and Mn^{2+} modified bentonite at 20 000x and 40 000x magnifications.

4.3.1.4 FTIR analysis

FTIR spectra analysis were carried out in order to evaluate the effect of Mn^{2+} ion on the surface chemistry of bentonite clay and also help in understanding the mechanism of F^- uptake by bentonite clay. Figure 4.3 shows the FTIR spectra of raw bentonite, Mn^{2+} modified bentonite and F^- loaded Mn^{2+} bentonite clay. According to Toor *et al.* (2014), three main absorption regions of bentonite clay are 3000-3800 cm^{-1},1300-1800 cm^{-1} and 500-1200 cm^{-1} and notable difference can be observed in each region of raw, Mn^{2+} and F^- loaded bentonite. The absorption band between 3619.12 and 3623.81 cm^{-1} is due to stretching vibrations of structural OH^- groups of montmorillonite and water. At lower frequency bentonite showed a strong broad band at 999.10 cm^{-1} due to the stretching and vibration of Si-OH of bentonite mineral. Band at 914.93 cm^{-1} is attributed to Al-OH-Al. The 795 cm^{-1} band corresponded to coupled Al–O and Si–O vibrations. Quartz was present as indicated by the bands at 791 cm^{-1}. Mn^{2+} bentonite showed an increased

© University of Venda

intensity of transmittance of all the IR spectrum indicating the formation of new bonds such as Mn-O, Mn-OH and Mn-H_2O at those frequencies. Spectra for F^- loaded Mn^{2+} bentonite showed that these bands absorption intensities were significantly reduced indicating that structural hydroxides groups and water molecules had important role in F^- adsorption process and the adsorption of F^- occurs through the exchange of OH^- in Mn, Al, Si oxides for F^-.

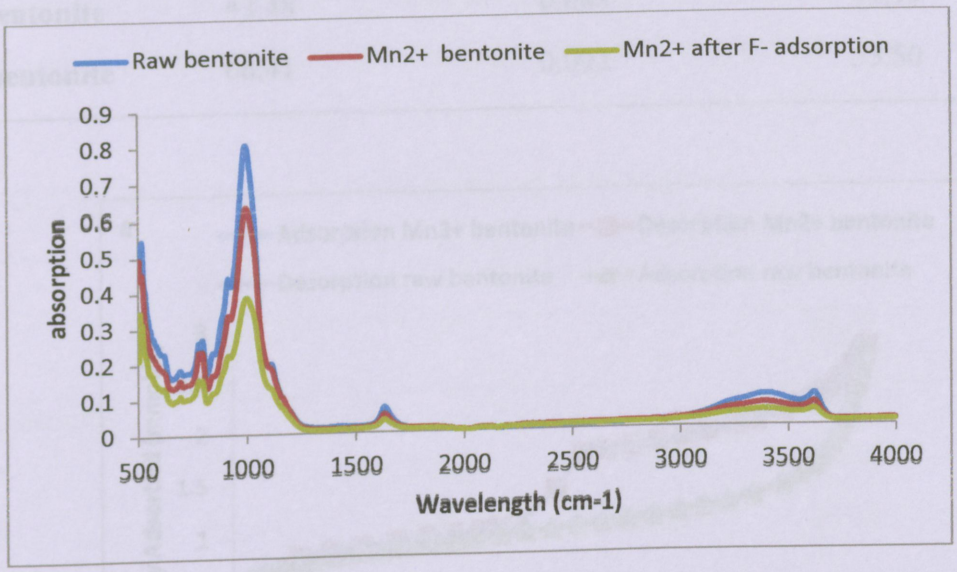

Figure 4.3: FTIR spectrum of raw bentonite, Mn^{2+} bentonite and the F^- loaded Mn^{2+} bentonite clay.

4.3.1.5 Surface area and pore distribution

BET and BJH analysis were carried out in order to assess the surface area, pore volume and the pore size and distribution of the raw and Mn^{2+} modified bentonite. Table 4.2 shows the BET surface area, pore size and pore volume of raw and Mn^{2+} modified bentonite clay. It was observed that there was an increase in total surface area and pore volume after the intercalation of Mn^{2+} ions. This may be attributed to swelling of the bentonite clay during intercalation of Mn ions. Pore width of raw bentonite was found to be higher compared to that of Mn^{2+} modified bentonite clay. This is indicating that Mn ions were incorporated onto the surface of the clay (Zhang *et al.*, 2012). Nitrogen adsorption-desorption isotherm of raw and Mn^{2+} modified bentonite is presented in figure 4.4a. Isotherms exhibited type IV isotherm with hysteresis loop (loop formed when desorption isotherm obscure the adsorption isotherm mainly at low pressure) at low relative pressure below 0.4 p/p°, desorption isotherm is obscuring the adsorption isotherm the indicating the mesoporous nature of the bentonite and Mn^{2+} modified bentonite clay. Figure 4.4b shows pore distribution of raw and Mn^{2+} modified bentonite it is observed that great amount

© University of Venda

of pores for both raw and Mn^{2+} bentonite are greater than 2 nm and smaller than 50 nm which provide evidence that bentonite clay is a mesoporous material.

Table 4.2: BET total surface area, pore volume and pore size.

	Surface area (m^2/g)	Pore volume (cm^3/g)	Pore size (Å)
Raw bentonite	43.48	0.088	79.99
Mn^{2+} bentonite	66.41	0.092	55.50

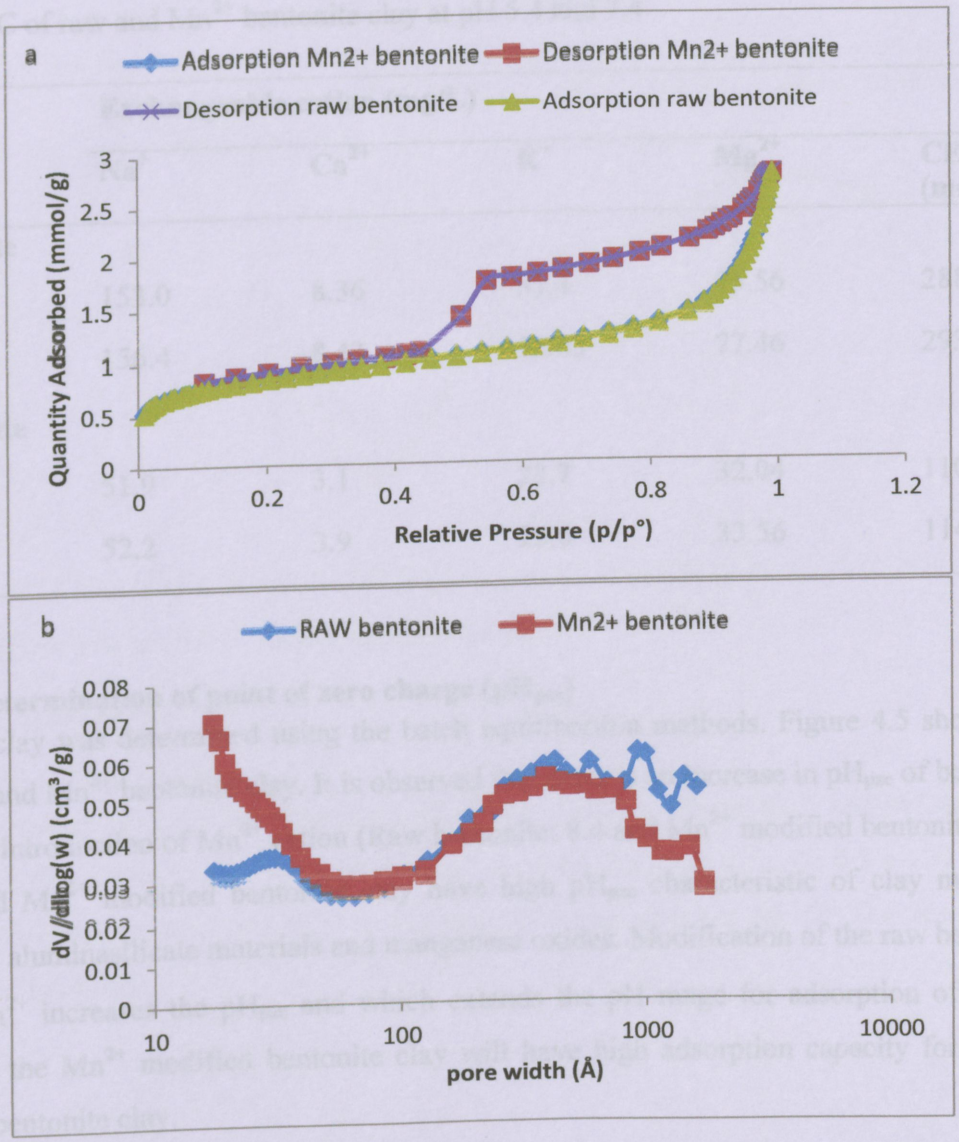

Figure 4.4: a) N_2 adsorption-desorption isotherm b) pore distribution of raw and Mn^{2+} modified bentonite clay.

© University of Venda

UNIVERSITY OF VENDA LIBRARY

University of Venda
Creating Future Leaders

4.3.1.6 Cation Exchange Capacity

Table 4.3 shows the concentration of the exchangeable cation and the calculated CEC of raw and Mn^{2+} modified bentonite clay extracted at pH 5.4 and 7.4. CEC for raw bentonite was found to be higher than the CEC of Mn^{2+} modified bentonite. This is the evidence that the dominant mechanism during the reaction of Mn^{2+} solution with raw bentonite is ion exchange. The CEC results show that Na^{+} is the main exchangeable cation. pH of the buffering media does not seem to have significant influence on the exchangeable cation concentration and subsequently the CEC.

Table 4.3: CEC of raw and Mn^{2+} bentonite clay at pH 5.4 and 7.4

	Exchangeable cation (mg/L)				
	Na^{+}	**Ca^{2+}**	**K^{+}**	**Mg^{2+}**	**CEC (meq/100 g)**
Raw bentonite					
pH 5.4	153.0	8.36	51.4	75.56	288.32
pH 7.4	156.4	8.43	52.03	77.46	293.92
Mn^{2+} bentonite					
pH 5.4	51.9	3.1	23.7	32.04	110.74
pH 7.4	52.2	3.9	25.0	33.56	114.66

4.3.1.7 Determination of point of zero charge (pH_{pzc})

pH_{pzc} of the clay was determined using the batch equilibration methods. Figure 4.5 shows the pH_{pzc} of raw and Mn^{2+} bentonite clay. It is observed that there is an increase in pH_{pzc} of bentonite clay after the introduction of Mn^{2+} cation (Raw bentonite: 8.4 and Mn^{2+} modified bentonite: 8.8). Both raw and Mn^{2+} modified bentonite clay have high pH_{pzc} characteristic of clay materials dominated by aluminasilicate materials and manganese oxides. Modification of the raw bentonite clay with Mn^{2+} increases the pH_{pzc} and which extends the pH range for adsorption of anions meaning that the Mn^{2+} modified bentonite clay will have high adsorption capacity for anions than the raw bentonite clay.

© University of Venda

University of Venda
Creating Future Leaders

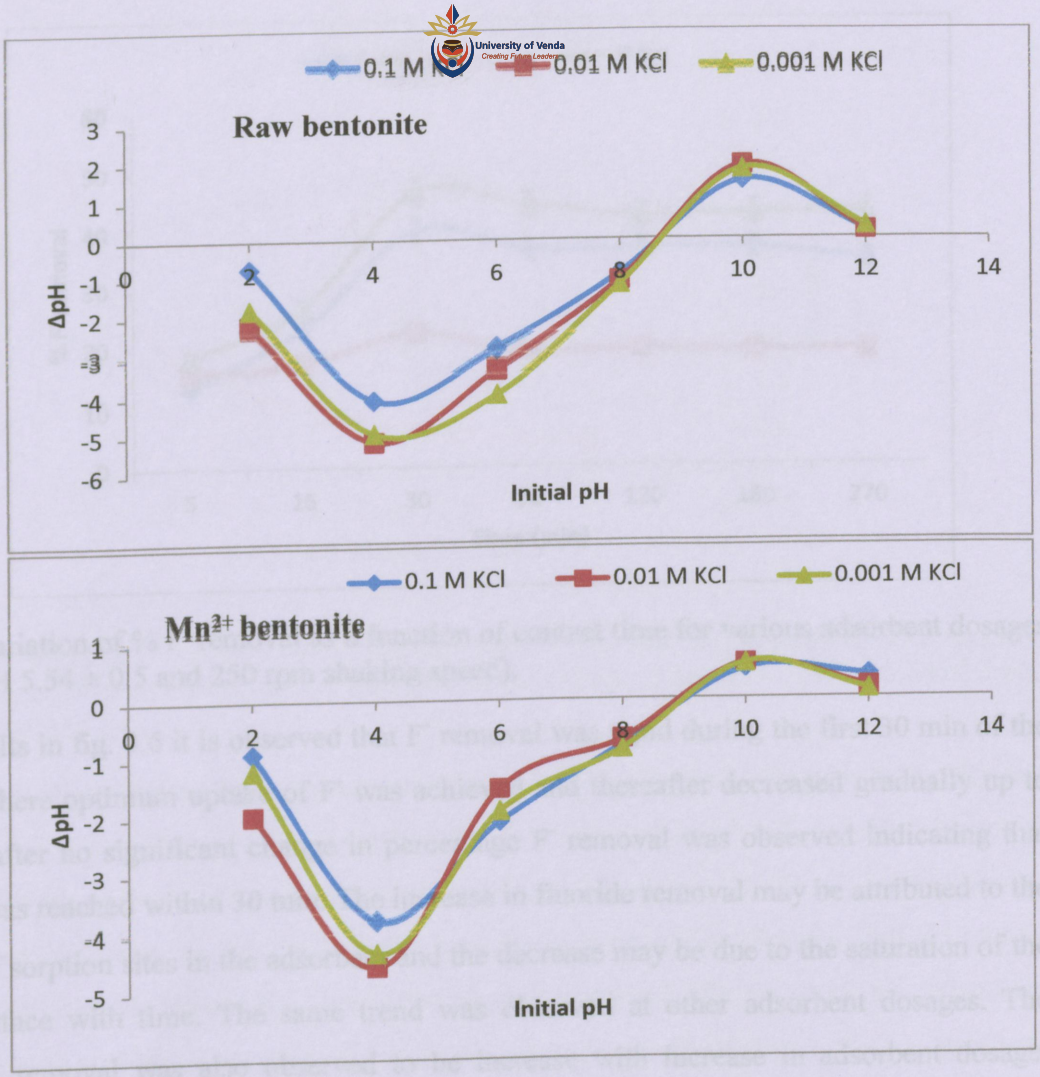

Figure 4.5: pH_{pzc} of raw and Mn^{2+} modified bentonite clay.

4.3.2 Batch experiments

4.3.2.1 Effects of contact time

The effect of contact time on the adsorption of F^- onto Mn^{2+} bentonite clay was evaluated by varying contact time from 5 to 270 min at various adsorbent dosages (0.1, 0.3, 0.5 g/100 mL), 3 mg/L initial F^- concentration, pH 5.54 ± 0.5 and 250 rpm shaking speed. The results are represented in Figure 4.6.

© University of Venda

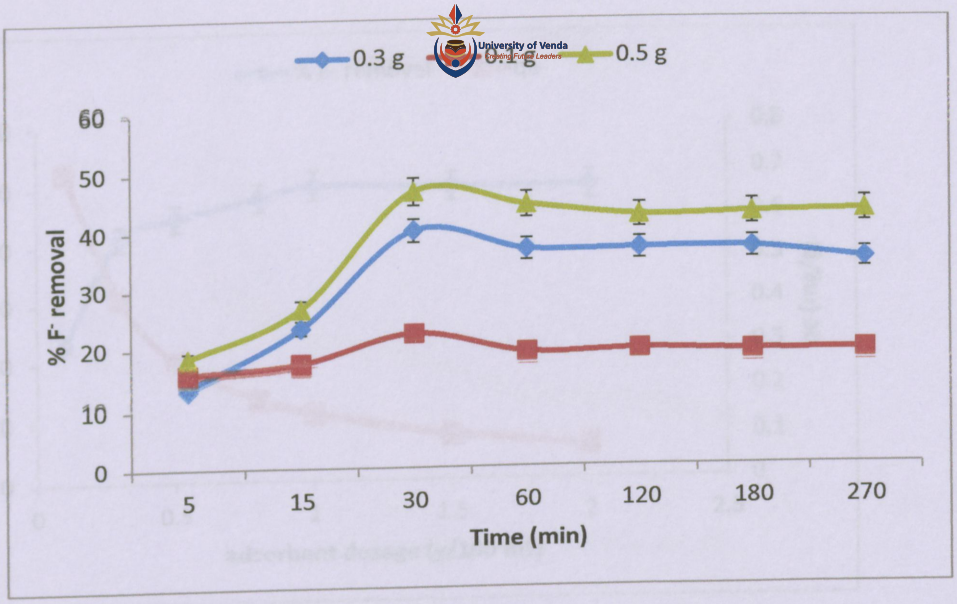

Figure 4.6: Variation of % F^- removal as a function of contact time for various adsorbent dosages (3 mg/L F^-, pH 5.54 ± 0.5 and 250 rpm shaking speed).

From the results in fig. 4.6 it is observed that F^- removal was rapid during the first 30 min of the experiment where optimum uptake of F^- was achieved and thereafter decreased gradually up to 60 min thereafter no significant change in percentage F^- removal was observed indicating that equilibrium was reached within 30 min. The increase in fluoride removal may be attributed to the availability of sorption sites in the adsorbent and the decrease may be due to the saturation of the adsorbent surface with time. The same trend was observed at other adsorbent dosages. The percentage F^- removal was also observed to be increase with increase in adsorbent dosage. Contact time of 30 min was taken as the optimum time and was applied in subsequent experiments.

4.3.2.2 Effect of adsorbent dosage

The effect of adsorbent dosage on the adsorption of F^- onto Mn^{2+} bentonite clay was evaluated at 30 min contact time at shaking speed of 250 rpm, 3 mg/L initial concentration of F^- and pH of 5.54 ± 0.5. The adsorbent dosage was varied from 0.1 g/100 mL to 2 g/100 mL. The plot of percentage fluoride removal and adsorption capacity against adsorbent dosage is presented in figure 4.7.

© University of Venda

University of Venda
Creating Future Leaders

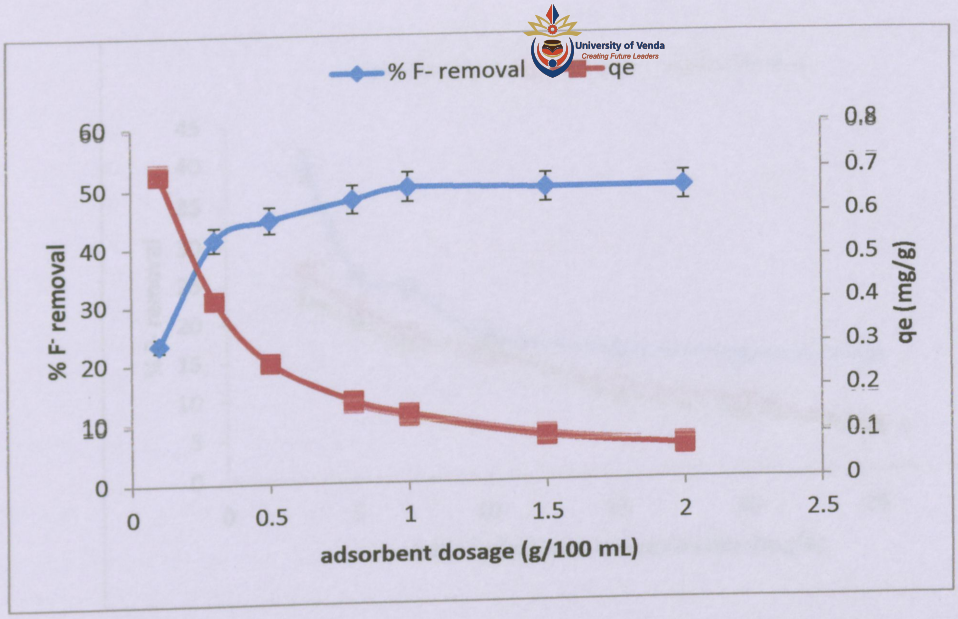

Figure 4.7: Variation % F^- removal and adsorption capacity by Mn^{2+} bentonite clay as a function of adsorbent dosage (contact time of 30 min, adsorbent dosage, 3 mg/L F^-, pH of 5.54±0.5 and shaking speed of 250 rpm).

Figure 4.7 shows the relationship between percentage fluoride removal, adsorption capacity and adsorbent dosage. It is observed that percentage fluoride removal onto Mn^{2+} modified bentonite clay increased with an increasing adsorbent dosage from 0.1 up to 1 g/100 mL were optimum uptake occurred. This may be attributed to the increase in the sorption sites for fluoride ions as the adsorbent dosage increases. No significant change observed after 1 g/100 mL adsorbent dosage this may be attributed to too many sites are available for limited quantity of adsorbate. The adsorption capacity on the other hand decreased with increase in adsorbent dosage. At the dosage of 1 g/100 mL, about 50% of fluoride was removed and this dosage was taken as the optimum and was used in subsequent experiments.

4.3.2.3 Effect of adsorbate concentration

The effect of initial concentration in the adsorption of F^- onto Mn^{2+} bentonite clay was evaluated at various contact times (30, 60 and 120 min) , at 250 rpm shaking speed, 1.0 g/100 mL adsorbent dosage and pH of 5.54±0.5. The initial concentration was varied from 3 mg/L to 25 mg/L. Plot of percentage removal with adsorbate concentration is presented in figure 4.8.

© University of Venda

University of Venda
Creating Future Leaders

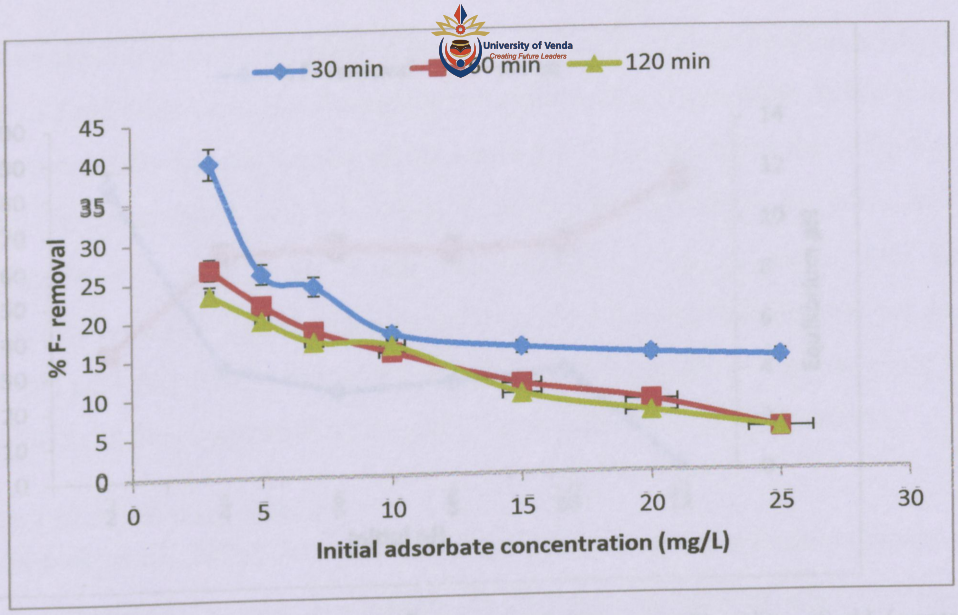

Figure 4.8: Variation of % F^- removal by Mn^{2+} bentonite clay as a function of adsorbate concentration at various contact times (adsorbent dosage 1.0 g/100 mL, pH of 5.54±0.5 and shaking speed of 250 rpm).

Figure 4.8 shows the effect of adsorbate concentration on the percentage fluoride removal at various contact times, it is observed that the percentage F^- removal decreased with an increase in the initial concentration, the same trend was observed at other contact times. This is due to availability of more fluoride ions in solution at higher concentration and the adsorption sites becomes the limiting factor in the adsorption process. At contact times > 30 min the adsorption capacity was lower, this was earlier observed in the contact time experiments where maximum absorption was at 30 min. Initial adsorbate of 3 mg/L was taken as the optimum concentration for subsequent experiments.

4.3.2.4 Effects of pH

To study the effects of pH in the adsorption of F^- onto Mn^{2+} bentonite clay, the initial pH was adjusted from 2 to 12 using 0.1 M NaOH and 0.1 M HCl. The effect of pH was evaluated under the condition of 30 min contact time at 250 rpm, 1.0 g/100 mL adsorbent dosage, 3 mg/L initial concentration. The plot of pH with percentage F^- removal is shown in figure 4.9 while figure 4.10 shows the change in pH ($pH_{initial} - pH_{final}$) as a function of initial pH.

© University of Venda

University of Venda
Creating Future Leaders

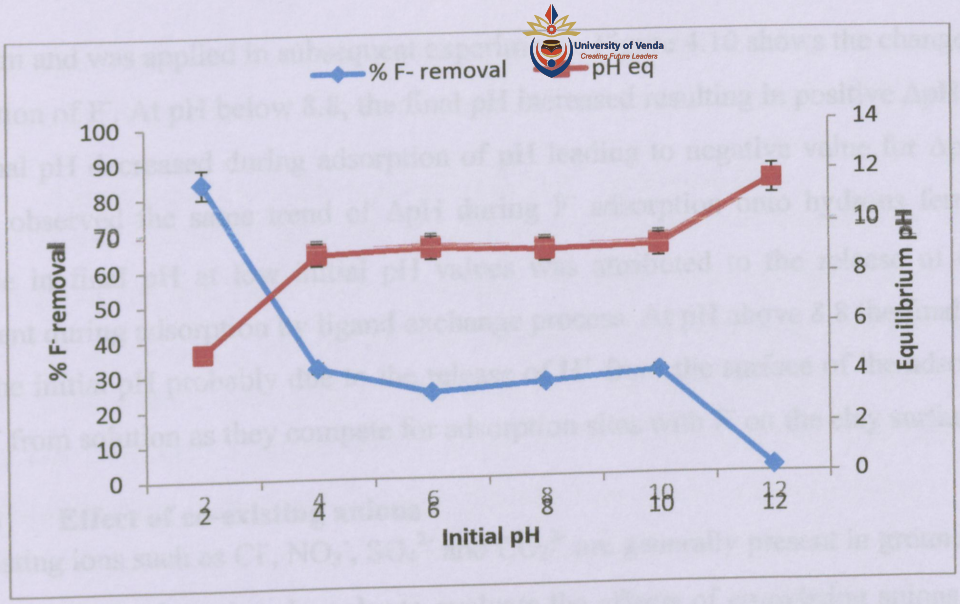

Figure 4.9: Variation of % F^- removal by Mn^{2+} bentonite clay as a function of pH (contact time 30 min, adsorbent dosage 1.0 g/100 mL, 3 mg/L F^- and shaking speed of 250 rpm).

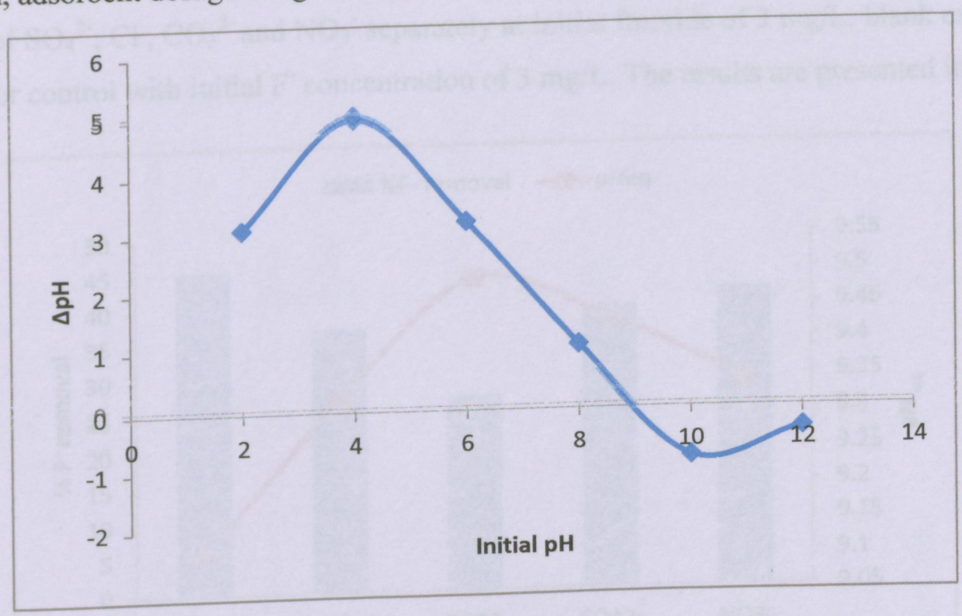

Figure 4.10: ΔpH during adsorption of F^- onto Mn^{2+} modified bentonite clay.

pH of the medium is the most important parameter that influences the fluoride removal and helps in elucidating fluoride uptake mechanisms of the adsorbent. From the results in figure 4.9, it is observed that % fluoride removal decreases with an increase in initial pH, from 84% removal at pH 2 to 24.33% at pH 6, thereafter a slight increase was observed up to 30% at pH 10. The drastic decrease in F^- removal was observed at pH beyond 10. This may be due to the abundance of OH^- ions in alkaline pH that compete with F^- for adsorption sites. pH 2 was then chosen as the

© University of Venda

optimum and was applied in subsequent experiments. Figure 4.10 shows the change of pH during adsorption of F^-. At pH below 8.8, the final pH increased resulting in positive ΔpH. At pH above 8.8, final pH decreased during adsorption of pH leading to negative value for ΔpH. Nur *et al.*, (2014) observed the same trend of ΔpH during F^- adsorption onto hydrous ferric oxide. The increase in final pH at low initial pH values was attributed to the release of OH^- from the adsorbent during adsorption by ligand exchange process. At pH above 8.8 the final pH decreased from the initial pH probably due to the release of H^+ from the surface of the adsorbent removal of OH^- from solution as they compete for adsorption sites with F^- on the clay surface.

4.3.2.5 Effect of co-existing anions

Co-existing ions such as Cl^-, NO_3^-, SO_4^{2-} and CO_3^{2-} are generally present in groundwater and can interfere with F^- adsorption. In order to evaluate the effects of co-existing anions on adsorption of fluoride by Mn^{2+} modified bentonite clay, defluoridation was conducted in the presence of 5 mg/L of SO_4^{2-}, Cl^-, CO_3^{2-} and NO_3^- separately at initial fluoride of 3 mg/L, blank experiment was done for control with initial F^- concentration of 3 mg/L. The results are presented in figure 4.11.

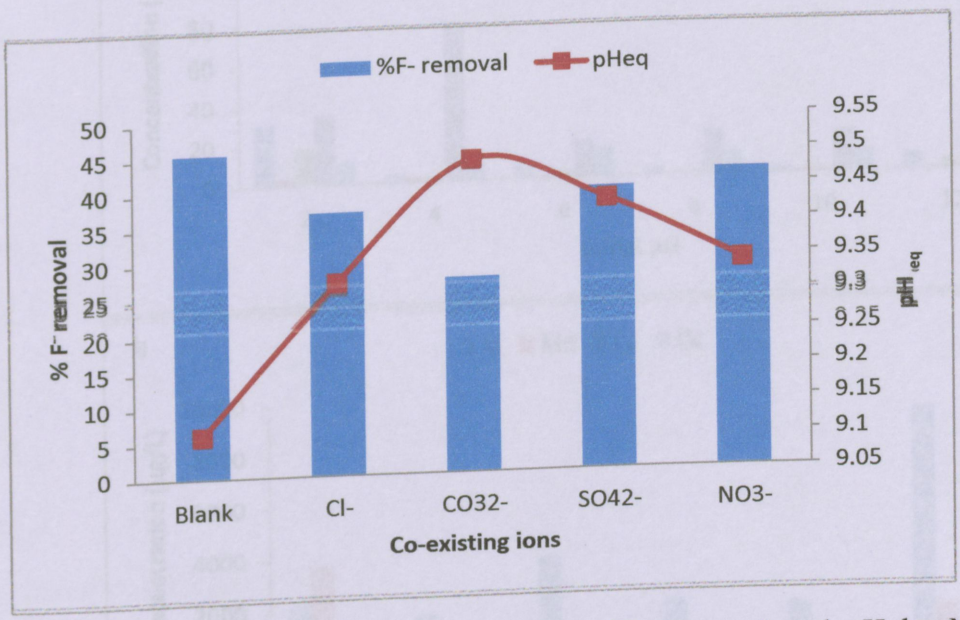

Figure 4.11: Effects of co-existing anions on fluoride removal and pH by Mn^{2+} modified bentonite clay soils (3 mg/L F^-, 1.0 g/100 mL adsorbent dosage, 30 min contact time at 250 rpm and pH of 6.5).

From figure 4.11, it was observed that percentage fluoride removal is slightly affected by the presence of Cl^-, NO_3^- and SO_4^{2-}. The presence of CO_3^{2-} decreased fluoride removal by up to 18%. This may be due to increased equilibrium pH which promoted competition for adsorption

© University of Venda

sites. The same observation was reported by Cher[illegible]11) and Yi *et al.* (2014). Effect of co-existing ion in adsorption of F^- increases in the following order: $NO_3^- > Cl^- > SO_4^{2-} > CO_3^{2-}$.

4.3.2.6 Leaching of chemical species from Mn^{2+} bentonite clay

Toxicity of Mn^{2+} modified bentonite for use in groundwater was assessed by determining the extent of metal and non-metal release from Mn^{2+} modified bentonite at different levels of initial pH. 100 mL of 3 mg/L F^- was mixed with 1.0 g of the clay, mixtures were then agitated for 30 min on a table shaker, after agitation, mixtures were then centrifuged at 2 500 rpm for 10 min, supernatants were then acidified with 3 drops of 2 M HNO_3 and then analysed for major and trace elements using Inductively Coupled Plasma-Mass Spectrometer (ICP-MS). The results are presented in figure 4.12a (mg/L) and figure 4.12b (µg/L).

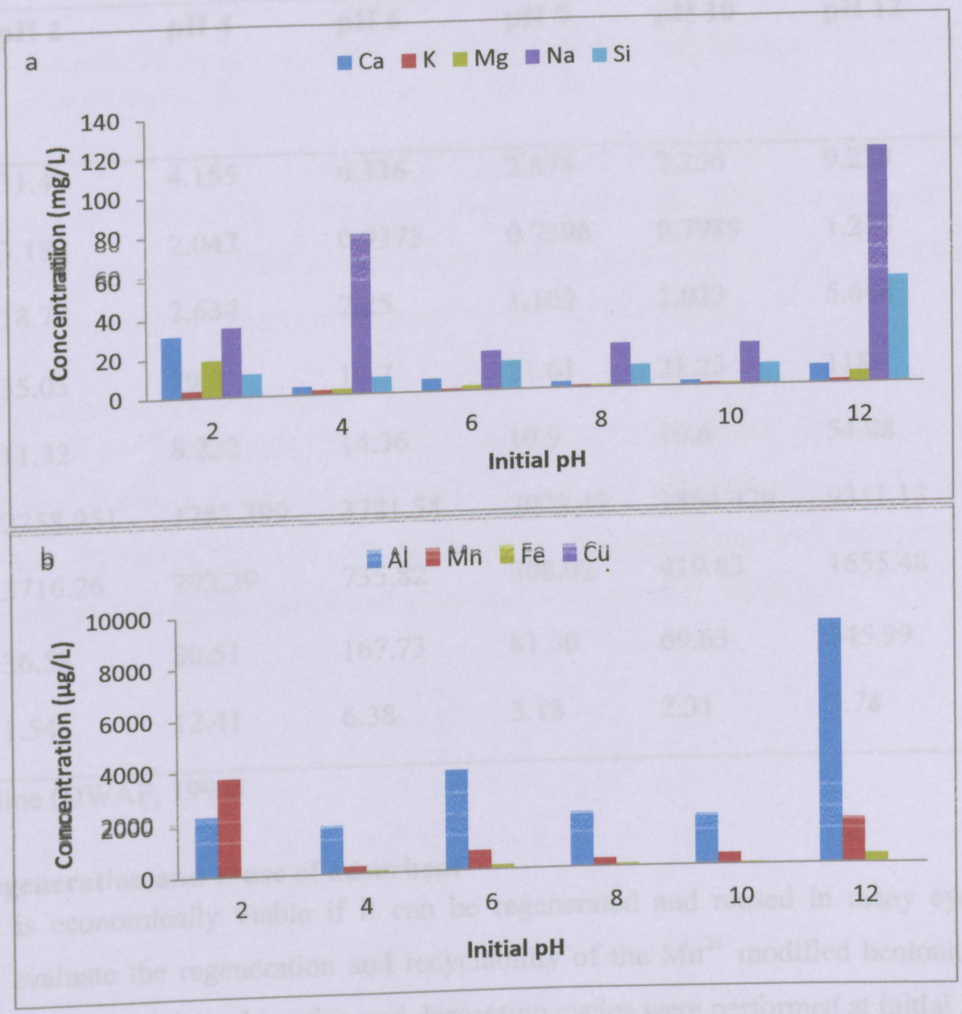

Figure 4.12: Concentration of chemical species in treated water at various pH. a) in mg/L, and b) in µg/L (1.0 g/100 mL adsorbent dosage, 3 mg/L initial F^- concentration and 30 min contact time at 250 rpm).

© University of Venda

University of Venda
Creating Future Leaders

It was observed that the concentration of Na was [illegible] at both pH levels, this may have been influenced by the use of NaOH for pH adjustment. High Si and Al concentration was observed at higher pH levels and this may have been influenced by dissolution of Si and Al at high alkaline conditions. Mn, Fe, Al and Cu were released at very trace concentration. The concentration of all chemical species was found to be within the DWAF recommended level (DWAF, 1996) (Table 4.4). Therefore, based on the obtained data, Mn^{2+} modified bentonite is a promising material for defluoridation of groundwater and moreover its stable at a wide pH range hence doesn't lead to release of secondary pollutants in the treated water.

Table 4.4: Comparison of species concentration at various pH with WHO guideline values for chemical species.

	pH 2	pH 4	pH 6	pH 8	pH 10	pH 12	DWAF guidelines (in mg/L)
Ca (mg/L)	31.48	4.155	6.336	2.874	2.256	9.238	0 – 32
K (mg/L)	3.182	2.042	0.9372	0.7396	0.7989	1.278	0 – 50
Mg (mg/L)	18.72	2.634	2.25	1.109	1.023	5.648	0 - 30
Na (mg/L)	35.05	79.2	19.7	21.61	21.23	118	0 - 100
Si (mg/L)	11.32	8.222	14.36	10.9	10.6	54.08	-
Al (µg/L)	2258.951	1782.399	3781.54	2028.43	1864.429	9341.13	0 - 0.15
Mn (µg/L)	3716.26	292.29	735.82	308.02	419.83	1655.48	0 - 0.05
Fe (µg/L)	36.58	80.51	167.73	81.50	69.63	345.99	0 - 0.1
Cu (µg/L)	1.54	12.41	6.38	3.18	2.31	3.78	0 - 1

DWAF guideline (DWAF, 1996)

4.3.2.7 Regeneration and reuse of adsorbent

An adsorbent is economically viable if it can be regenerated and reused in many cycles of operation. To evaluate the regeneration and recyclability of the Mn^{2+} modified bentonite clay, experiments of five successive adsorption and desorption cycles were performed at initial 3 mg/L F^- concentration, at pH 5.54 and contact time of 30 min. The results are presented in figure 4.13.

© University of Venda

University of Venda
Creating Future Leaders

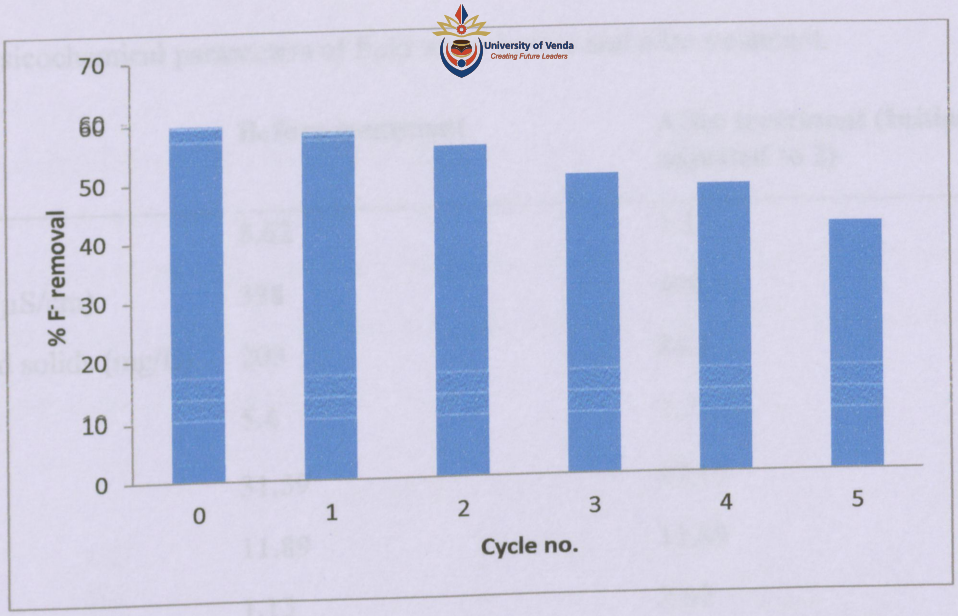

Figure 4.13: % Fluoride removal onto Mn^{2+} modified bentonite clay in successive regeneration cycles (3 mg/L, 30 min contact time at 250 rpm and pH 5.54).

From the results in figure 4.13, it can be observed that percentage fluoride removal decreases with increasing cycles of reuse. However a very slight decrease was observed up to the second cycle and a drastic decrease by 20% was observed at fifth cycle. Jia *et al.* (2015) reported the same trend and attributed it to in adequate regeneration of the adsorbent.

4.3.2.8 Defluoridation of field water

The effectiveness of Mn^{2+} bentonite clay in fluoride removal was tested on field water from Siloam community borehole containing 5.4 mg/L fluoride ion concentration. Field water was treated under the optimized pH of 2, adsorbent dosage 1.0 g/100 mL and the mixture was agitated for 30 min at 250 rpm shaking speed. Results are presented in Table 4.5.

© University of Venda

UNIVERSITY OF VENDA LIBRARY

Table 4.5: Physicochemical parameters of field water before and after treatment.

Parameters	Before treatment	After treatment (Initial pH adjusted to 2)
pH	8.62	3.2
Conductivity (µS/cm)	338	402
Total dissolved solids (mg/L)	203	84.1
F^- (mg/L)	5.4	2.7
Cl^- (mg/L)	31.59	37.15
SO_4^{2-} (mg/L)	11.89	11.89
NO_3^- (mg/L)	1.13	2.07
Br^- (mg/L)	2.08	ND
PO_4^{3-} (mg/L)	2.67	ND

ND=Not detected

Percentage F^- removal of 55.89% was achieved from field water at optimized conditions this is lower than the percentage F^- removal achieved at the same conditions from the synthetic F^- solution (84.0%) (Fig.4.9). This may be attributed to the competition for adsorbent surface between co-existing anion and F^- ion. Table 4.5 shows that there was reduction in Br^- and PO_4^{3-} ions after defluoridation indicating that they were also adsorbed during the process. The results indicate that the fabricated adsorbent would be suitable for treatment of groundwater with F- concentration ≤ 3 mg/L to achieve the recommended concentration of 1.5 mg/L.

4.4 Adsorption isotherms

Adsorption isotherms are generally used to describe the equilibrium relationship between adsorbate concentration and the amount of adsorbate adsorbed on the surface of adsorbent (Chen *et al.*, 2011). Langmuir and Freundlich are the two widely used isotherm models. Langmuir isotherm model is applicable to homogeneous adsorption where adsorption process has equal activation energy it assumes that assumes that the adsorbent surface is uniform, i.e., all the adsorption sites are equivalent and adsorption molecules do not interact (Zhang *et al.*, 2011; Sun *et al.*, 2011). The linear equation for Langmuir is expressed by equation 4.3:

© University of Venda

University of Venda
Creating Future Leaders

$$\frac{C_e}{Q_e} = \frac{1}{Q_m b} + \frac{C_e}{Q_m} \quad (4.3)$$

Where, C_e is the equilibrium concentration (mg/L), Q_e is the adsorption capacity (mg/L), Q_m is theoretical maximum adsorption capacity (mg/g) and b is the Langmuir constant related to enthalpy of adsorption (L/mg). Q_m and b are determined from the slope and intercept of the plot of $\frac{C_e}{Q_e} Vs\ C_e$. Calculated Langmuir constants are presented in Table 4.6. The Langmuir plots at various contact times are shown in figure 4.14.

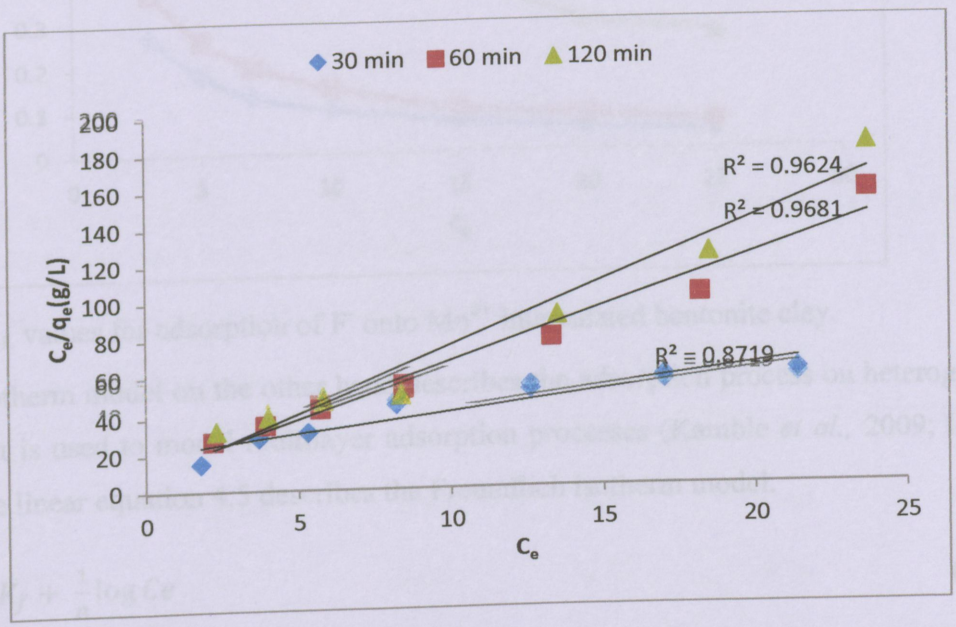

Figure 4.14: Langmuir isotherm plot for fluoride removal onto Mn^{2+} incorporated bentonite clay at 30, 60 and 120 min contact time 250 rpm shaking speed, pH 5.54 ± 0.5 and adsorbent dosage of 1 g/100 mL.

The plots showed higher correlation coefficient for both contact times which shows the applicability of Langmuir adsorption isotherm. Furthermore, in order to reveal the feasibility of the isotherm, the dimensionless parameter of the equilibrium or adsorption intensity (R_L) was used for further analysis of Langmuir equation. The values of R_L were calculated using equation 4.4:

$$R_L = \frac{1}{1+bC_o} \quad (4.4)$$

Where C_o is the initial concentration and b is the Langmuir constant. The value of R_L less than 1 generally indicate favourable adsorption and greater than 1 indicate unfavourable adsorption.

© University of Venda

Calculated R_L values in figure 4.15 lie within the range 0-1 indicating adsorption process was favourable at room temperature for all the adsorbate concentrations tested.

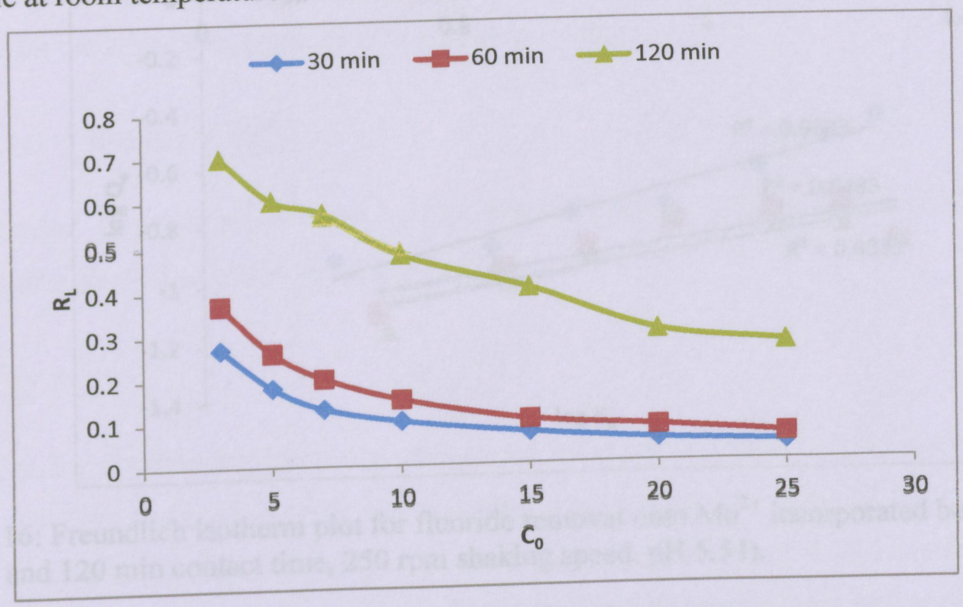

Figure 4.15: R_L values for adsorption of F^- onto Mn^{2+} intercalated bentonite clay.

Freundlich isotherm model on the other hand describes the adsorption process on heterogeneous surfaces and it is used to model multilayer adsorption processes (Kamble *et al.*, 2009; Chen *et al.*, 2011). The linear equation 4.5 describes the Freundlich isotherm model.

$$\log Q_e = \log K_f + \frac{1}{n}\log Ce \qquad (4.5)$$

Where, Ce is the equilibrium concentration (mg/L), Qe is the amount adsorbed at equilibrium (mg/g), K_f is the Freundlich constant related to adsorption capacity and represents the strength of adsorptive bonds and $1/n$ is the adsorption intensity . The value of K_f and $1/n$ are obtained from the slope and intercepts of linear plot of log Q_e vs log C_e and calculated values are shown in the Table 4.6. The value of $1/n$, Freundlich constants, indicates the type of isotherm. When $0 < 1/n < 1$, the adsorption is favourable; when $1/n = 1$, the adsorption is irreversible; and when $1/n > 1$, the adsorption is unfavourable. Figure 4.16 shows Freundlich isotherm plots for fluoride adsorption onto Mn^{2+} intercalated bentonite clay.

© University of Venda

University of Venda
Creating Future Leaders

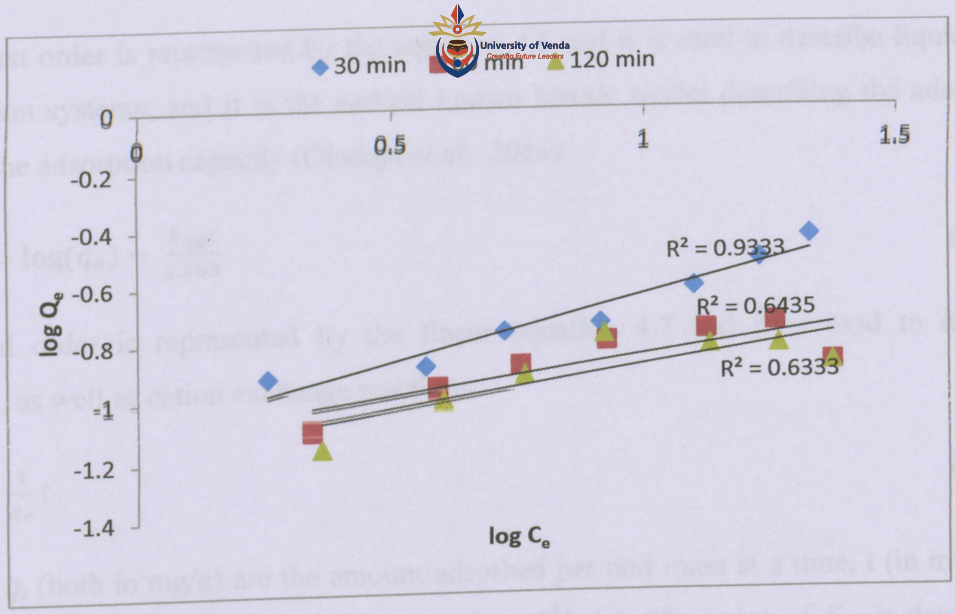

Figure 4.16: Freundlich isotherm plot for fluoride removal onto Mn^{2+} incorporated bentonite clay at 30, 60 and 120 min contact time, 250 rpm shaking speed, pH 5.54).

Table 4.6: Constant values for Langmuir and Freundlich isotherm.

	Langmuir isotherm			**Freundlich isotherm**		
	q_m (mg/g)	**b (L/mg)**	**R^2**	**K_f (mg/g)**	**1/n**	**R^2**
30 min	0.14	0.88	0.99	0.08	0.45	0.93
60 min	0.17	0.55	0.96	0.07	0.26	0.64
120 min		0.10	0.87	0.06	0.27	0.63

Based on the correlation coefficient values (R^2), the experimental data fitted well to Langmuir and adsorption of fluoride occurred on a monolayer surface. The value of R_L, dimensionless equilibrium parameter and the value of *1/n* Freundlich adsorption intensity were both between 0 and 1, which indicates that the adsorption of F^- onto Mn^{2+} bentonite was favourable.

4.5 Adsorption kinetics

The adsorption kinetics was evaluated to determine the mechanism of fluoride adsorption onto Mn^{2+} bentonite as well as the potential rate controlling steps. Pseudo first and second order kinetics reaction based and the Webber Morris intra-particle diffusion models were used to explain the kinetics.

© University of Venda

The pseudo first order is represented by the equation 4.6 and it is used to describe liquid–solid phase adsorption systems, and it is the earliest known kinetic model describing the adsorption rate based on the adsorption capacity (Oladoja *et al.*, 2014).

$$\log(q_e - q_t) = \log(q_e) - \frac{k_{ad}t}{2.303} \quad (4.6)$$

Pseudo second order is represented by the linear equation 4.7 and it is used to describe chemisorption, as well as cation exchange reactions.

$$\frac{t}{q_t} = \frac{1}{K_{2ads}q_e^2} + \frac{1}{q_e}t \quad (4.7)$$

Where q_e and q_t (both in mg/g) are the amount adsorbed per unit mass at a time, t (in min). K_{ad} and K_{2ads} are first and second order rate constant (g.mg^{-1}/min). The value of K_{ad} is determined from the slope and intercepts of log (q_e- q_t) vs t (min) and the value of K_{2ads} is determined from the slope and intercepts of t/q_t vs q_e. Plots of log (q_e-q_t) values against time for various adsorbent doses are shown in figure 4.17. Adsorption of fluoride ion onto Mn^{2+} bentonite did not follow the pseudo first order process since it did not yield a straight line.

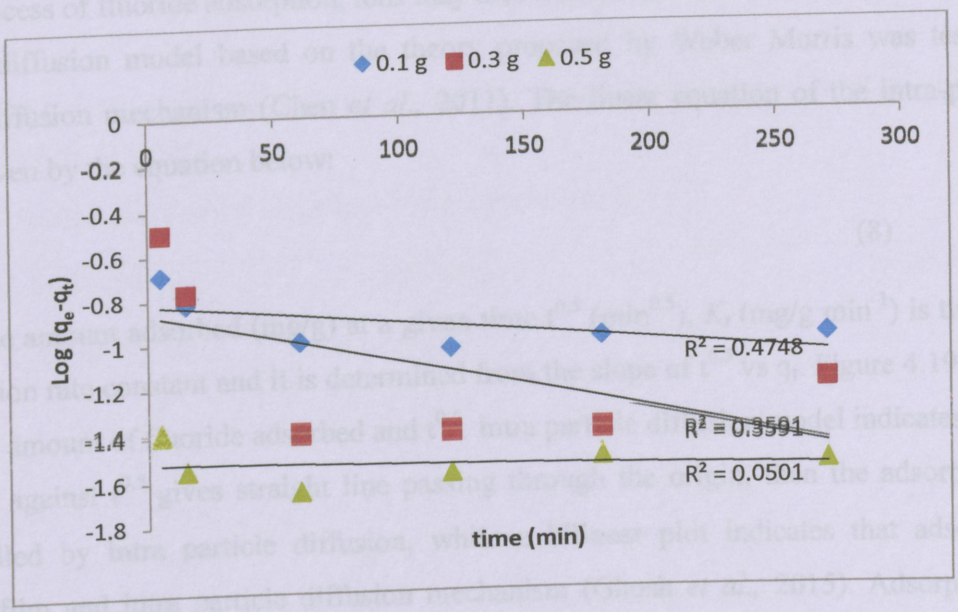

Figure 4.17: Pseudo first order plot at various adsorbent doses (3 mg/L F^-, pH 5.54 and shaking speed of 250 rpm).

Plots of t/q with time are shown in figure 4.18. The plots are linear and gave a high correlation coefficient at both adsorbent doses. This implies that fluoride sorption onto Mn^{2+} modified

© University of Venda

bentonite clay followed pseudo second order kinetic chemisorption. The constant values of pseudo first and second order are presented in Table 4.7.

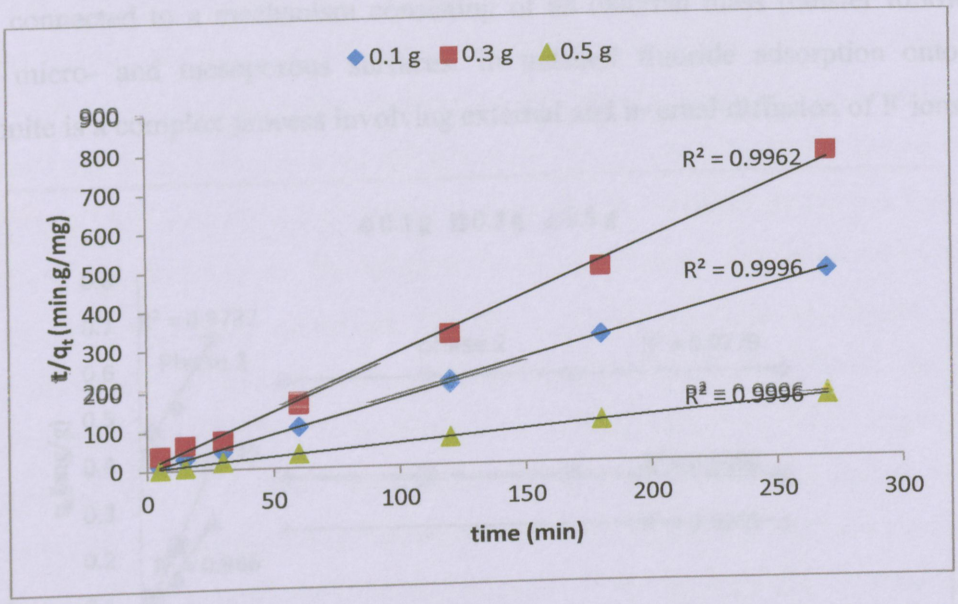

Figure 4.18: Pseudo second order plot at various adsorbent doses (3 mg/L F^-, pH 5.54 and shaking speed of 250 rpm).

During the process of fluoride adsorption, ions may also diffuse into the interior of the adsorbent. Intra-particle diffusion model based on the theory proposed by Weber Morris was tested to identify the diffusion mechanism (Chen *et al.,* 2011). The linear equation of the intra-particle diffusion is given by the equation below:

$$q_t = K_i t^{0.5} \quad (8)$$

Where q_t is the amount adsorbed (mg/g) at a given time $t^{0.5}$ ($min^{0.5}$), K_i (mg/g min^{-1}) is the intra particle diffusion rate constant and it is determined from the slope of $t^{0.5}$ vs q_t. Figure 4.19 shows the plot of the amount of fluoride adsorbed and $t^{0.5}$. Intra particle diffusion model indicates that if the plot of q_t against $t^{0.5}$ gives straight line passing through the origin, then the adsorption is solely controlled by intra particle diffusion, while a bilinear plot indicates that adsorption occurred via film and intra particle diffusion mechanism (Ghosh *et al.,* 2015). Adsorption of fluoride onto Mn^{2+} bentonite showed bilinear plot with the initial plot (phase 1) indicating external diffusion and the second plot (Phase 2) indicates intra-particle diffusion. The intra-particle rate constants K_{i1} and K_{i2} obtained from the plot are presented in Table 4.7. At both adsorbent dosages, K_{i1} value is greater than the K_{i2} value, indicating that the initial step is faster

© University of Venda

University of Venda
Creating Future Leaders

than the final step where equilibrium was established. This may be attributed to difference in the rate of mass transfer in the initial and final stages of adsorption (Jia *et al.*, 2015). This observation is connected to a mechanism consisting of an external mass transfer followed by diffusion into micro- and mesoporous surfaces. In nutshell fluoride adsorption onto Mn^{2+} modified bentonite is a complex process involving external and internal diffusion of F^- ions.

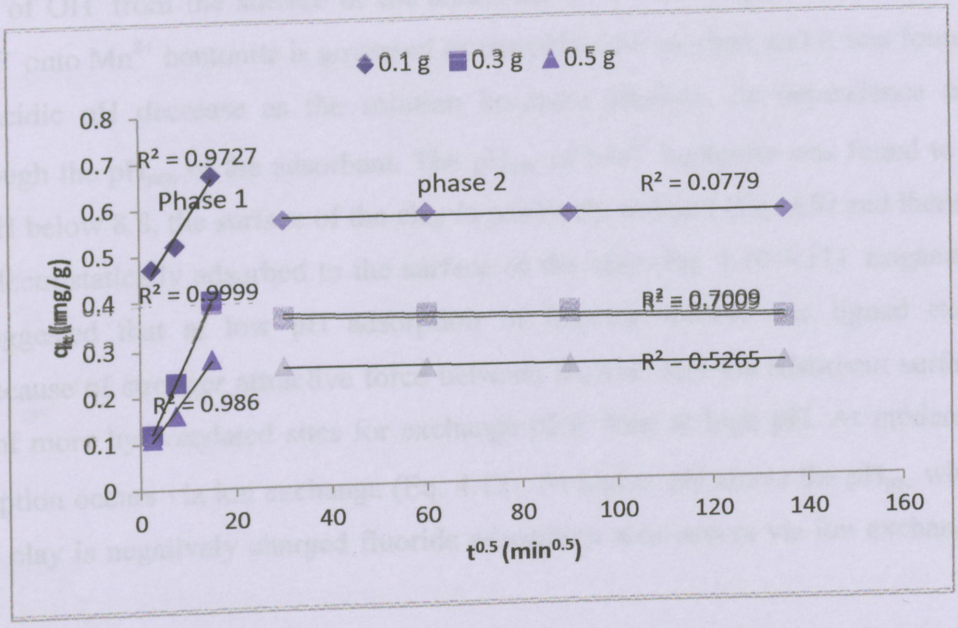

Figure 4.19: plot for intra-particle diffusion at various adsorbent dosages (3 mg/L F^-, pH 5.54 and shaking speed of 250 rpm).

Table 4.7: Pseudo first and second order kinetics constant values.

	Pseudo first order		**Pseudo second order**			**Intra-particle diffusion**	
	K_{ad}(min^{-1})	R^2	q_e(mg/g)	K_{2a} (g/mg/min)	R^2	K_{i1}	K_{i2}
0.1 g/100 mL	2.1×10^{-2}	0.47	0.56	2.73	0.99	0.016	-3×10^{-5}
0.3 g/100 mL	5.06×10^{-3}	0.35	0.33	1.36	0.99	0.022	-0.2×10^{-5}
0.5 g/100 mL	4.6×10^{-3}	0.05	2.4	0.52	0.99	0.13	-8×10^{-8}

© University of Venda

University of Venda
Creating Future Leaders

4.6 Mechanistic aspect of F^- adsorption onto Mn^{2+} bentonite clay

Ma *et al.* (2012) indicated that fluoride adsorption depends on the number of hydroxyl sites. FTIR spectra (Fig. 4.3) showed that Mn^{2+} modified bentonite structure has highly accessible hydroxyl groups positioned on the layers which favours F^- adsorption. After F^- adsorption a decrease in intensity of transmittance was observed which indicates that during adsorption, there was exchange of OH^- from the surface of the adsorbent for F^- ion. Figure 4.9 shows that the adsorption of F^- onto Mn^{2+} bentonite is governed by the pH of the medium and it was found to be optimum at acidic pH decrease as the solution becomes alkaline. Its dependence may be explained through the pH_{pzc} of the adsorbent. The pH_{pzc} of Mn^{2+} bentonite was found to be 8.8 (fig 4.5). At pH below 8.8, the surface of the clay is positively charged (Eq. 4.9) and therefore F^- ions will be electrostatically adsorbed to the surface of the clay (Eq. 4.10-4.11). Loganathan *et al.* (2013) suggested that at low pH adsorption of fluoride follows the ligand exchange mechanism because of stronger attractive force between fluoride and the adsorbent surface and the presence of more hydroxylated sites for exchange of F^- than at high pH. At moderate pH, fluoride adsorption occurs via ion exchange (Eq. 4.12). At higher pH above the pH_{pzc} where the surface of the clay is negatively charged fluoride adsorption also occurs via ion exchange (Eq. 4.13).

$$\equiv M(OH)_2 + H^+ \leftrightarrow \equiv MOH_3^+ \quad (4.9)$$

$$\equiv MOH + H_3O^+ + F^- \leftrightarrow \equiv MOH_2^+ - F^- + H_2O \quad (4.10)$$

$$\equiv MOH + H_2O + F^- \leftrightarrow \equiv MOH_2^+ - F^- + 2OH^- \quad (4.11)$$

$$\equiv MOH + F^- \leftrightarrow MF + OH^- \quad (4.12)$$

$$\equiv M(OH)_2^- + 2F^- \leftrightarrow MF_2 + 2OH^- \quad (4.13)$$

Where ≡ M represent Metal in the adsorbent surface (Mn, Si, and Al).

© University of Venda

University of Venda
Creating Future Leaders

4.7 Comparison of Mn^{2+} modified bentonite adsorption capacity with other reported adsorbents

Comparison of the adsorption capacity of Mn^{2+} modified bentonite is presented in Table 4.8. From the table it can be noted that Mn^{2+} modified bentonite has low adsorption capacity for fluoride compared to other adsorbent. In their preliminary study, Kamble *et al.* (2009) also report that Mn^{2+} modified bentonite has low adsorption capacity.

Table 4.8: Comparison of different adsorption capacities of different adsorbents for fluoride

Adsorbent	Adsorption capacity (mg/g)	Experimental conditions	Reference
Mg^{2+} bentonite clay	2.25	pH 2-10, 5 mg/L initial F^-	Thakre *et al.* (2010)
Ceramic adsorbent	2.16	pH 4, 10 mg/L initial F^-	Chen *et al.* (2010)
Fe^{3+} bentonite clay	2.91	pH 2, 20 mg/L initial F^-	Gitari *et al.* (2013)
Alum bentonite	5.7	pH 2-10, 60 mg/L initial F^-	Vhahangwele *et al.* (2014)
Mn^{2+} bentonite	0.25	pH 2, 3 mg/L initial F^-	Present study

4.8 Conclusions

Bentonite clay was successfully modified by intercalation of Mn^{2+} in the interlayers through ion exchange. Mineralogical characterization revealed main mineral phase in raw and Mn^{2+} bentonite is montmorillonite. Elemental characterization showed that silica and alumina are the main components in bentonite clay. Mn loading onto raw bentonite was very low and this is attributed to the exchange rate of Mn^{2+} ions with the exchangeable ions in bentonite clay. Mn^{2+} intercalation increased the surface area and the pore volume of the bentonite clay. pH_{pzc} of Mn^{2+} bentonite clay was observed to be higher than that of raw bentonite. Optimum conditions for adsorption of F^- were established to be 30 min contact time, 1.0 g/100 mL adsorbent dosage, 3 mg/L adsorbate concentration and pH of 2. A maximum F^- removal of 84.0% was achieved at the optimized batch conditions. Co-existing ions decreased the percentage fluoride removal. Regeneration study revealed that Mn^{2+} bentonite can be successfully regenerated with 0.1 M NaOH. Leaching assessment showed that there is minimal release of chemical species from the adsorbent at various pH levels. The adsorption isotherm data fitted well to Langmuir model suggestion a monolayer adsorption. Kinetic modelling suggested chemisorption as the main mechanism of F^- adsorption. Adsorption of F^- was observed to be a complex process involving external and internal particle diffusion. Fluoride adsorption onto Mn^{2+} bentonite occurred via

© University of Venda

University of Venda
Creating Future Leaders

ligand exchange at lower pH and ion exchange at higher pH. Mn^{2+} bentonite clay showed low F^- adsorption capacity compared to other adsorbent. The optimal adsorption capacity was at low pH which would limit application in rural areas due to requirement for pH adjustment. This aspect should be investigated further in a bid to improve its adsorption capacity at wide pH range.

© University of Venda

University of Venda
Creating Future Leaders

References

Chen, N., Zhang, Z., Feng, C., Li, M., Zhu, D., Chen, R. & Sugiura, N., 2010. An excellent fluoride sorption behavior of ceramic adsorbent. *Journal of Hazardous Materials,* 183, pp.460–465

Chen, N., Zhang, Z., Feng C., Li M., Zhu D., Sugiura N., 2011. Studies on fluoride adsorption of iron-impregnated granular ceramics from aqueous solution. *Journal of material and physics*, 125, pp. 293-298.

Department of Water Affairs and Forestry (DWAF). 1996. South African Water Quality Guidelines for Domestic Use, 1st ed., Department of Water Affairs and Forestry, Pretoria. Available from: www.dwaf.gov.za.

Ghosh, A., Pal, M., Biswasb, K., Ghosh, U. C., & Manna, B. 2015. Manganese oxide incorporated ferric oxide Nano composites (MIFN): A novel adsorbent for effective removal of Cr(VI) from contaminated water. *Journal of Water Process Engineering*, 7, pp. 176–186

Gitari W. M., Ngulube T, Masindi V., & Gumbo J. R., 2013. Defluoridation of groundwater using Fe^{3+}- modified bentonite clay: Optimization of adsorption condition. *Desalination & water treatment*., pp 1-13.

Jia Y., Zhu B. S., Zhang K. S., Jin Z., Luo T., Yu X. Y., Kong., L. T., & Liu J. H., 2015. Porous 2-line ferrihydrite/byerite composite (LFBC): Fluoride removal performance and mechanism. *Chemical Engineering Journal,* 268, pp. 325-336.

Kamble, S. Dixit, P. Rayalu, S. S. & Labhsetwar, N. K., 2009. Defluoridation of drinking water using chemically modified bentonite clay. *Desalination and water treatment journal,* 249, pp.687-693.

Loganathan, P., Vigneswaran, S., Kandasamy, J. & Naidu, R., 2013. Review: Defluoridation of drinking water using adsorption processes. *Journal of Hazardous Materials*, 248 (249), pp.1–19.

Ma, Y., Wang, S. G., Fan, M., Gong, W. X. & Gao, B. Y., 2012. Characteristics and defluoridation performance of granular activated carbons coated with manganese oxides. *Journal of Hazardous Materials*, 168, pp1140–1146

Meenakshi, S. K. & Maheshwari, R. C., 2006. Fluoride in drinking water and its removal. *Journal of Hazardous Matter,* 137(1), pp. 456-463

Mudzielwana R., 2014. Defluoridation of groundwater using Mn^{2+} bentonite: preliminary study. Honours mini-dissertation submitted at University of Venda, School of Environmental Sciences.

© University of Venda

University of Venda
Creating Future Leaders

Nur, T., Loganathan, P. Nguyen, T. C., Vigneswaran, S., Singh, G. & Kandasamy J., 2014. Batch and column adsorption and desorption of fluoride using hydrous ferric oxide: Solution chemistry and modelling. *Chemical Engineering Journal*, 247, pp. 93–102.

Oladoja N. A. & Helmreich B., (2014) Batch defluoridation appraisal of aluminium oxide infused diatomaceous earth. *Chemical Engineering Journal*. 258: 51–61

Sun, Y., Fang, Q. Dong, J., Cheng X, & Xu, J., 2011. Removal of fluoride from drinking water by natural stilbite zeolite modified with Fe (III) *Desalination*, 277, pp. 121–127.

Thakre, D., Rayalu, S., Kawade, R,. Meshram, S., Subrt, J. & Labhsetwar, N., 2010. Magnesium incorporated Bentonite clay for defluoridation of drinking water. *Journal of Hazardous Materials,* 180, pp.122-130.

Toor M., Jin B., Dai S., Vimonoses V., 2014. Activating natural bentonite as a cost effective adsorbent for removal of Congo red in waste water, *J. industrial & engineering chemistry*, 1979, pp. 1-9.

Vhahangwele, M., Mugera, G.W., Tholiso, N., 2014. Defluoridation of drinking water using Al^{3+}-modified bentonite clay: optimization of fluoride adsorption conditions. *Toxicol. Environ. Ch*em. 96, 1–16.

World Health Organzation, 2011. *Guideline for drinking water, world health organization.* Geneva.

Yi, Z., Ying, X., Hao, C., Bingjie., L, Xiang, G., Dongfeng., W, & Peng., L. (2014). La (III)-loaded bentonite/chitosan beads for defluoridation from aqueous solution. *Journal of Rare Earths*, 32 (5), 2014, pp. 458.

Zhang, Y., Zhao Y., Zhu, Y., Wu, H., Wang, H., & Lu, W., 2012. Adsorption of mixed cationic-nonionic surfactant and its effect on bentonite structure. *Journal of Environmental Sciences,* 24(8), pp.1525–1532

Zhang, Z., Tan, Y. & Zhong, M., 2011. Defluoridation of wastewater by calcium chloride modified natural zeolite. *Desalination*, 276, pp. 246–252

© University of Venda

University of Venda
Creating Future Leaders

Chapter 5: Surface coating of NaOH activated bentonite with MnO_2 and its potential application on groundwater defluoridation

Abstract

Presence of fluoride ion in groundwater has drawn worldwide attention due to its considerable impact on human health. The assimilation of water containing fluoride concentration greater than 1.5 mg/L may lead to dental fluorosis and still higher may lead to major health hazards such as skeletal fluorosis. This work aims at the synthesis of MnO_2 coated bentonite and to evaluate its implication on fluoride removal. Bentonite clay was activated using NaOH and then coated with MnO_2 through *in-situ* reduction of $KMnO_4$. Physicochemical and mineralogical properties of the adsorbent were evaluated using XRD, XRF, BET, SEM, FTIR and pH_{pzc}. XRD showed that coating Na-bentonite leads to formation of new minerals such as, Jacobsite, cryptomelane and pyrolusite. Optimum conditions (contact time, adsorbent dosage, Initial concentration and pH) for fluoride removal were evaluated using batch experiments and optimized. Optimum conditions were found to be, 30 min contact time at 250 rpm, 1.5 g/100 mL adsorbent dosage, 5 mg/L adsorbate concentration, and pH of 8. Maximum F^- removal of ≈94.66% was achieved under optimum conditions. The adsorption data fitted well to Langmuir adsorption isotherm while the kinetics data fitted well to pseudo second order of reaction kinetics. Intra-particle diffusion model of Weber-Morris indicated that the removal of fluoride by MnO_2 coated Na-bentonite is a highly complex process, involving boundary layer diffusion and intra-particle diffusion as well as equilibrium adsorption. Sorption of fluoride occurred via ligands exchange mechanism at pH below 3 and at pH above 3 it occurred via ion exchange mechanism. The regeneration study showed that MnO_2 coated Na-bentonite can be successfully regenerated up to 5th cycle with 0.1 M NaOH. When applied to the groundwater MnO_2 coated bentonite was able to remove fluoride from 5.4 mg/L up to 0.98 mg/L. The toxicity assessment showed that MnO_2 coated Na-bentonite leaches out Mn ions which can result in secondary contamination. The study recommends that MnO_2 coated Na-bentonite can be used for defluoridation of groundwater in areas where no alternative sources of safe clean water are available and it recommend that further studies should be carried out to make MnO_2 coated Na-bentonite more stable.

Keywords: *MnO_2 coated bentonite, adsorption, groundwater, adsorption isotherms and kinetics.*

© University of Venda

5.1 Introduction

The presence of elements such as fluoride in high concentration in drinking water is a serious concern from the health point of view. Fluoride is classified as one of the major contaminants of water for human consumption by the Word Health Organization (WHO, 2011). The consumption of water containing fluoride concentration above 1.5 mg/L for extended period of time may lead to dental fluorosis and still higher concentrations lead to major health hazards such as deformation of bones (skeletal fluorosis) (Ncube and Schutte, 2005). In South Africa dental fluorosis has been observed in provinces such as, Limpopo, North West, Mpumalanga, Kwazulu Natal and Northern Cape (Ncube and Schutte, 2005; Odiyo and Makungo, 2012). Fluorosis is an incurable disease and as such efforts should be directed towards prevention. In trying to reduce the effect of fluoride, World Health Organization (WHO) has set a standard for fluoride concentration in water at 1.5 mg/L (WHO, 2011) while South African water standard is also set at 1.5 mg/L (DWAF, 1996). Ncube and Schutte (2005) suggested that areas with fluoride concentration above the permissible limit will require defluoridation. They further recommended that proper research must be initiated into investigating cheap and technologically simple processes for small-scale removal of fluoride from fluoride rich groundwater or developing alternative methods of fluoride free water supply in such areas. Chapter 3 and 4 discussed the application of black smectite rich clay soils from Mukondeni and Mn^{2+} modified bentonite in defluoridation of groundwater respectively. The two adsorbents showed higher percentage fluoride removal at acidic pH of 2 which limit their application for defluoridation of groundwater in rural area. There is therefore need to develop a high adsorption capacity fluoride adsorbents based on locally available clay materials which can show high fluoride binding capacity at wide range of pH and which also offer the advantage of large surface area. Coating adsorbents with MnO_2 increased the surface area of the adsorbent and MnO_2 coated adsorbent showed higher fluoride binding efficiency at wider range of pH (Teng *et al.,* 2009; Li *et al.,* 2013). The objectives for this section were therefore: (i) to activate bentonite clay with dilute NaOH this was done with the aim of exchanging anions in the clay soil with Na ions, (ii) to optimise conditions for coating activated bentonite with MnO_2, (iii) to evaluate the physicochemical and mineralogical properties of the modified bentonite, (iv) to evaluate optimum conditions for removing fluoride using MnO_2 coated bentonite, its regeneration and reuse potential.

© University of Venda

University of Venda
Creating Future Leaders

5.2 Material and Methods

5.2.1 Sample collection

Bentonite clay used in this project was collected from ECCA pty (Ltd) in Cape Town. Field water was collected from a community borehole in Siloam, Vhembe district in South Africa. All reagents including TISAB-III were obtained from Rochelle Chemicals and Lab Equipment CC, South Africa Ltd. A stock solution containing 1000 mg/L fluoride was prepared by dissolving 2.21 g analytical grade sodium fluoride in 1 L of ultra-pure water (18.2 MΩ/cm). Fluoride solutions for batch experiments were prepared from fresh stock fluoride solution by appropriate dilution.

5.2.2 Adsorbent preparation

MnO_2 coated bentonite was prepared as follows: prior coating, optimum conditions of activating bentonite with NaOH i.e. contact time and NaOH concentrations were evaluated using batch experiments. The obtained Na-bentonite was then coated in-situ through the reduction of $KMnO_4$ with HCl.

5.2.2.1 Optimising condition for activating bentonite clay with NaOH

Optimum conditions such as contact time and concentration were evaluated using batch experiments. To evaluate contact time, 100 mL of 0.1 M NaOH was pipetted into five bottles of 250 mL then 0.1 g of bentonite clay was added to make S/L ratio of 0.1 g/100 mL. The mixture was agitated for 5, 15, 30, 60, 120 min on a table shaker at 250 rpm shaking speed. After agitation the samples were filtered through 0.45 µm pore filter membrane. Samples were then analysed for F^-, Cl^- and SO_4^{2-} using Ion Chromatography (Metrohm 850 professional IC). The concentration of Na, Ca, Mg, K, Al, Si, Fe, Mn and other metals were analysed using inductively coupled plasma-mass spectrometer (ICP-MS). To evaluate the effect of NaOH concentration, 0.1, 0.3 and 0.5 M NaOH were prepared by dissolving known mass of NaOH pellets in 1 L. Thereafter 100 mL of each concentration was pipetted into three bottles of 250 mL, mixtures were agitated for 15 min at 250 rpm on a table shaker. After agitation samples were treated and analysed as above mentioned procedure. The obtained bentonite was then termed Na-bentonite.

© University of Venda

University of Venda
Creating Future Leaders

5.2.2.2 Optimizing conditions for coating Na-bentonite with MnO_2

In order to prepare MnO_2 coated Na-bentonite, the following parameters were optimized: Concentration, Na-bentonite clay amount and reaction time. To evaluate effect of $KMnO_4$ concentration various concentration of $KMnO_4$ (1.5, 3, 4.5 and 6 M) were prepared by dissolving appropriate amount of $KMnO_4$ in 20 mL of distilled water in beaker and kept in a water bath at 90° C for 15 min. To this 5 g of Na-bentonite was added and the suspension was mixed gently and heated in a water bath and kept in water bath for 10 min. Then 250 mL of 2 M HCl was added and suspension was stirred at 300 rpm on a magnetic stirrer, followed by water bath heating for 30 min under continuous stirring. The formation of Manganese oxide can be explained through equation 5.1 (Taffarel *et al.*, 2010):

$$2KMnO_4 + 8HCl \leftrightarrow 2MnO_2 + 2KCl + 3Cl_2 + 4H_2O \quad (5.1)$$

After the completion of reaction, mixtures were left for 15 min to cool and then filtered through 0.45 µm cellulose filter membrane, obtained residues were further rinsed with 0.05 M perchloric acid and distilled water until the runoff was clear and then dried in an oven at 110 °C for 6 hr. To find optimum concentration of $KMnO_4$ for coating Na-bentonite with MnO_2, batch defluoridation experiments were conducted. In order to evaluate the effect of clay dosage, clay dosage was varied from 2.5 to 10 g. and to evaluate the effect of reaction time, time was varied from 30 to 120 min. Samples prepared and treated following the procedure used to evaluate concentration.

5.2.2.3 Synthesis of MnO_2 coated Na-bentonite

MnO_2 coated bentonite was prepared as follows: prior to the coating procedure bentonite clay was converted to its Na form by suspending 12 g of bentonite in 300 mL of 0.1 M NaOH solution. The mixture was agitated for 15 min, after agitation the suspension was centrifuged for 10 min at 2 500 rpm, the obtained residues were then rinsed with MILLIQ water (18.2 MΩ/cm) and then dried at 110 °C for 12 hrs in the oven. Resulting Na-bentonite was then coated with MnO_2 through *in-situ* reduction of $KMnO_4$ with 2 M HCl. Concentration of 1.5 M $KMnO_4$ was prepared by dissolving 5.0 g of $KMnO_4$ in 20 mL of distilled water in 500 mL beaker and kept in a water bath at 90 °C for 15 min. To this 2.5 g of Na-bentonite was added and the suspension was mixed gently and kept in a water bath for 5 min. To this 300 mL of 2 M HCl was then added and the mixture was then vigorously stirred at 300 rpm using a magnetic stirrer followed by

© University of Venda

University of Venda
Creating Future Leaders

continuous heating in a water bath at 90 °C for 60 min under continuous stirring. After the completion of reaction, mixtures were left for 15 min to cool. pH of the mixture was measured and found to be 3.2. The mixture was then filtered through 0.45 µm pore cellulose filter membrane, obtained residues were further rinsed with 0.05 perchloric acid and distilled water until the runoff was clear and then dried in an oven at 110 °C for 12 h in the oven. Obtained MnO_2 coated Na-bentonite was then milled to pass through <250 µm sieve and stored in lockable sample bags.

5.2.3 Physiochemical and mineralogical characterization

Mineralogical and chemical composition of MnO_2 bentonite clay was evaluated using XRD and XRF techniques respectively. Surface morphology was determined using Scanning electron microscopy (SEM) (Leo1450 SEM, at 10Kv, working distance 14mm). Functional groups and surface chemistry was determined using Fourier transform infrared spectroscopy (FTIR). Surface area and pore volume was determined by Brunauer Emmet Teller (BET) method using micrometrics TriStar II. The surface charge and point of zero charge (PZC) was determined using solid addition method as described by Kumar *et al.* (2011).

5.2.4 Batch defluoridation experiments

Batch experiments were carried out to evaluate the effects of contact time, effect of adsorbent dosage, adsorbate initial concentration and the effect of pH on fluoride adsorption. The fluoride concentration in the treated samples was measured using an ion selective electrode 9609 BNWP Orion (USA) attached to Thermo Scientific Orion Star ISE/pH/EC meter. Similar ion meter coupled with pH and EC electrode was used for measuring pH and EC of the treated samples. For residual fluoride, ion selective electrode was calibrated with four standards containing 1 mL of total ionic strength buffer (TISAB III) per 10 mL of solution. Same ratio was maintained for the sample. TISAB was added to decomplex F^- from Al^{3+}, Fe^{3+} and Si^{4+} fluorocomplexes and to maintain pH at between 5.2 and 5.5. Metrohm 850 professional IC was used to measure other anionic species concentration and Inductively Coupled Plasma-Mass Spectrometer (ICP-MS) was used to measure cationic species. All experiments were conducted in triplicate for better accuracy and the mean values were reported. Equation 5.2 and 5.2 were used to calculate the percentage removal and adsorption capacity respectively.

$$\%\, removal = \left(\frac{C_o - C_e}{C_o}\right) \times 100 \qquad (5.2)$$

© University of Venda

University of Venda
Creating Future Leaders

Where: Co is initial fluoride ion concentration and Ce is equilibrium fluoride ion concentration.

$$Q = \left(\frac{C_o - C_e}{m}\right) \times v \quad (5.3)$$

Where: C_o= initial F^- concentration (mg/L), C_e = F^- concentrations at equilibrium (mg/L),

V = Volume of solution (L) and m = Weight of the adsorbent (g)

5.2.5 Regeneration of MnO_2 coated Na-bentonite clay

Regeneration of the adsorbent was carried out as follows; 1.5 g of fluoride loaded clay was agitated with 100 mL of 0.1 M NaOH for 30 min on a Table shaker. NaOH was used because the material was not stable and effective for reuse when regenerating with other solutions. After agitation, the adsorbent was filtered through 0.45 µm pore membrane filter and the filtrate was diluted to 100 mL and then analysed for desorbed fluoride. The collected adsorbent on filter membrane was washed with MILLIQ water and then dried at 110 °C for 3 hrs. Regenerated adsorbent was then re-used for defluoridation for up to five times.

5.3 Results and discussion

5.3.1 Optimizing conditions for activating bentonite with NaOH

5.3.1.1 Effect of contact time

Figure 5.1 shows the concentration of anionic and cationic species leached from bentonite clay during activation of bentonite with NaOH. Results showed that the leaching of both anionic and cationic species was high at initial 15 min contact time and decrease at time > 15 min. Therefore 15 min was then chosen to be the optimum contact time for the subsequent experiments.

© University of Venda

University of Venda
Creating Future Leaders

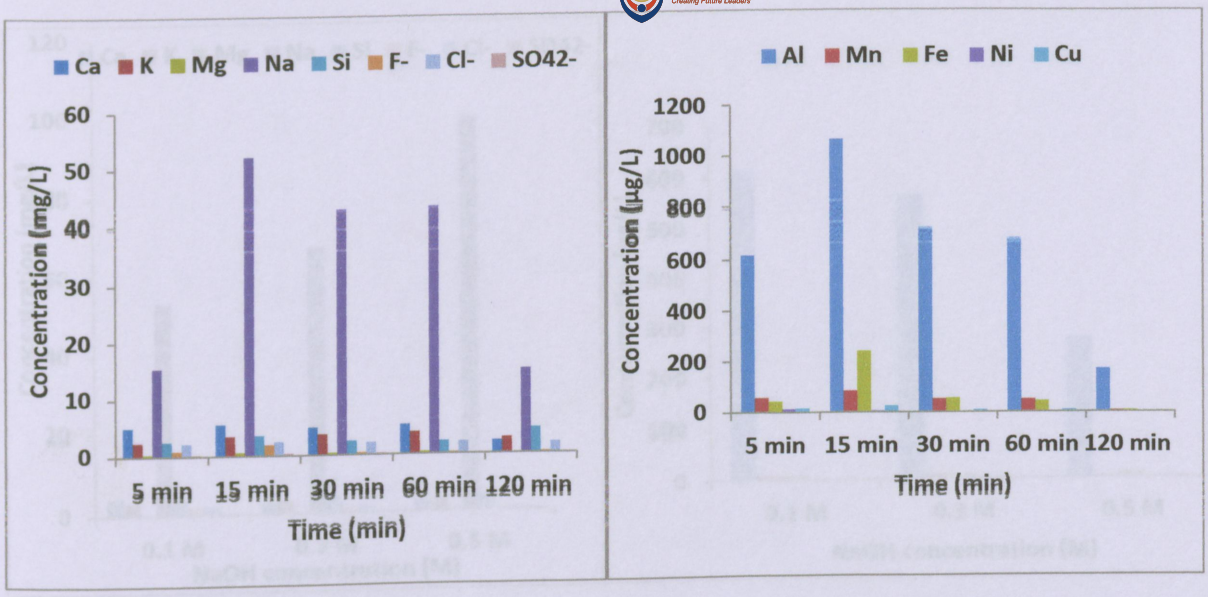

Figure 5.1: Variation of species concentration in mg/L and µg/L with contact time (0.1 M NaOH concentration, 0.1 g/100 mL adsorbent dosage).

5.3.1.2 Effect of concentration

Figure 5.2 showed the effect of concentration on the leaching of chemical species from bentonite clay. From the results it was observed that as the concentration increases from 0.1 to 0.5 M, the concentration of both anionic and cationic species decreases except for Na which increased with increased concentration which may be due to the increase in Na added in the form of NaOH at higher concentration. Therefore 0.1 M NaOH concentration was then chosen to be the optimum concentration for activating bentonite clay.

© University of Venda

University of Venda
Creating Future Leaders

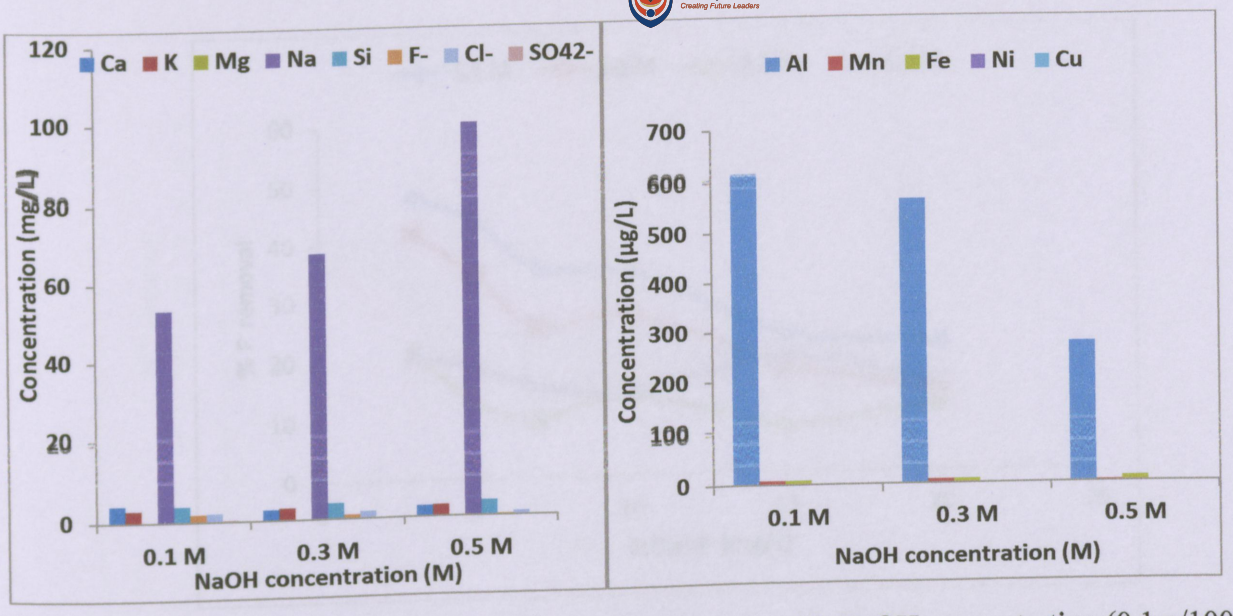

Figure 5.2: Variation of chemical species in mg/L and µg/L with NaOH concentration (0.1 g/100 mL adsorbent dosage and 15 min contact time).

Based on the above results the optimum conditions for activating bentonite with NaOH were concluded to be 15 min contact time and 0.1 M NaOH concentration.

5.3.2 Optimisation of conditions for coating Na-bentonite with MnO_2

5.3.2.1 Effect of $KMnO_4$ concentration

To find optimum concentration of $KMnO_4$ for coating Na-bentonite with MnO_2, clay prepared under different concentrations were subjected to defluoridation experiments. Various concentrations of F^- ranging from 3-20 mg/L were prepared by appropriate dilution from 1000 mg/L stock solution. 100 mL of F^- solution was pipetted into 250 mL and then 0.5 g of modified clay was added, mixtures were agitated for 30 min in a Table shaker at a speed of 250 rpm. The results are presented in figure 5.3 in terms of % F^- removal and initial fluoride.

© University of Venda

University of Venda
Creating Future Leaders

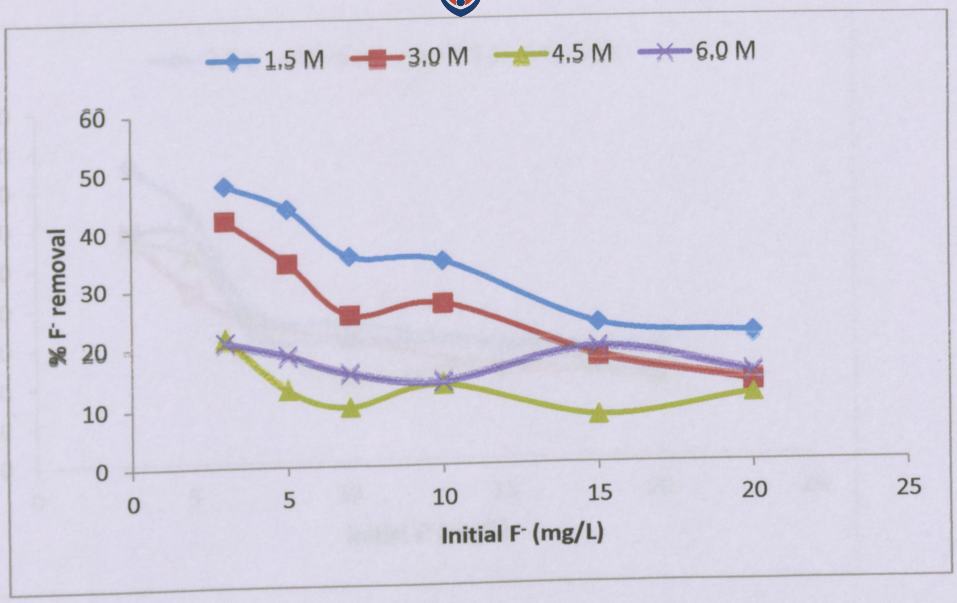

Figure 5.3: Variation of % F^- removal with initial fluoride concentration (1.5, 3.0, 4.5 and 6.0 M $KMnO_4$ concentration, 0.5 g/100 mL adsorbent dosage, 30 min contact time at 250 rpm and initial pH 5.54±0.5).

From the figure, it can be noted that % F^- removal of 1.5 M-MnO_2 coated Na-bentonite was fairly higher compared to clays coated at higher concentration of $KMnO_4$. 1.5 M $KMnO_4$ was then chosen to be the optimum for further experiments.

5.3.2.2 Effect of clay amount

To find optimum clay amount of $KMnO_4$ for coating Na-bentonite with MnO_2, clay prepared under different clay doses were subjected to defluoridation experiments. Various concentrations of F^- ranging from 3-20 mg/L were prepared by appropriate dilution from 1000 mg/L stock solution. 100 mL of F^- solution was pipetted into 250 mL and then 0.5 g of modified clay was added, mixtures were agitated for 30 min in a Table shaker at a speed of 250 rpm. The results are presented in figure 5.4 in terms of % F^- removal and initial fluoride.

© University of Venda

University of Venda
Creating Future Leaders

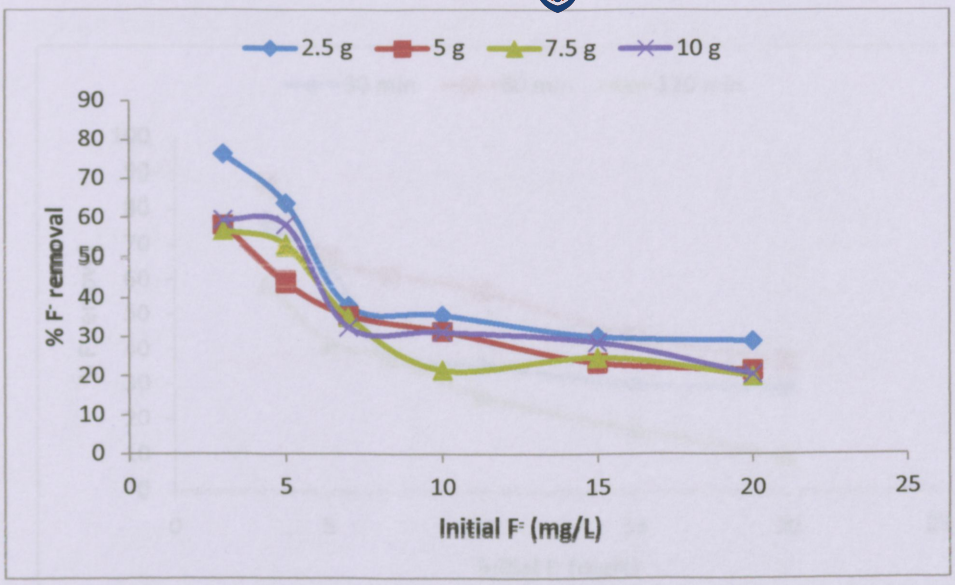

Figure 5.4: Variation of % F^- removal with initial fluoride concentration (Na-bentonite doses: 2.5, 5, 7.5 and 10 g. Adsorption conditions: 0.5 g/100 mL adsorbent dosage, 30 min contact time at 250 rpm and initial pH 5.54±0.5).

From fig 5.4 it can be observed that 2.5 g MnO_2 clay showed higher % F^- removal compared to higher dosages and it was then chosen to be optimum for the next experiment.

5.3.2.3 Effect of reaction time

To find optimum concentration of $KMnO_4$ for coating Na-bentonite with MnO_2, clay prepared under different concentrations were subjected to defluoridation experiments. Various concentrations of F^- ranging from 3-20 mg/L were prepared by appropriate dilution from 1000 mg/L stock solution. 100 mL of F^- solution was pipetted into 250 mL and then 0.5 g of modified clay was added, mixtures were agitated for 30 min in a Table shaker at a speed of 250 rpm. The results are presented in figure 5.5 in terms of % F^- removal and initial fluoride.

© University of Venda

University of Venda
Creating Future Leaders

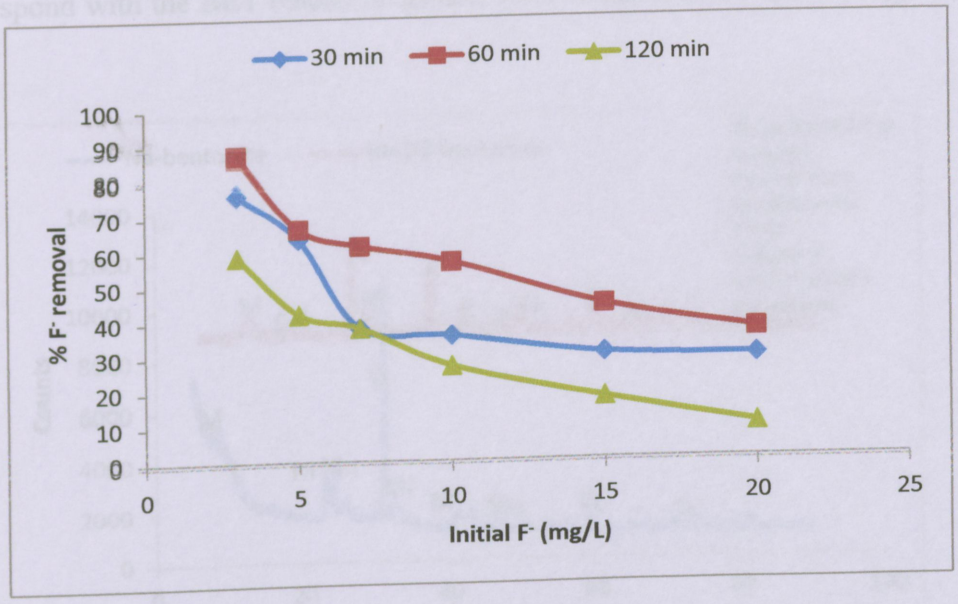

Figure 5.5: Variation of % F^- removal with initial fluoride concentration (reaction times for coating bentonite clay: 30, 60 and 120 min, Adsorption conditions: 0.5 g/100 mL adsorbent dosage, 30 min contact time at 250 rpm and initial pH 5.54±0.5).

It was observed during the experiment that for both initial concentrations 60 min MnO_2 clay showed higher percentage F^- removal compared to other clays and it was then chosen to be the optimum reaction time.

Based on the above results the following optimum conditions for coating Na-bentonite with MnO_2 were established: 1.5 M $KMnO_4$ concentration, 2.5 g clay amount and 60 min reaction time.

5.4 Physicochemical and mineralogical characterization

5.4.1 X ray diffraction analysis

XRD analysis was carried out to evaluate the change in mineralogical content of Na-bentonite after modification with manganese oxide. Figure 5.6 presents the XRD spectra of Na-bentonite and MnO_2 modified bentonite clay. The results showed that the Na-bentonite clay contains quartz, montmorillonite as the main minerals. After modification with manganese oxide analysis revealed that there was formation of new minerals such as cryptomelane (KMn_8O_{16}) jacobsite ($(Mn_6Fe_4)O_4$ and pyrolusite (MnO_2) in the Na-bentonite which are both the oxides of manganese. Interlayer spacing below 20 degree 2 theta shows the low crystallinity nature of the material and

© University of Venda

University of Venda
Creating Future Leaders

this correspond with the BET results in section 5.4.4 which showed that the clay is mesoporous in nature.

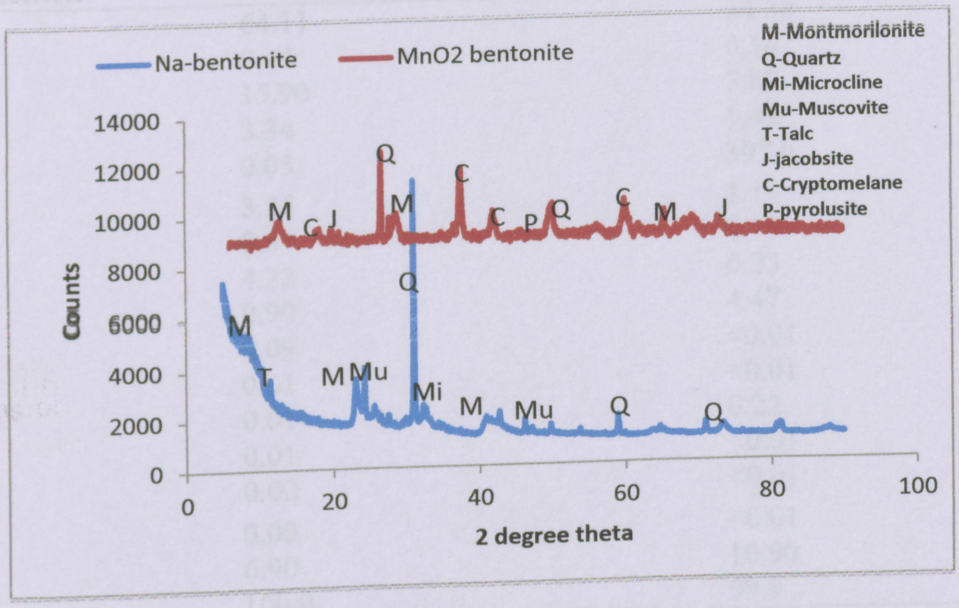

Figure 5.6: XRD spectra for Na-bentonite and MnO_2-bentonite.

5.4.2 X ray fluorescence

Table 5.1 shows the elemental composition of Na-bentonite and manganese oxide coated Na-bentonite respectively. The result shows that SiO_2 and Al_2O_3 are the main oxides of Na-bentonite followed by Na_2O, MgO and Fe_2O_3. After coating Na-bentonite with MnO_2 there was a decrease in major oxides which is may be attributed to their dilution due to the introduction of MnO_2 and increase in K_2O.

© University of Venda

University of Venda
Creating Future Leaders

Table 5.1: Elemental composition of Na-bentonite and MnO_2 coated Na-bentonite.

Composition	Na-bentonite	MnO_2 coated
SiO_2	64.11	34.30
TiO_2	0.44	0.16
Al_2O_3	15.90	7.80
Fe_2O_3	3.34	1.41
MnO	0.05	39.20
MgO	3.35	1.17
CaO	0.81	0.10
Na_2O	4.22	0.23
K_2O	0.90	4.47
P_2O_5	0.09	<0.01
Cr_2O_3	0.01	<0.01
NiO	0.01	0.22
V_2O_5	0.01	<0.01
ZrO_2	0.02	<0.01
CuO	0.00	<0.01
LOI	6.90	10.90
Total	100.0	99.9

5.4.3 Scanning Electron Microscopy

Figure 5.7 presents the morphology of Na-bentonite clay and MnO_2 coated Na-bentonite clay at 5 000x and 20 000x magnifications. The morphology of Na-bentonite is largely granular with irregular structures. After modification with MnO_2 the morphology appears largely fibrous coatings on the granules which indicate precipitates of manganese oxides on the surface of the clay. The qualitative SEM-EDS in Table 5.2 confirmed the presence of Mn (44.17%) on the surface of the MnO_2 coated bentonite clay. The analysis also revealed that coating Na-bentonite with MnO_2 decreased the concentration of the main elements of Na-bentonite this includes Si, Al, Na and Mg. However increase in K and Cl was observed which may be due to $KMnO_4$ and HCl used for coating. The results of quantitative EDS correspond with the XRF results, this is noted by the increase in chemical species of Mn and K and also a decrease in other such as Na, Al, Fe, C, and Si which was observed by both XRF and EDS. This confirms the intercalation of Mn ions into the clay surface.

© University of Venda

University of Venda
Creating Future Leaders

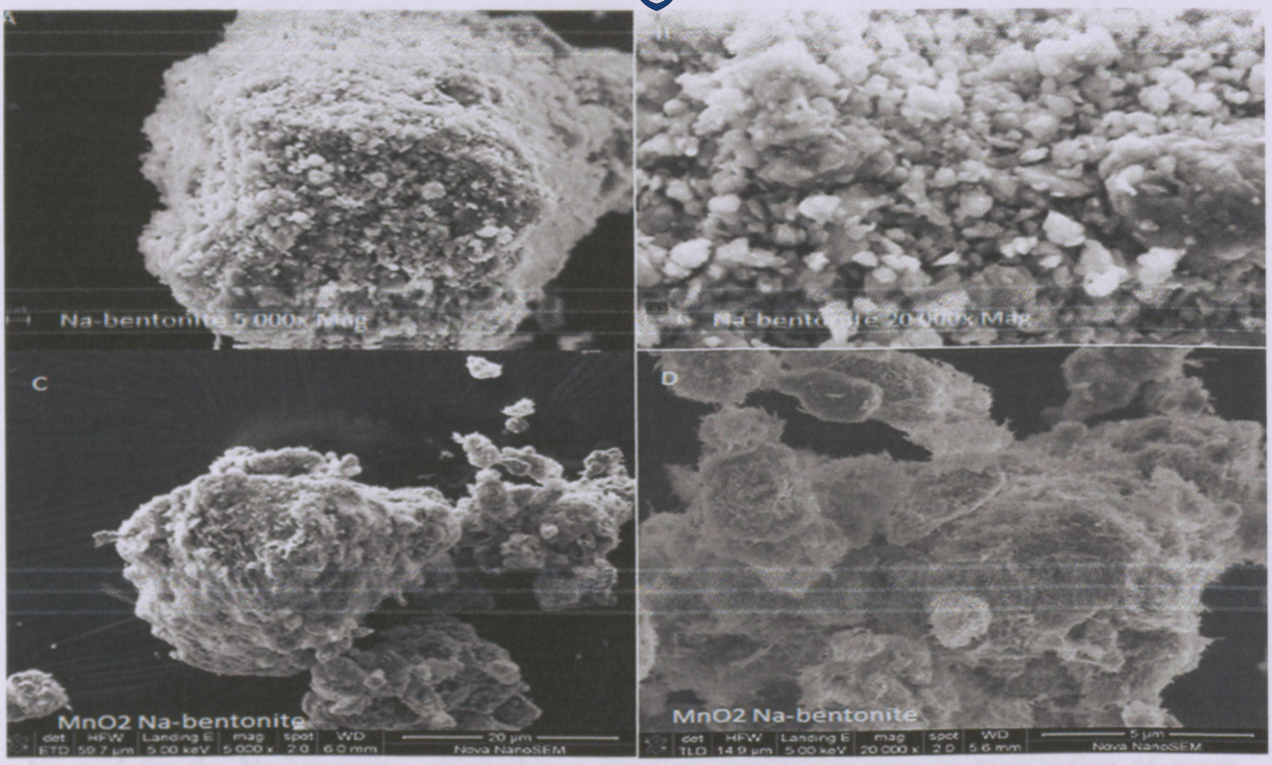

Figure 5.7: Surface morphology for Na-bentonite and MnO_2 coated bentonite.

Table 5.2: Qualitative SEM-EDS of Na-bentonite and MnO_2 coated Na-bentonite

Elements	Na-bentonite	MnO_2 coated
O	59.33	36.29
Si	26.57	10.51
Al	8.32	3.99
Na	4.07	-
Mg	2.65	-
C	13.20	-
Fe	1.73	-
K	0.95	3.23
Mn	-	44.17

© University of Venda

University of Venda
Creating Future Leaders

5.4.4 Surface area, pore distribution and pore volume

The surface area and pore distribution are the important physical properties of the adsorbent. In order to determine the surface area and pore distribution of the adsorbent, BET and BJH techniques were used and the results were reported in Table 5.3. After coating with MnO_2 the surface area of Na-bentonite increased from 29.03 m^2/g to 58.25 m^2/g which is two fold. An increase in the external surface area could be due to surface adsorption and surface precipitation of manganese oxides from solution. An increase in surface area makes the MnO_2 coated Na-bentonite clay a better adsorbent. Figure 5.8a and b shows the nitrogen adsorption-desorption curves and the pore distribution for Na-bentonite and MnO_2 coated Na-bentonite respectively. The N_2 adsorption-desorption curves for both Na-bentonite and the MnO_2 coated Na-bentonite in fig 5.8a displayed type IV type of isotherm with wider hysteresis loop at high relative pressures suggesting that both Na-bentonite and MnO_2 coated bentonite are mesoporous in nature. Similar isotherms were reported by Xu *et al.* (2013) for the hydrous manganese oxide. Fig 5.8b shows the pore distribution of Na-bentonite and MnO_2 coated Na-bentonite. The sharp peak was observed for the Na-bentonite which shows the pore size is monomodal distribution of pores meaning pore are almost of the same size with the average of 12.83 nm. The pore distribution curve for MnO_2 coated Na-bentonite showed that greater amount of pores lies between 17.35-100 Å (1.75 -10 nm) indicating that the pore size ranges from micro-mesoporous with the average 5.39 nm. Pore size of the Na-bentonite decreased after coating with MnO_2. Wang *et al.* (2012) also reported decrease in pore size for the MnO_2 coated bamboo charcoal. Modification of bentonite with Mn^{2+} and MnO_2 increased the surface area of the bentonite clay. However, the surface of Mn^{2+} bentonite is slightly higher compared to the surface area of MnO_2 coated bentonite. The pore diameter of the two materials is almost of the same structure and size, both ranging between 5.5 and 5.9 nm.

Table 5.3: Surface area, pore diameter and pore volume of Na bentonite and MnO_2 coated bentonite clay

	Surface area (m^2/g)	Pore diameter (nm)	Pore volume (cm^3/g)
Na-bentonite clay	29.03	12.45	0.092
MnO_2 coated	52.5142	5.91	0.11

© University of Venda

University of Venda
Creating Future Leaders

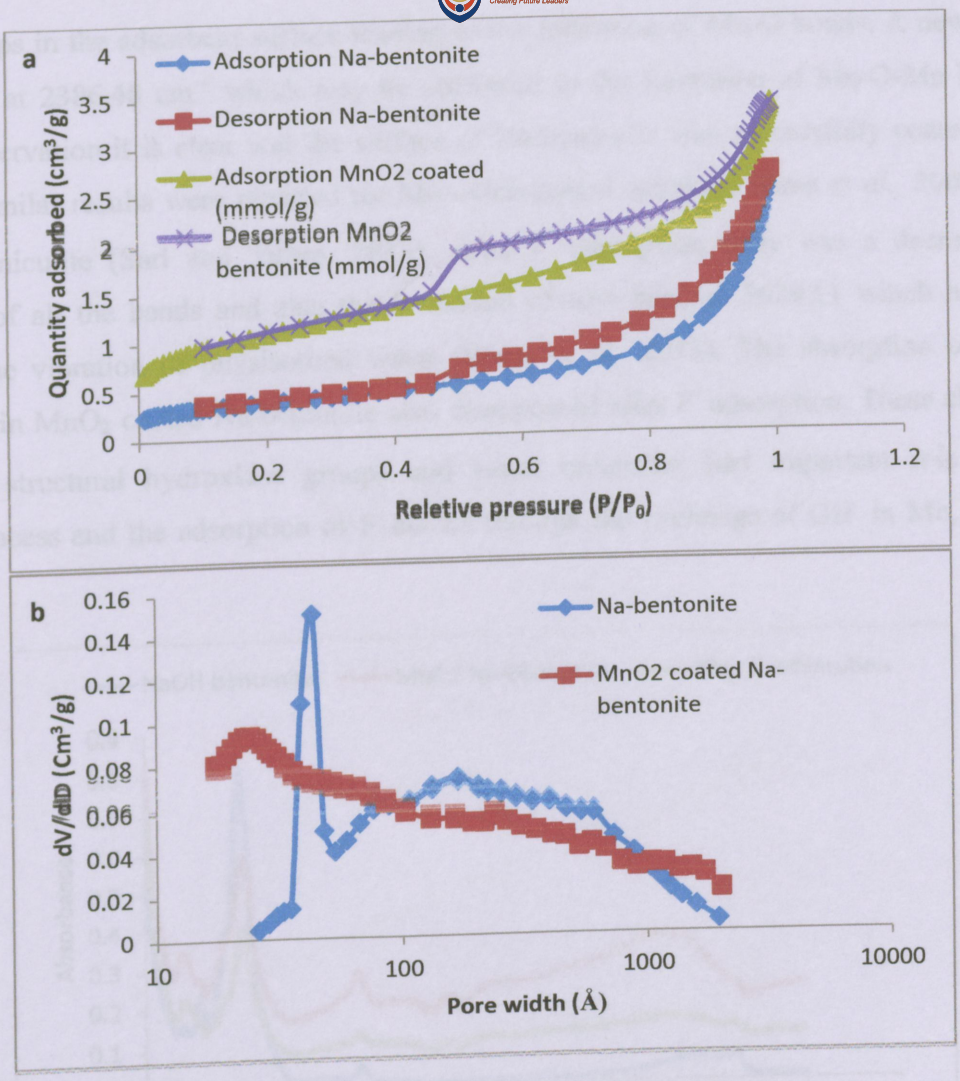

Figure 5.8: N_2 adsorption-desorption isotherms (a) and pore distribution (b).

5.4.5 FTIR analysis

FTIR was used for identification of functional groups of the adsorbent as well as for characterisation of the chemical interaction responsible for F^- adsorption. Figure 5.9 shows the FTIR spectra of Na-bentonite, MnO_2 coated Na-bentonite and F^- loaded MnO_2 coated Na-bentonite respectively. From the Na-bentonite in the main absorption band were observed at the wavelength range of 3628.25, 1649.35, 1037 and 797.73 which may be due to the vibration and stretching of H-O-H, Si-OH, Al-OH and Si-O-Al groups. The bands observed at lower wavelength range may be ascribed to the metal-oxygen-metal bonds vibrations. After coating Na-bentonite with MnO_2 there was a shift in these bands to 3343.36, 1626.70, 1040.64 and 713.40 cm^{-1} from 3628.25, 1649.35, 1037 and 797.73 cm^{-1}. Their transmission intensity also increased. This may be ascribed to the interaction between the Mn oxides and the silanol and

© University of Venda

University of Venda
Creating Future Leaders

aluminol groups in the adsorbent surface leading to the formation of Mn-O bonds. A new band was observed at 2386.48 cm^{-1} which may be attributed to the formation of Mn-O-Mn bonds. From this observation it is clear that the surface of Na-bentonite was successfully coated with MnO_2. The similar results were reported for Mn oxide coated bentonite (Eren *et al.*, 2009) and modified vermiculite (Sari and Tuzen, 2013). After F^- adsorption there was a decrease in transmission of all the bands and also the formation of new band at 3629.11 which may be ascribed to the vibration of physisorbed water (Wang *et al.*, 2013). The absorption band at 2386.48 cm^{-1} in MnO_2 coated Na-bentonite also disappeared after F^- adsorption. These changes indicate that structural hydroxides groups and water molecules had important role in F^- adsorption process and the adsorption of F^- occurs through the exchange of OH^- in Mn, Al, Si oxides for F^-.

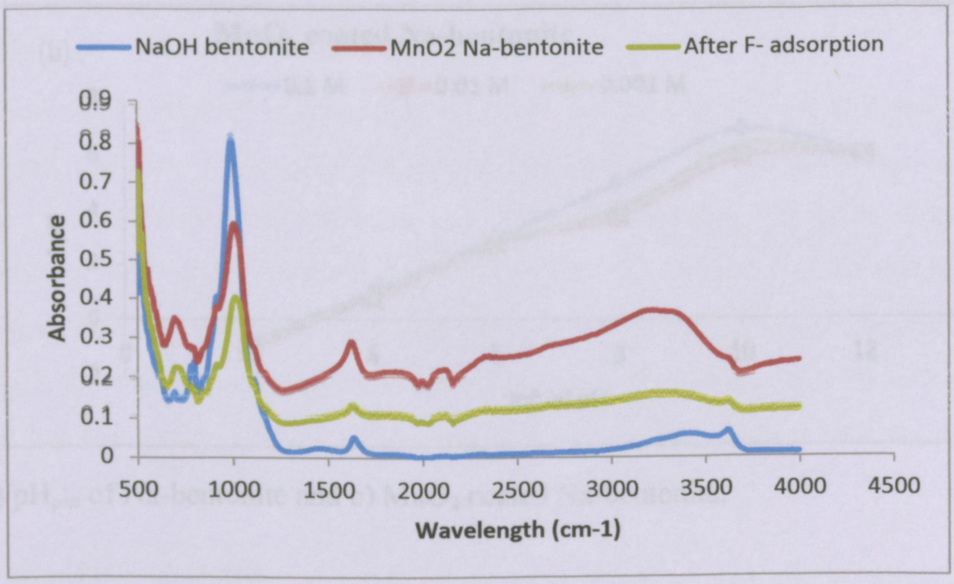

Figure 5.9: FTIR spectra of Na-bentonite, MnO_2 coated Na-bentonite and F^- loaded MnO_2 coated Na-bentonite.

5.4.6 Determination of pH point of zero charge (pH_{pzc})

Point of zero charge is the pH where the material has net zero surface charge. pH below the pH_{pzc} the clay surface is positively charged and above the clay surface is negatively charged. Figure 5.10a and b shows the pH_{pzc} of Na-bentonite and MnO_2 coated Na-bentonite respectively. It can be observed that coating Na-bentonite with MnO_2 decreased the pH_{pzc} of the clay from 8.4 to 3.0±0.2. Ma *et al.* (2012) and Teng *et al.* (2009) also reported low pH_{pzc} for MnO_2 coated adsorbents and it was attributed to acidic nature of the adsorbent. The pH_{pzc} helps to understand

© University of Venda

University of Venda
Creating Future Leaders

the region where the adsorption of F^- will be optimum. Adsorption of F^- onto MnO_2 coated Na-bentonite is likely to be optimum at pH below 3.0±0.2.

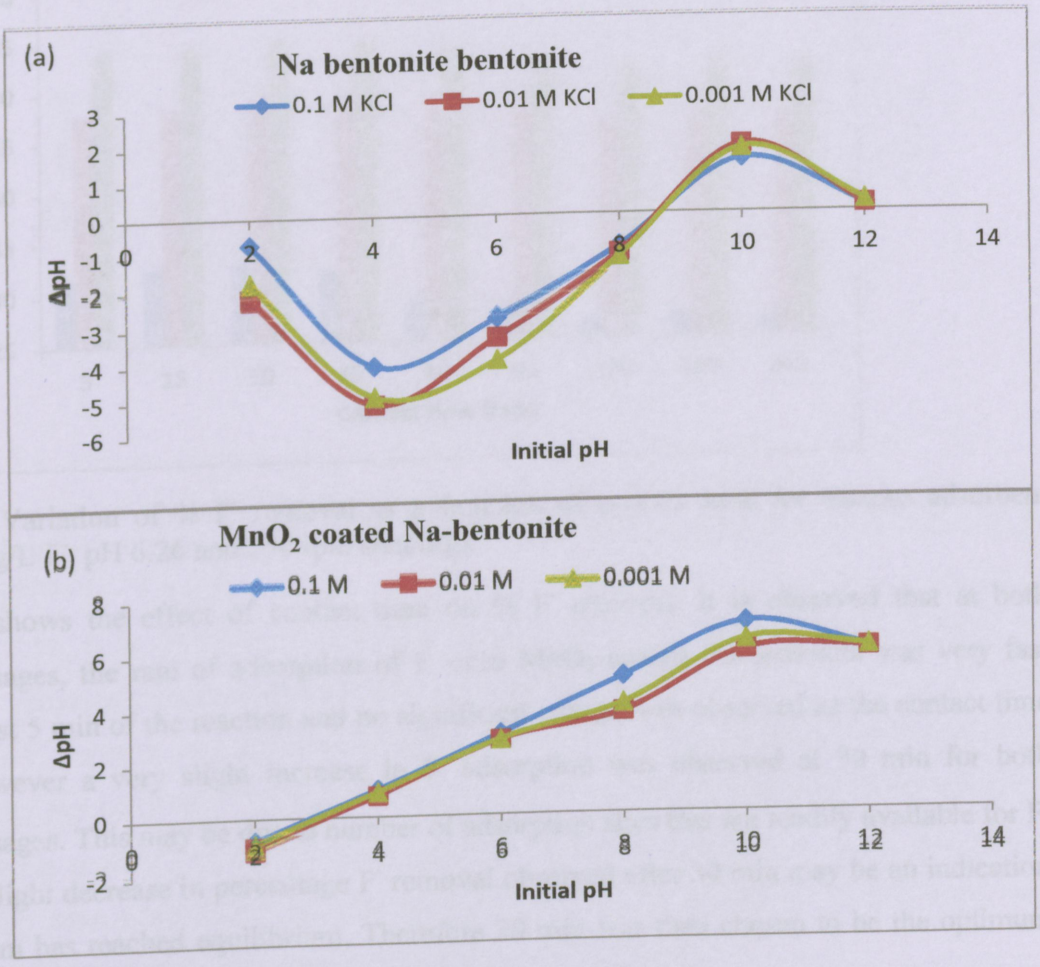

Figure 5.10: a) pH_{pzc} of Na-bentonite and b) MnO_2 coated Na-bentonite.

5.5 Batch defluoridation

5.5.1 Effect of contact time

The effect of contact time in the adsorption of F^- onto MnO_2 coated Na-bentonite clay was evaluated by varying contact time from 5 to 240 min at various adsorbent dosages (0.1 , 0.3 and 0.5 g/100 mL), 5 mg/L initial F^- concentration, initial pH of 6.26 and shaking speed of 250 rpm. Figure 5.11 presents the variation of % F^- removal with contact time.

© University of Venda

University of Venda
Creating Future Leaders

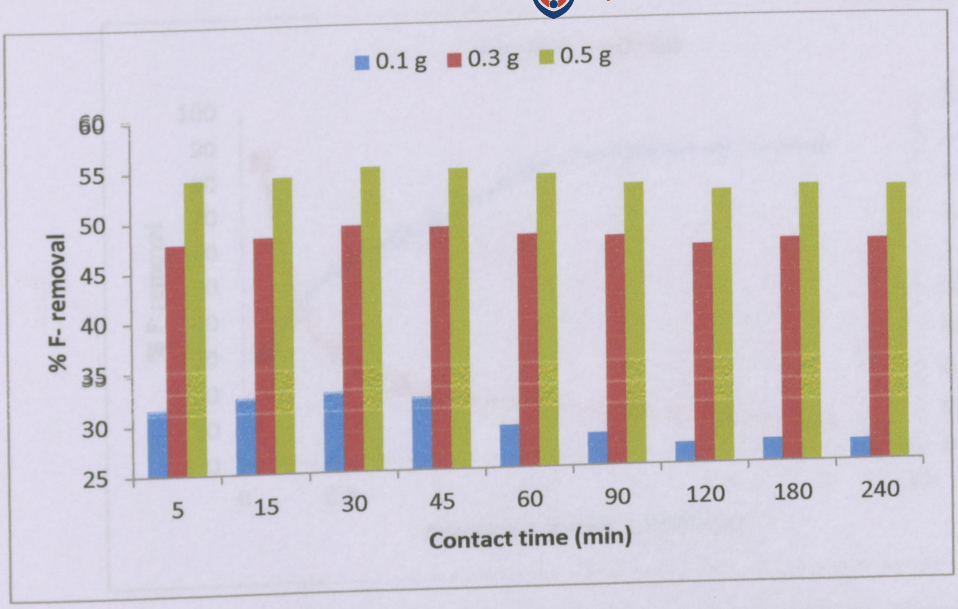

Figure 5.11: Variation of % F^- removal as a function of contact time for various adsorbent dosages (5 mg/L F^-, pH 6.26 and 250 rpm shaking).

Figure 5.11 shows the effect of contact time on % F^- removal. It is observed that at both evaluated dosages, the rate of adsorption of F^- onto MnO_2 coated Na-bentonite was very fast during the first 5 min of the reaction and no significant change was observed as the contact time increases however a very slight increase in F^- adsorption was observed at 30 min for both adsorbent dosages. This may be due to number of adsorption sites that are readily available for F^- adsorption. Slight decrease in percentage F^- removal observed after 30 min may be an indication that the system has reached equilibrium. Therefore 30 min was then chosen to be the optimum contact time for the subsequent experiments.

5.5.2 Effect of adsorbent dosage

The effect of adsorbent dosage on the adsorption of F^- onto MnO_2 coated Na-bentonite clay was evaluated at 30 min contact time at shaking speed of 250 rpm, 5 mg/L initial concentration of F^- and pH of 6.24. The adsorbent dosage was varied from 0.1 g/100 mL to 3 g/100 mL. The plot of percentage of fluoride removal and adsorption capacity against adsorbent dosage is presented in figure 5.12

© University of Venda

University of Venda
Creating Future Leaders

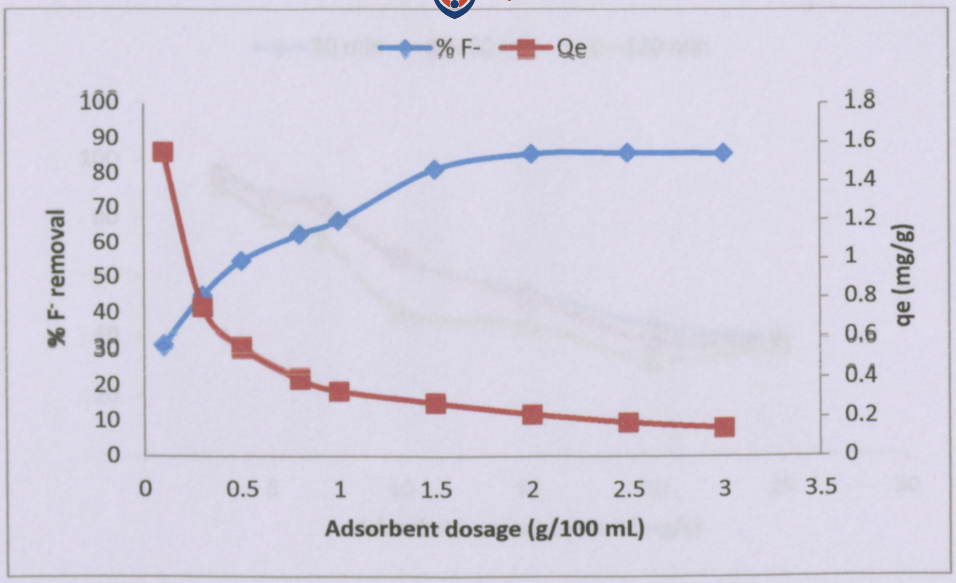

Figure 5.12: Variation % F^- removal and adsorption capacity by MnO_2 bentonite clay as a function of adsorbent dosage (contact time of 30 min, adsorbent dosage, 5 mg/L F^-, pH of 6.24 and shaking speed of 250 rpm).

From figure 5.12, it is observed that for the fixed initial F^- concentration of 5 mg/L the percentage F^- removal increased with increase in adsorbent dosage from 0.1 to 1.5 g /100 mL where 81.24% F^- removal was achieved. However further increase in sorbent dose did not show any remarkable increase in % F^- removal. This may be attributed to high density of the adsorbent particles limiting mobility of the F^- hence limiting access to adsorption sites. Adsorption capacity on the other hand decreased with increasing dosage. A dosage of 1.5 g/100 mL was adopted as the optimum adsorbent dosage for subsequent experiments.

5.5.3 Effect of initial adsorbate concentration

Effect of adsorbate concentration was evaluated by varying initial concentration from 3 mg/L to 25 mg/L at 30, 60 and 120 min contact time at 250 rpm shaking speed and 1.5 g/100 mL dosage. Results in percentage F^- removal are presented in figure 5.13.

© University of Venda

University of Venda
Creating Future Leaders

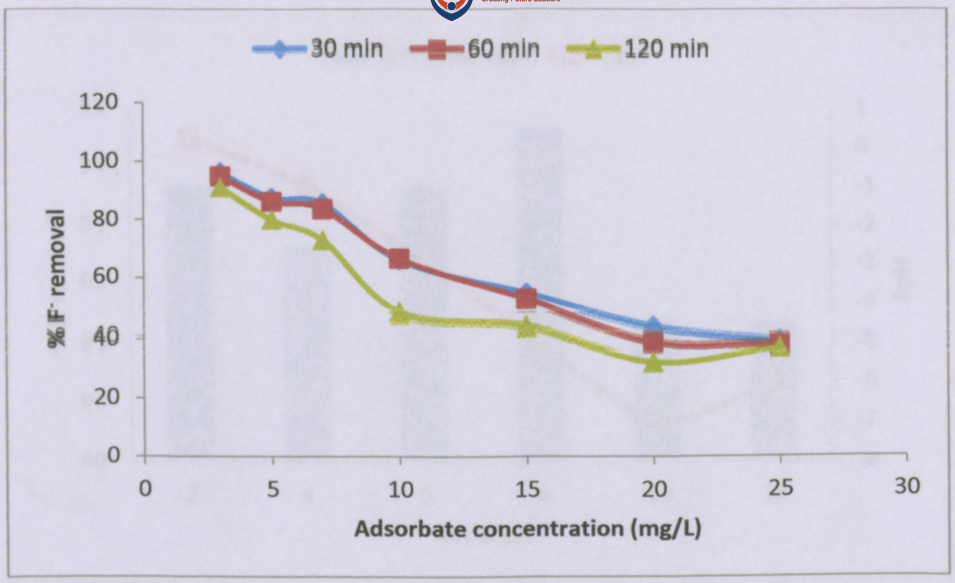

Figure 5.13: Variation of % F^- removal with initial concentration at various contact time (adsorbent dosage 1.5 g/100 mL, pH 5.54 and shaking speed of 250 rpm).

From the figure it can be observed that the % F^- removal decreased with increase in initial concentration and reached a plateau at initial concentration above 20 mg/L indicating that the adsorbent was saturated. This was observed at all contact times. The decrease may be attributed to decrease in the binding capacity of the adsorbent as the concentration increases (Thakre *et al.*, 2010). The percentage of removal remained almost equal for 30 min and 60 min contact times and decreased at 120 min. This was earlier observed in the contact time experiments where maximum absorption was at 30 min. Therefore 5 mg/L was then chosen to be the optimum initial adsorbate concentration for subsequent experiments. This was chosen because in Limpopo groundwater in most of the areas has F^- concentration below 5 mg/L.

5.5.4 Effects of pH

To evaluate the effect of pH on F^- removal, 100 mL of 5 mg/L solution was pipetted into six bottles of 250 mL each, 1.5 g was added and the initial pH of the mixture was adjusted to values ranging from 2 to 12 using 0.1 M NaOH and 0.1 M HCl. Mixtures were then agitated for 30 min at 250 rpm. The results are presented in figure 5.14 in terms of % F^- removal.

© University of Venda

University of Venda
Creating Future Leaders

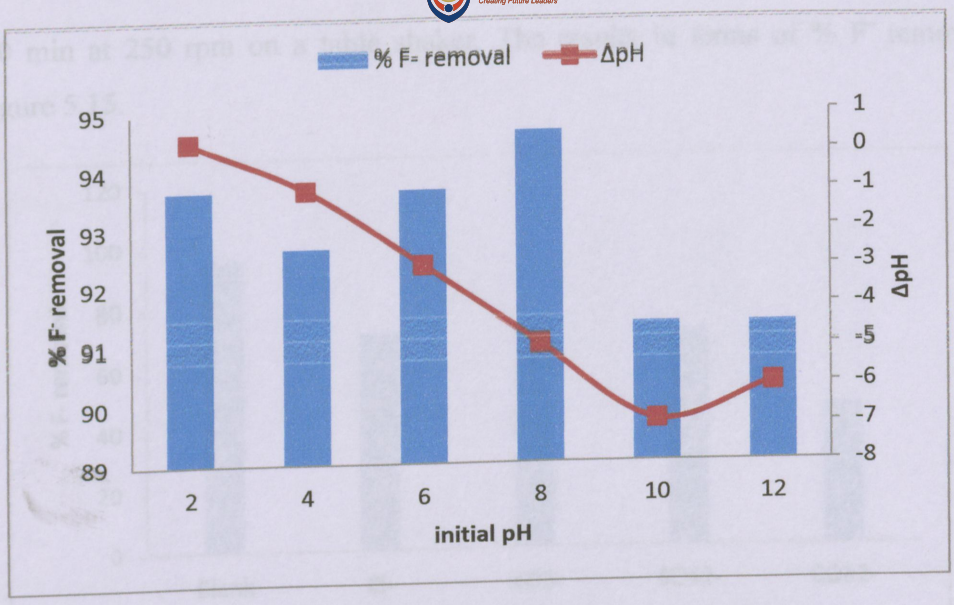

Figure 5.14: Variation of % F^- removal and ΔpH with initial pH (3 mg/L, 1.5 mg/L, and 30 min contact time at 250 rpm).

The pH of the medium is one of the important parameters, which significantly affects the fluoride adsorption. From figure 5.15 it is observed that % F^- removal in MnO_2 coated Na-bentonite is above 90% at all evaluated pH levels (2 - 12). Initially % F^- removal decreased from 93.66% at pH 2 to 92.66% at pH 4 and increased again to 94.66% at pH 8 thereafter decreased to 93.33% at pH 12. The decrease in % removal at pH >8 may be due to the presence of OH^- ions which compete with F^- for adsorption. ΔpH trend showed that at initial pH 2, the equilibrium pH of the mixture increased leading to positive value of ΔpH. This may be due to the release of OH^- from the surface of the adsorbent during F^- adsorption. At pH 4 and above, the final pH decreased leading to negative value of ΔpH. This may be due to the release of H^+ ions and adsorption of OH^- ions by the adsorbent. pH 8 was then chosen as the optimum pH for the subsequent experiments

5.5.5 Effects of Co-Existing ions

Various anionic species such as Cl^-, NO_3^-, SO_4^{2-}, and CO_3^{2-} are generally present in groundwater and may compete with F^- for adsorption. To evaluate their effects in adsorption of F^-, 10 mg/L concentration of the anionic species was prepared by dissolving known mass of their respective salts (KCl, KNO_3, Na_2CO_3 and K_2SO_4) in the presence of 5 mg/L F^-. A control solution of 5 mg/L F^- was included. Adsorbent dose of 1.5 g/100 mL was added and the mixtures were

© University of Venda

University of Venda
Creating Future Leaders

agitated for 30 min at 250 rpm on a table shaker. The results in terms of % F^- removal are presented in figure 5.15.

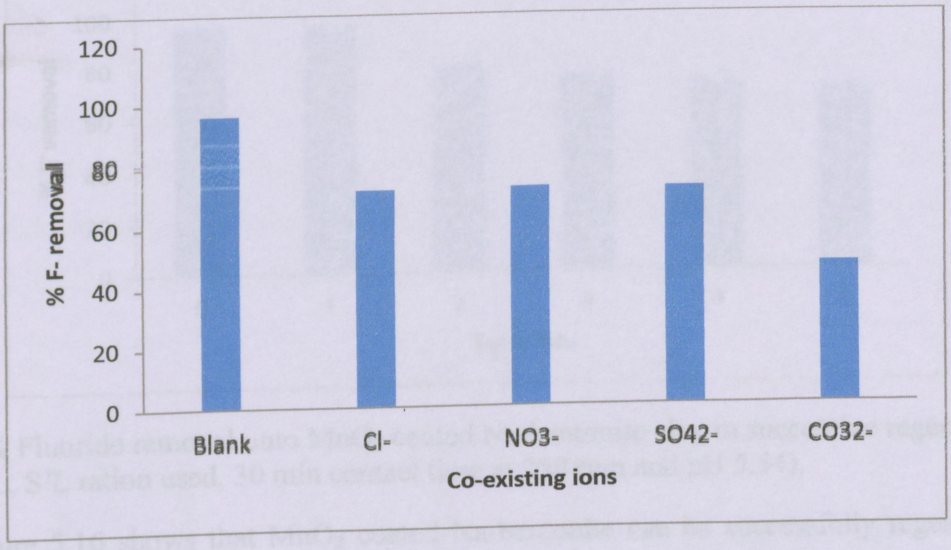

Figure 5.15: Effects of co-existing anions on fluoride removal by MnO_2 coated Na-bentonite (5 mg/L F^-, 10 mg/L of co-existing ions, 1.5 g/100 mL adsorbent dosage, pH 8 and 30 min contact time at 250 rpm).

From the results in figure 5.15 it is observed that the presence of Cl^-, NO_3^- and SO_4^{2-} decreased the % F^- removal by ≈24% while the presence of CO_3^{2-} decreased the % F^- removal significantly by ≈50%. Zhang *et al.* (2011) also reported significant decrease in % F^- removal in the presence of CO_3^{2-} and attributed it to the competition between F^- and CO_3^{2-} for active sites on adsorbent surface.

5.5.6 Regeneration and Reuse of the adsorbent

For the adsorbent to be cost effective, it must be regenerable and reused for fluoride adsorption. To evaluate the regeneration potential of MnO_2 coated Na-bentonite, 0.1 M NaOH was used as the adsorbent regenerating agent. Experiments of five successive adsorption and desorption cycles were performed at initial 5 mg/L F^- concentration, at pH 8 and contact time of 30 min. The results are presented in figure 5.16.

© University of Venda

University of Venda
Creating Future Leaders

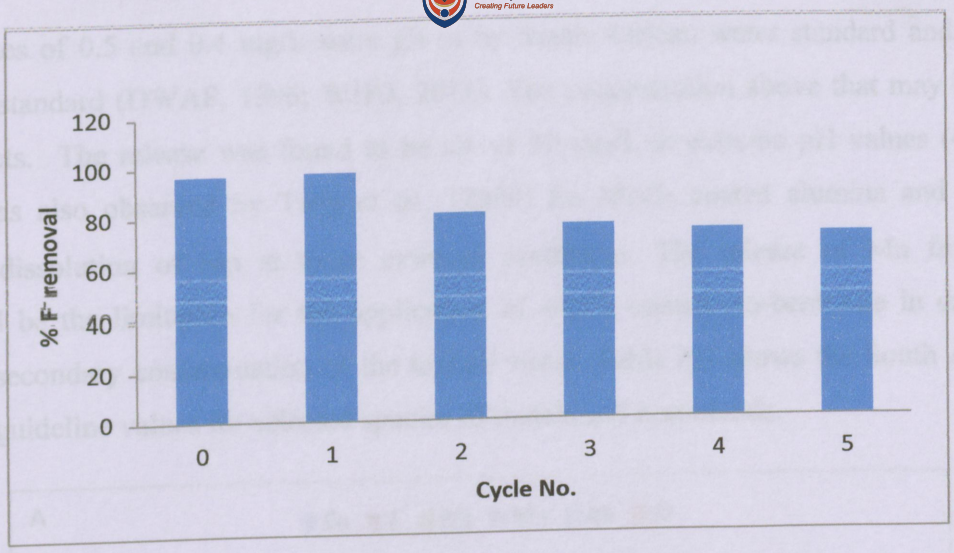

Figure 5.16: % Fluoride removal onto MnO_2 coated Na-bentonite clay in successive regeneration cycles (5 mg/L, S/L ration used, 30 min contact time at 250 rpm and pH 5.54).

Results in figure 5.16 shows that MnO_2 coated Na-bentonite can be successfully regenerated. After the first regeneration cycle, MnO_2 coated Na-bentonite showed significantly high percentage fluoride removal of 97.8% which is almost equal to the percentage of removal achieved by the fresh adsorbent. Thereafter the percentage of removal decreased with increasing cycle of reuse up to fifth cycle where up to 71.6% F^- was achieved. The decrease of fluoride adsorption ratio is probably due to the gradual dissolution of MnO_2 at alkaline conditions from the surface of the adsorbent during the regeneration process (Xiang *et al.*, 2014).

5.5.7 Chemical stability of the adsorbent

The chemical stability of MnO_2 coated Na-bentonite was assessed by measuring the release of metals and non-metals species at various pH levels (2-12). The results are presented in figure 5.17a and b in mg/L and µg/L respectively. The results showed that pH has significant impact on the stability of chemical species both metals and non-metals. At pH below 8, the leaching of Al and Ni was observed to be higher which may be attributed to the dissolution at extreme conditions. The leaching of Na was observed to be increasing with increasing pH. This may be attributed to the NaOH used during pH adjustment. However concentration of these species was found to be within the South African water guideline (DWAF, 1996). The leaching of K was also observed to be higher at both pH levels which may be an indication that K was not stable in the adsorbent. The South African and the WHO water guideline do not provide definitive guideline for Mn in drinking water since it does not have a considerable health impact however the

© University of Venda

University of Venda
Creating Future Leaders

guideline values of 0.5 and 0.4 mg/L were given by South African water standard and WHO water quality standard (DWAF, 1996; WHO, 2011). The concentration above that may lead to aesthetic effects. The release was found to be above 10 mg/L at extreme pH values (4< and >10). This was also observed by Teng *et al.*, (2009) for MnO_2 coated alumina and it was attributed to dissolution of Mn at those extreme conditions. The release of Mn from the adsorbent will be the limitation for the application of MnO_2 coated Na-bentonite in drinking water due to secondary contamination of the treated water. Table 5.4 shows the South African water quality guideline values for selected species of metals and non-metals.

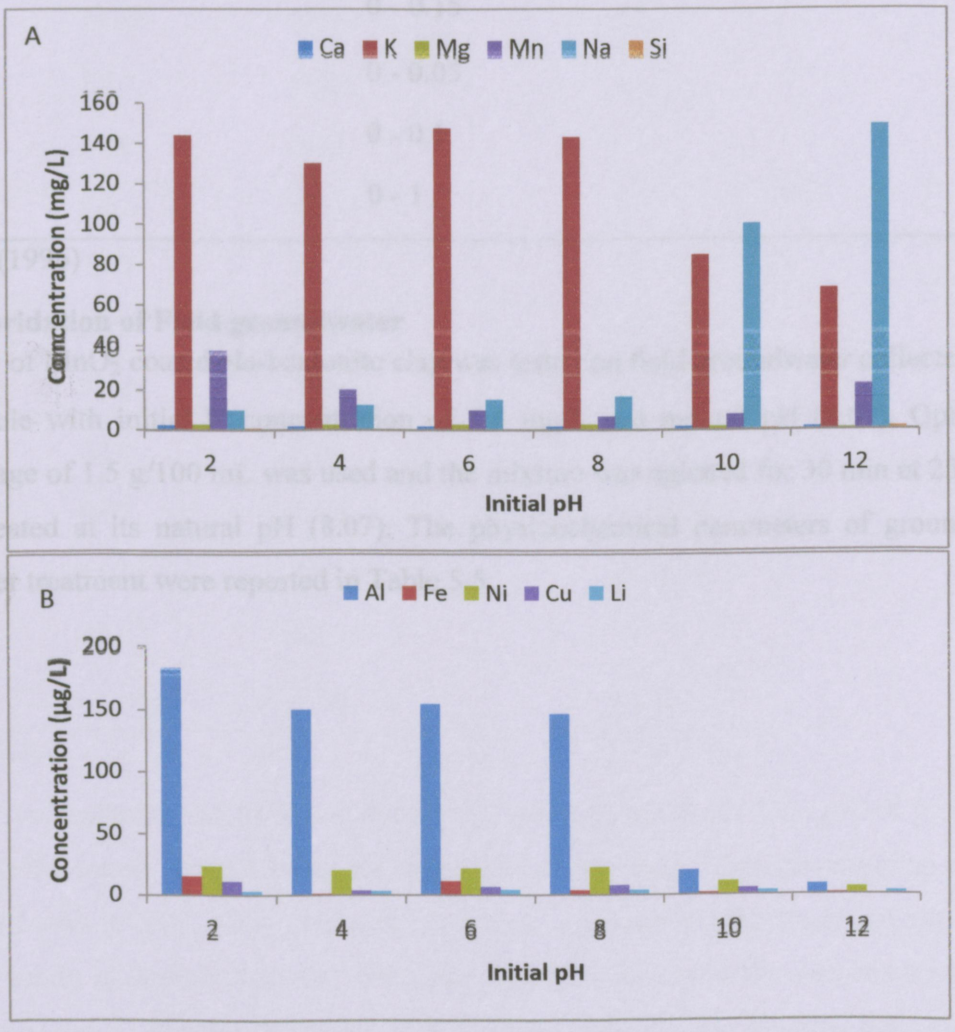

Figure 5.17: Concentration of chemical species in treated water at various pH. a) in mg/L, and b) in µg/L (1.5 g/100 mL adsorbent dosage, 3 mg/L initial F^- concentration and 30 min contact time at 250 rpm).

© University of Venda

University of Venda
Creating Future Leaders

Table 5.4: The South African water quality guideline of selected species.

Elements	DWAF (1996) (mg/L)
Ca	0 – 32
K	0 – 50
Mg	0 - 30
Na	0 - 100
Si	-
Al	0 - 0.15
Mn	0 - 0.05
Fe	0 - 0.1
Cu	0 - 1

Note: DWAF (1996)

5.5.8 Defluoridation of Field groundwater

The efficiency of MnO_2 coated Na-bentonite clay was tested on field groundwater collected from Siloam borehole with initial F^- concentration of 5.4 mg/L and natural pH (8.07). Optimized adsorbent dosage of 1.5 g/100 mL was used and the mixture was agitated for 30 min at 250 rpm. Water was treated at its natural pH (8.07). The physicochemical parameters of groundwater before and after treatment were reported in Table 5.5.

© University of Venda

University of Venda
Creating Future Leaders

Table 5.5: Physicochemical parameters of groundwater before and after treatment.

Parameter	Before treatment	After treatment	DWAF guideline values (mg/L)
pH	8.07	5.72	6.0-9.0
EC (µS/cm)	194	451	<150
TDS (mg/L)	116.7	270	<600
F^- (mg/L)	5.4	0.98	1.5
Cl^- (mg/L)	31.59	72.9	250
SO_4^{2-} (mg/L)	11.89	N.D	250
NO_3^- (mg/L)	1.13	N.D	-
Br^- (mg/L)	2.08	N.D	-
PO_4^{3-} (mg/L)	2.67	N.D	-
Ca (mg/L)	2.09	3.3	0 – 32
K (mg/L)	2.74	112.90	0 – 50
Na (mg/L)	71.91	79.85	0 - 100
Mg (mg/L)	0.04	2.84	0 - 30
Mn (mg/L)	0.02	1.66	0 - 0.05
Al (µg/L)	11.11	102.69	0 - 0.15
Si (mg/L)	46.31	42.26	-
Fe (µg/L)	16.55	1.06	0 - 0.1

N.D= Not detected.

MnO_2 coated Na-bentonite was able to reduce F^- in groundwater from 5.4 mg/L to 0.98 mg/L which is below the South African water standard value of 1.5 mg/L. The concentration of other co-existing ions such as SO_4^{2-}, NO_3^-, Br^- and PO_4^{3-} were not detected after treatment with MnO_2 coated Na-bentonite indicating that they were also adsorbed. However the concentration of Cl^- increased after treatment which may be due to the release of residue Cl^- resulting from treatment with HCl during modification. pH of the mixture decreased from 8.07 to 5.72 after treatment and this may be due to the release of H^+ ions into the solution while the increase in TDS an EC may

© University of Venda

University of Venda
Creating Future Leaders

be attributed to dissolution of chemical species such as Na^+, Cl^- in to the solution which increases the salinity of the treated water.

5.6 Adsorption isotherms

In order to explain the relationship between the equilibrium amount of solute on the adsorbent and the solute concentration in solutions two commonly used isotherms i.e. Langmuir and Freundlich adsorption isotherms were employed (Tang and Zhang, 2016; Mariapan *et al.*, 2015). Langmuir adsorption isotherm model is based on mono layered adsorption on uniform homogeneous surface with sites of identical nature. The linear equation of Langmuir adsorption is expressed by equation 5.4 as follows:

$$\frac{C_e}{Q_e} = \frac{1}{Q_m b} + \frac{C_e}{Q_m} \qquad (5.4)$$

Where, C_e is the equilibrium concentration (mg/L), Q_e is the adsorption capacity (mg/g), Q_m is theoretical maximum adsorption capacity (mg/g) and b is the Langmuir constant related to enthalpy of adsorption (L/mg). Q_m and b are determined from the slope and intercept of the plot of $\frac{C_e}{Q_e} Vs\ C_e$. Figure 5.18 shows the plots for Langmuir adsorption isotherm at different contact times.

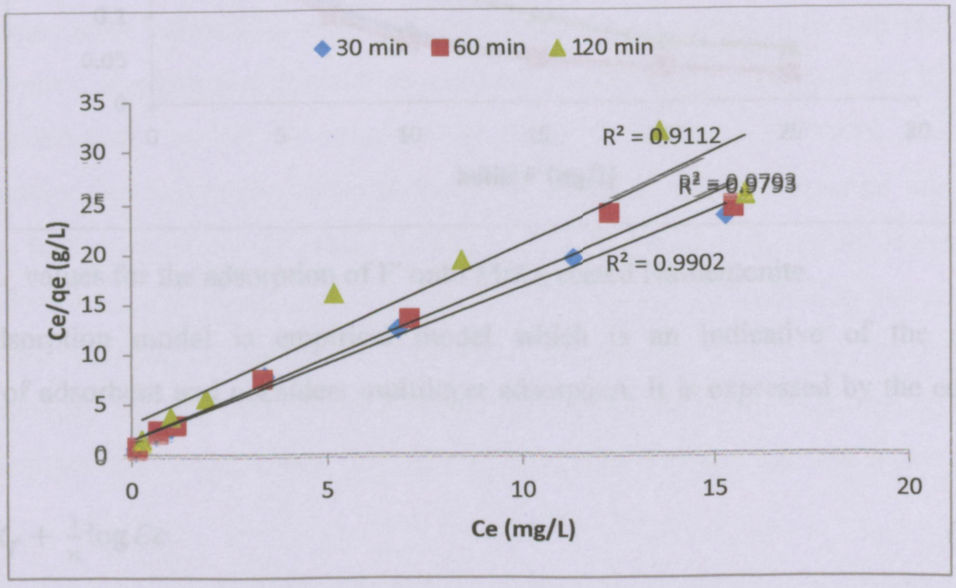

Figure 5.18: Langmuir adsorption isotherm (30 min, 60 min, 120 min contact times at 250 rpm, 1.5 g/100 mL, pH 6.2).

© University of Venda

University of Venda
Creating Future Leaders

From fig 5.18, it can be observed that the data yielded straight line with higher correlation co-efficient at both contact times. The essential characteristic of the Langmuir isotherm can be denoted by the dimensionless constant called equilibrium parameter, R_L, expressed by:

$$R_L = \frac{1}{1+bC_o} \quad (5.5)$$

Where C_o is the initial concentration and b is the Langmuir constant. $R_L = 1$ represents linear adsorption while $R_L = 0$ stands for the irreversible adsorption process. $R_L < 1$ is for favourable adsorption, while $R_L > 1$ represents unfavourable adsorption. Calculated values of R_L for different initial concentrations is presented is figure 5.19. Calculated values lie between 0 and 1 indicating that the adsorption of F^- onto MnO_2 coated Na-bentonite was favourable.

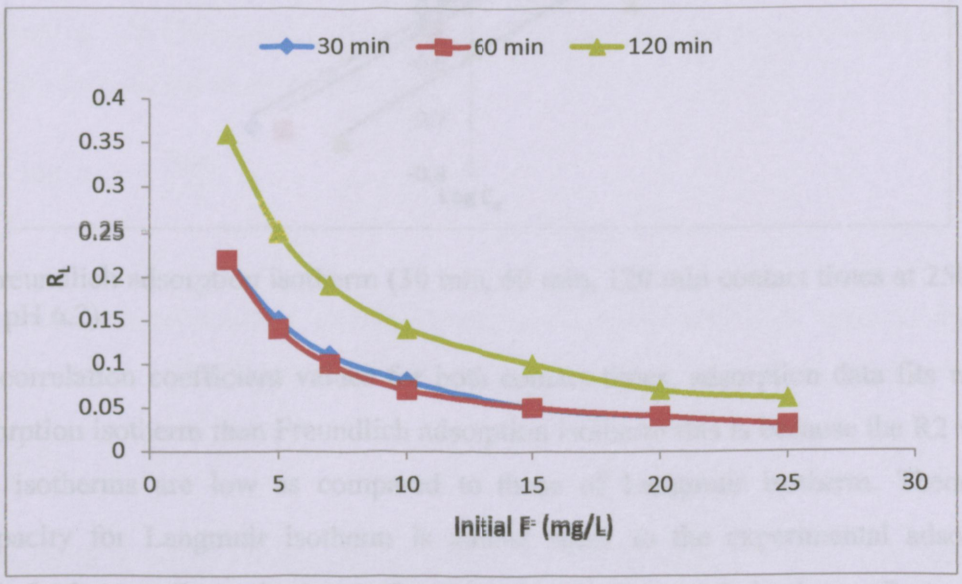

Figure 5.19: R_L values for the adsorption of F^- onto MnO_2 coated Na-bentonite.

Freundlich adsorption model is empirical model which is an indicative of the surface heterogeneity of adsorbent and considers multilayer adsorption. It is expressed by the equation 5.6:

$$\log Q_e = \log K_f + \frac{1}{n}\log Ce \quad (5.6)$$

Where, Ce is the equilibrium concentration (mg/L), Qe is the amount adsorbed at equilibrium (mg/g), K_f is the Freundlich constant related to adsorption capacity and represents the strength of adsorptive bonds and $1/n$ is the adsorption intensity. When $0 < 1/n < 1$, the adsorption is

© University of Venda

University of Venda
Creating Future Leaders

favourable; when $1/n = 1$, the adsorption is irreversible; and when $1/n > 1$, the adsorption is unfavourable. The value of K_f and $1/n$ are obtained from the slope and intercepts of a linear plot of log Q_e vs log C_e. Figure 5.20 shows a plot of Freundlich isotherm. Calculated values of K_f and $1/n$ are reported in Table 5.6.

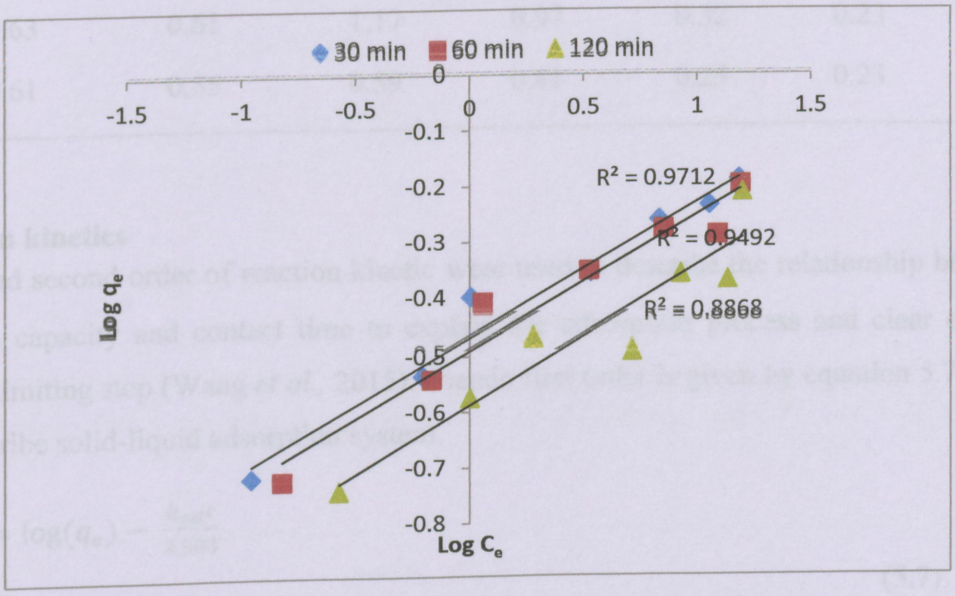

Figure 5.20: Freundlich adsorption isotherm (30 min, 60 min, 120 min contact times at 250 rpm, 1.5 g/100 mL, pH 6.2).

Based on the correlation coefficient values for both contact times, adsorption data fits well to Langmuir adsorption isotherm than Freundlich adsorption isotherm this is because the R2 values of Freundlich isotherms are low as compared to those of Langmuir isotherm. Theoretical adsorption capacity for Langmuir isotherm is almost equal to the experimental adsorption capacity which further confirms the better fit of the data to Langmuir isotherm. Better fit of Langmuir isotherm model suggests monolayer adsorption coverage. Calculated model constants for Langmuir and Freundlich isotherms are shown in Table 5.6. The value of R_L, dimensionless equilibrium parameter and the value of $1/n$ Freundlich adsorption intensity were both between 0 and 1, which indicate that the adsorption of F^- onto MnO_2 coated Na-bentonite was favourable.

© University of Venda

University of Venda
Creating Future Leaders

Table 5.6: Constant values for Langmuir and Freundlich isotherms.

	Langmuir isotherm				Freundlich isotherm		
	q_{exp} (mg/g)	Q_m (mg/g)	b (L/mg)	R^2	K_f (mg/g)	1/n	R^2
30 min	0.64	0.65	1.12	0.99	0.34	0.23	0.97
60 min	0.63	0.61	1.17	0.97	0.32	0.23	0.94
120 min	0.61	0.55	0.59	0.91	0.25	0.23	0.88

5.7 Adsorption kinetics

Pseudo first and second order of reaction kinetic were used to describe the relationship between the adsorption capacity and contact time to explain the adsorption process and clear out the potential rate-limiting step (Wang *et al.*, 2015). Pseudo first order is given by equation 5.7 and it is used to describe solid-liquid adsorption system.

$$\log(q_e - q_t) = \log(q_e) - \frac{k_{ad}t}{2.303} \tag{5.7}$$

Pseudo second order is represented by the linear equation 5.8 and it is used to describe chemisorption, as well as cation exchange reactions.

$$\frac{t}{q_t} = \frac{1}{K_{2ads}q_e^2} + \frac{1}{q_e}t \tag{5.8}$$

Where q_e and q_t (both in mg/g) are the amount adsorbed per unit mass at a time, t (in min). K_{ad} (min^{-1}) and K_{2ads} ($g.mg^{-1}/min$) are first and second order rate constant ($g.mg^{-1}/min$). The value of K_{ad} is determined from the slope and intercepts of log ($q_e - q_t$) vs t (min) and the value of K_{2ads} is determined from the slope and intercepts of t/q_t vs t. Figure 5.21 and 5.22 shows plots of pseudo first and second order respectively. The plots of pseudo second order yielded straight lines and higher correlation coefficient at both concentrations. The plots of pseudo first order did not give straight lines, this shows that adsorption of fluoride onto MnO_2 coated Na-bentonite followed pseudo second order and it occurred through chemisorption. Calculated model constants for pseudo first and second order are presented in Table 5.7.

© University of Venda

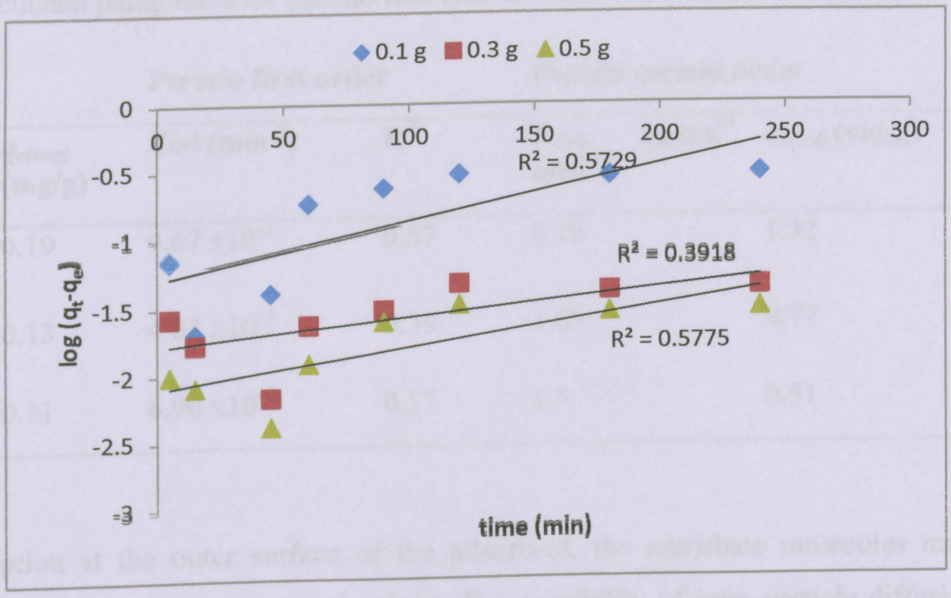

Figure 5.21: Pseudo first order plot at various adsorbent dosages (5 mg/L F^-, pH 6.24 and 250 rpm shaking).

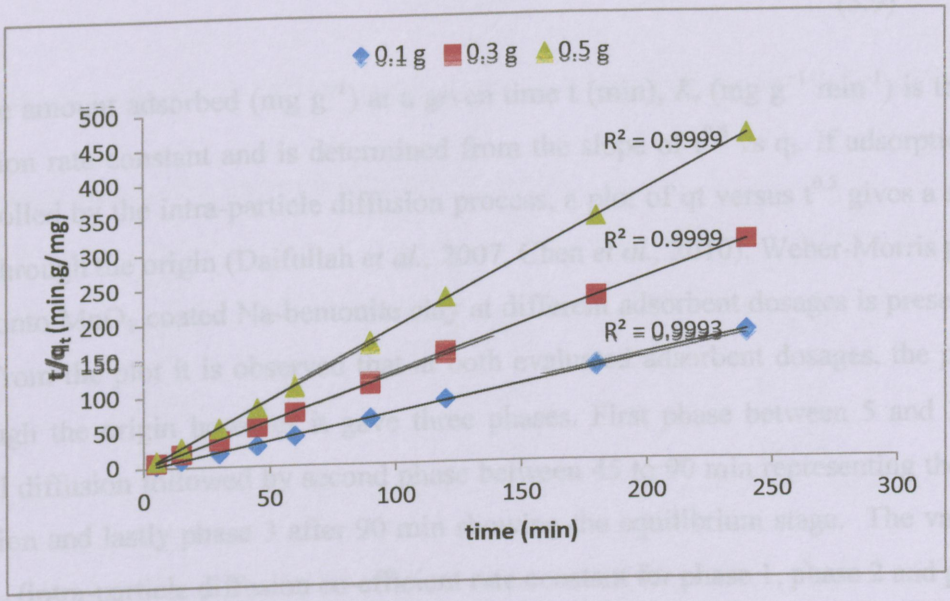

Figure 5.22: Pseudo second order plot at various adsorbent dosages (5 mg/L F^-, pH 6.24 and 250 rpm shaking).

© University of Venda

University of Venda
Creating Future Leaders

Table 5.7: Calculated parameters for pseudo first and second order reaction kinetics model

		Pseudo first order		Pseudo second order		
	$q_{e(exp)}$ (mg/g)	Kad (min^{-1})	R^2	K_{2ad} ($g.mg^{-1}$ min^{-1})	$q_{e(cal)}$ (mg/g)	R^2
3 mg/L	0.19	9.67×10^{-3}	0.57	0.18	1.32	0.99
5 mg/L	0.13	4.83×10^{-4}	0.39	1.09	0.77	0.99
10 mg/L	0.21	6.90×10^{-4}	0.57	1.5	0.51	0.99

Besides adsorption at the outer surface of the adsorbent, the adsorbate molecules may also diffuse into the interior of the porous adsorbent. The possibility of intra-particle diffusion was evaluated using Weber-Morris intra-particle diffusion model represented by equation 5.9.

$$q_t = K_i t^{0.5} \quad (5.9)$$

Where q_t is the amount adsorbed (mg g^{-1}) at a given time t (min), K_i (mg g^{-1} min^{-1}) is the intra particle diffusion rate constant and is determined from the slope of $t^{0.5}$ vs q_t. If adsorption of a solute is controlled by the intra-particle diffusion process, a plot of qt versus $t^{0.5}$ gives a straight line and pass through the origin (Daifullah *et al.*, 2007, Chen *et al.*, 2010). Weber-Morris plots of F^- adsorption onto MnO_2 coated Na-bentonite clay at different adsorbent dosages is presented in Figure 5.23. From the plot it is observed that at both evaluated adsorbent dosages, the plot did not pass through the origin however it gave three phases. First phase between 5 and 30 min shows external diffusion followed by second phase between 45 to 90 min representing the intra-particle diffusion and lastly phase 3 after 90 min showing the equilibrium stage. The values of K_{i1}, K_{i2} and K_{i3} (intra-particle diffusion co-efficient rate constant for phase 1, phase 2 and phase 3 respectively) obtained from the plots are shown in Table 8. For both adsorbent dosages the values of K_{i1} is higher than the value of K_{i2} and K_{i3} indicating that the first phase was faster compared to phase 2 and 3 (Shang and Gou, 2013; Tang and Zhang, 2016). This may be due to difference in the rate of mass transfer in the initial and final phase of adsorption. The Correlation coefficient values for the phase 2 was higher compared to phase 1 and 3. This may be an indication that intra-particle diffusion dominated the adsorption process. Pore distribution

© University of Venda

analysis showed that the pores of the MnO_2 coated Na-bentonite ranged from micro to macro pores with average pores being mesoporous. External diffusion occurred in the micro pores, followed by intra-particle diffusion in the mesoporous and lastly equilibrium adsorption in the macro-porous of the adsorbent. These results show that adsorption of F^- onto MnO_2 coated Na-bentonite is not only controlled by intra-particle diffusion and it is therefore a complex process.

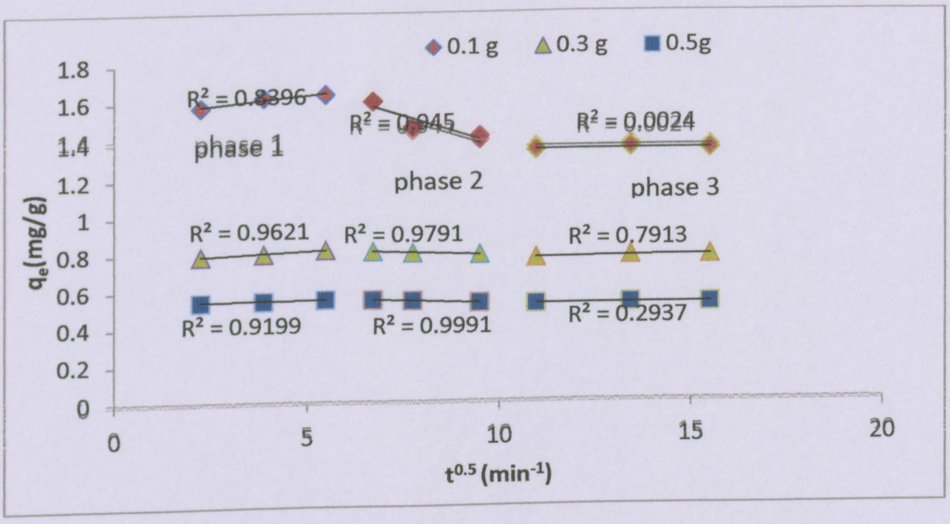

Figure 5.23: Intra-particle plot at various adsorbent dosages (5 mg/L F^-, pH 6.24 and 250 rpm shaking)

Table 5.8: Constant values of intra-particle diffusion model

	K_{i1}	K_{i2}	$Ki3$
0.1 g/100 mL	0.021	-0.064	0.0001
0.3 g/100 mL	0.092	-0.007	0.002
0.5 g/100 mL	0.0025	-0.0072	0.0005

© University of Venda

5.8 Mechanistic aspect

Possible mechanism for fluoride adsorption onto MnO_2 coated bentonite can be elucidated by looking at the effect of pH on F^- adsorption and the change in pH during F^- adsorption fig. 5.14. At pH below 3, where final pH was higher than the initial pH and the surface of the adsorbent is positive, fluoride adsorption would be via ligands exchange mechanism because of stronger attractive force between fluoride and the adsorbent surface and the presence of more hydroxylated sites for exchange of F^- (eq. 5.10 and 5.11). At solution pH above 3, the surface of the adsorbent becomes negatively charged and stronger electrostatic repulsion between active sites and F^- ions exists. The fluoride removal would be mainly due to the ion exchange mechanism (eq. 5.12-5.13).

$$\equiv MOH + H_3O^+ + F^- \leftrightarrow \equiv MOH_2^+ - F^- + H_2O \quad (5.10)$$

$$\equiv MOH + H_2O + F^- \leftrightarrow \equiv MOH_2^+ - F^- + 2OH^- \quad (5.11)$$

$$\equiv MOH + F^- \leftrightarrow MF + OH^- \quad (5.12)$$

$$\equiv M(OH)_2^- + 2F^- \leftrightarrow MF_2 + 2OH^- \quad (5.13)$$

Where ≡ M represent Metal in the adsorbent surface (Mn, Si, and Al).

5.9 Comparison with other MnO_2 coated adsorbents

Comparison between MnO_2 coated Na-bentonite and previously reported MnO_2 coated was made based on the pH, Initial F^- concentration and maximum adsorption capacity. The comparison is presented in Table 5.9. It seemed as MnO_2 coated Na-bentonite has lower adsorption capacity compared to other MnO_2 coated adsorbents except for activated alumina (Tripathy *et al.*, 2008). Although MnO_2 coated Na-bentonite showed lower maximum adsorption capacity compared to other adsorbents, the adsorption capacity was sufficient for F^- removal from groundwater. Moreover the percentage F^- removal was above 90% at evaluated pH values (2-12).

© University of Venda

University of Venda
Creating Future Leaders

Table 5.9: Comparison of different adsorption capacities of different adsorbents for fluoride.

Adsorbent	pH	Initial F^- (mg/L)	Adsorption capacity (mg/g)	Reference
MnO_2 activated alumina	7	10	0.15	Tripathy *et al.* (2008)
MnO_2 granular activated carbon	7.5-8	10	0.82	Ma *et al.* (2009)
Hydrous MnO_2 coated activated alumina	3.5- 7	6	7.1	Teng *et al.* (2009)
MnO_2 coated earthenware	7.5	2	1.55	Sivasankar *et al.* (2011)
MnO_2 graphene oxide	5.5-6.7	10	4.35	Li *et al.* (2013)
MnO_2 coated Na-bentonite	8	5	0.65	Present study

5.10 Conclusions

Na-bentonite was successfully coated with MnO_2 through *in-situ* reduction of $KMnO_4$. From the study the following major conclusions were made:

- Coating Na-bentonite with manganese oxides changes the mineralogical as well as the morphological properties of bentonite clay and further increases the surface area.
- Percentage F^- removal above 91.0% was achieved at all evaluated pH levels (2-12), 5 mg/L F^- initial concentration, optimum dosage of 1.5 mg/L and contact time of 30 min and shaking speed of 250 rpm.
- Regeneration study showed that MnO_2 coated Na-bentonite can be successfully regenerated with 0.1 M NaOH
- Chemical stability test revealed that Mn, Na and K ions were leached at concentrations above the South African drinking standards in drinking water. Elements such as Al, Si, Fe and Li were leached at concentrations below the within the South African guideline

© University of Venda

University of Venda
Creating Future Leaders

values in drinking water. Data fitted well to Langmuir isotherm model indicating that adsorption occurred on a mono layered surface

- Adsorption kinetics data fitted well to pseudo second order reaction kinetics indicating that the adsorption occurred through chemisorption.
- Intra-particle diffusion model of Weber-Morris indicated that the removal of fluoride by MnO_2 coated Na-bentonite is a highly complex process, involving boundary layer diffusion and intra-particle diffusion as well as equilibrium adsorption.
- Sorption of fluoride occurred via ligands exchange mechanism at pH below 3 and at pH above 3 it occurred via ion exchange mechanism.
- This work recommends that MnO_2 coated Na-bentonite is a potential adsorbent for defluoridation of groundwater and further studies should be carried out to improve its chemical stability.

© University of Venda

References

Chen, N., Zhang, Z., Feng, C., Li, M., Zhu, D., Chen, R. & Sugiura, N., 2010. An excellent fluoride sorption behaviour of ceramic adsorbent. *Journal of Hazardous Materials,* 183, pp.460–465

Daifullah, A. A. M., Yakout, S.M., Elreefy, S. A., 2007. Adsorption of fluoride in aqueous solutions using $KMnO_4$-modified activated carbon derived from steam pyrolysis of rice straw. *Journal of Hazardous Materials,* 147, pp. 633–643.

Department of Water Affairs and Forestry (DWAF). 1996. South African Water Quality Guidelines for Domestic Use, 1st ed., Department of Water Affairs and Forestry, Pretoria. Available at: www.dwaf.gov.za.

Eren, E., Afsin, B. & Onal, Y.,2009. Removal of lead ions by acid activated and manganese oxide-coated bentonite. *Journal of Hazardous Materials*, 161, pp. 677–685.

Li, Y., Du, Q., Wang, J., Liu, T., Sun, J., Wang, Y., Wang, Z., Xia, Y., Xia, L., (2013). Defluoridation from aqueous solution by manganese oxide coated graphene oxide. *Journal of Fluorine Chemistry*, 148, pp. 67–73

Ma, Y., Wang, S. G., Fan, M., Gong, W. X. & Gao, B. Y., 2012. Characteristics and defluoridation performance of granular activated carbons coated with manganese oxides. *Journal of Hazardous Materials*, 168, pp1140–1146

Mariappan, R., Vairamuthu, R. & Ganapathy., A. 2015. Use of chemically activated cotton nut shell carbon for the removal of fluoride contaminated drinking water: Kinetics evaluation. Chinese Journal of *Chemical Engineering*, pp. 1-12

Ncube, E. J., & Schutte, C. F., 2005. The occurrence of fluoride in South African groundwater: A water quality and health problem. *Water S.A*, 31 (1), pp. 35-40.

Odiyo J. O., & Makungo, R., 2012. Fluoride concentrations in groundwater and impact on human health in Siloam Village, Limpopo Province, South Africa. *Water S.A*, 38 (5). 731-732.

Sari, A & Tuzen, M., 2013. Adsorption of silver from aqueous solution onto raw vermiculite and manganese oxide-modified vermiculite. *Microporous and Mesoporous Materials,* 170, pp. 155–163.

Shan, Y. & Guo, H., 2013. Fluoride adsorption on modified natural siderite: Optimization and performance. *Chemical Engineering Journal*, 223, pp.183–191

Taffarel, S. & R., Rubio, J., 2010. Removal of Mn^{2+} from aqueous solution by manganese oxide coated zeolite. *Minerals Engineering*, 23, pp. 1131–1138

© University of Venda

University of Venda
Creating Future Leaders

Tang, D., Zhang, G. 2016. Efficient removal of fluoride by hierarchical Ce–Fe bimetal oxides adsorbent: Thermodynamics, kinetics and mechanism. *Chemical Engineering Journal,* 283, pp. 721–729.

Teng, S., Wang, S., Gong, W., Liu, X. & Gao, B., 2009. Removal of fluoride by hydrous manganese oxide-coated alumina: Performance and mechanism. *Journal of Hazardous Materials*, 168, pp.1004–1011.

Thakre, D., Rayalu, S., Kawade, R,. Meshram, S., Subrt, J. & Labhsetwar, N., 2010. Magnesium incorporated Bentonite clay for defluoridation of drinking water. *Journal of Hazardous Materials,* 180, pp.122-130.

Wang, J., Dongjuan Kang, D., Yu, X., Ge, M., Chen, Y. 2015. Synthesis and characterization of Mg-Fe–La trimetal composite as an adsorbent for fluoride removal. *Chemical Engineering Journal.,* 264, pp. 506–513.

Wang, Y., Wang, X., Wang, X., Liu, M., Yang, L., Wu, Z., Xia, S. & Zhao., J., 2012. Adsorption of Pb(II) in aqueous solutions by bamboo charcoal modified with $KMnO_4$ via microwave irradiation. *Colloids and Surfaces A: Physicochem. Eng. Aspects,* 414, pp.1– 8.

World Health Organisation, 2011. *Guideline for drinking water, world health organization.* Geneva.

Xiang, W., Zhang, G., Zhang, Y., Tang, D & Wang., J., 2014. Synthesis and characterization of cotton-like Ca–Al–La composite as an adsorbent for fluoride removal. *Chemical Engineering Journal*, 250, pp. 423–430

Zhang, Z., Tan, Y. & Zhong, M., 2011. Defluoridation of wastewater by calcium chloride modified natural zeolite. *Desalination*, 276, pp. 246–252

Xu, M., Wang, H., Di Lei D., Qu, D., Zhai, Y & Wang, Y. 2013. Removal of Pb (II) from aqueous solution by hydrous manganese dioxide: Adsorption behavior and mechanism. *Journal of Environmental Sciences*, 25(3) pp.479–486

© University of Venda

University of Venda
Creating Future Leaders

Chapter 6: Fabrication of smectite rich clay soil MnO_2 coated bentonite composites and potential application in groundwater defluoridation

Abstract

Presence of fluoride in drinking water is a threat to human health. Recent studies have focused on the development of fluoride adsorbents that are flexible and sustainable for use in rural areas. This study evaluated the potential application of MnO_2 coated Na-bentonite clay/smectite rich clay soils composite in fluoride removal from drinking water. Composite was prepared by mixing MnO_2 coated Na-bentonite and smectite rich clay soils at various ratios. The ratio of MnO_2 coated Na-bentonite clay/smectite rich clay soils for fabricating the composite was established to be 1:3. Pellets were then prepared by moulding the clay manually. To find the optimum calcination temperature, fabricated pellets were calcined at various temperatures ranging from 150-750 °C and the optimum calcination temperature was found to be 550 °C. The composite was characterised for mineralogy using XRD, chemical composition using XRF, Surface morphology using SEM. XRD showed that quartz, albite, cryptomelane and microcline are the main minerals in the composite and montmorillonite which was found to be the main mineral in MnO_2 coated Na-bentonite and smectite rich clay soils was not found in composite clay soils. XRF showed that the clay consist of SiO_2, Al_3O_2 and MnO oxides. SEM showed that the composite has platy like morphology. Adsorption capacity of the pellets was evaluated using batch experiments. Pellets prepared under the established optimum conditions removed ≈63.3% F^- from an initial F^- concentration of 10 mg/L. the study concluded that fabricated clay composite pellets can be used for fluoride removal of groundwater and it recommended that further studies should be conducted to evaluate its application in a dynamic flow set-up.

Keywords: Composite, pellets, calcination, characterisation and batch experiments.

© University of Venda

University of Venda
Creating Future Leaders

6.1 Introduction

Fluoride is a health affecting substance often considered as two edged sword. This is because depending on its concentration, fluoride can have beneficial as well as harmful effects on human health. If available at concentrations below 1.5 mg/L fluoride promote dental caries and above 1.5 mg/L it lead to dental fluorosis and still higher concentration lead to major health hazards. Department of water affairs in South Africa has stipulated the value of 1.5 mg/L as the guideline value of fluoride in groundwater (DWAF, 1996). In many of the regions of South Africa groundwater has concentration above 1.5 mg/L and as such it will require defluoridation. The previous three chapters discussed the application of black smectite rich clay soils from Mukondeni, Mn^{2+} modified bentonite clay as well as the MnO_2 coated Na-bentonite on defluoridation of groundwater. Smectite rich clay as well as Mn^{2+} modified bentonite showed high fluoride removal efficiency at acidic pH. This limited their application on groundwater defluoridation. MnO_2 coated Na-bentonite showed higher fluoride removal efficiency at wide range of pH levels (2-12) however toxicity assessment showed that it leads to the leaching of Mn ions from the adsorbent. Therefore there is a need to develop an adsorbent that will have high fluoride removal efficiency and do not give rise to secondary pollutant. Recently granular ceramic as well as composite adsorbents were reported to exhibit high fluoride removal capacities and it was reported to be stable (Chen *et al.*, 2011; Jia *et al.*, 2015; Oladoja *et al.*, 2015). In this work a ceramic composite adsorbent was fabricated by mixing smectite rich clay soils with MnO_2 coated Na-bentonite and moulded into pellets. Physicochemical and mineralogical characteristics of the composite adsorbent were evaluated using XRD, XRF and SEM. The adsorbent was then tested for its fluoride removal efficiency using batch experiments.

6.2 Material and Methods

6.2.1 Sample collection

Smectite rich clay soil was collected from Mukondeni Village, Vhembe district in South Africa. Field water was collected from community borehole in Siloam, Vhembe district in South Africa MnO_2 coated Na-bentonite was prepared using the method developed in chapter 5. All reagents and TISAB-III were obtained from Rochelle Chemicals & Lab Equipment CC, South Africa Ltd and they were of analytical grade. A stock solution containing 1000 mg/L fluoride was prepared by dissolving 2.21 g NaF in 1 L of MILLIQ water (18.2 MΩ/cm) and fluoride solutions for batch experiments were prepared from fresh stock fluoride solution by appropriate dilution.

© University of Venda

University of Venda
Creating Future Leaders

6.2.2 Adsorbent preparation

In order to prepare smectite rich clay soil/MnO_2 Na-bentonite clay composite adsorbent, two factors were evaluated, i.e. clay mixing ratio and the calcination temperature.

6.2.2.1 Clay mixing ratio

In order to find the optimum clay mixing ratio, MnO_2 coated bentonite clay and smectite rich clay soils were mixed at mass ratios of 1:1, 1:2, 1:3, 2:1 and 3:1 and put into 50 mL glass beaker. To this 20 mL of MILLIQ water was added and the mixture was stirred to homogenise for 15 min. After stirring, mixtures were then centrifuged at 2500 rpm and the solid residues were then dried at 110 °C for 12 hours in an oven. Thereafter samples were then milled to pass through <250 µm pore sieve. In order to find the optimum clay mixing ratio, defluoridation experiments were conducted as follows: 100 mL of 5 mg/L F^- solution was prepared and pipetted into five (5) 250 mL plastic bottles, to this 0.3 g of composite adsorbent prepared at various ratios was added to make up S/L ratio of 0.3 g/100 mL. Mixtures were then agitated for 30 min at 250 rpm on a Table shaker. After agitation samples were then filtered using 0.45 µm pore filter membrane. Filtrates were analysed for residual fluoride using ion selective electrode calibrated with four standards containing 1 mL of total ionic strength buffer (TISAB-III) per 10 mL of solution. Same ratio was maintained for the sample. MnO_2 coated Na-bentonite/smectite rich clay soil ratio of 1:3 was found to be the optimum based on F^- adsorption efficiency and was used for subsequent experiment.

6.2.2.2 Effect of calcination temperature

In order to evaluate the effect of calcination temperature, the clay was mixed at ratio of 1:3 as explained in section 6.2.2.1 and moulded manually into pellets. The pellets were then air dried for 3 hours followed by oven drying at 110 °C for 12 hours. After drying pellets were calcined at various temperatures ranging from 150 to 750 °C for 1 hour in a marble furnace. The obtained pellets were then used for defluoridation of synthetic fluoride solutions. In order to evaluate the effect of calcination temperature on defluoridation, pellets prepared were used for fluoride removal and the experiments were conducted as follows: 100 mL of 10 mg/L F^- solution was prepared and pipetted into five (5) 250 mL plastic bottles, to this 2 g of pellets composite adsorbent prepared at various calcination was added to make up S/L ratio of 2 g/100 mL. Mixtures were then agitated for 30 min at 250 rpm on a table shaker. After agitation samples were then filtered using 0.45 µm pore filter membrane. Filtrates were analysed for residual

© University of Venda

University of Venda
Creating Future Leaders

fluoride using ion selective electrode calibrated with four standards containing 1 mL of total ionic strength buffer (TISAB-III) per 10 mL of solution. Same ratio was maintained for the sample. The Material that was calcined at 750 was found the optimum and was then characterised, its properties were compared to those of smectite clay and MnO2 coated bentonite clay.

6.2.3 Physicochemical and mineralogical characterisation

Mineralogical and chemical composition of the composite adsorbent were determined using X-ray diffraction (XRD) (PANalytical X'Pert pro power) and X-ray fluorescence (XRF) (Thermo Fisher ARL9400 XP+ Sequential XRF with WinXRF software) respectively. Surface morphology was determined using Scanning electron microscopy (SEM) (Leo1450 SEM, voltage is 10Kv, working distance 14mm). Properties were compared with those of MnO_2 Na-bentonite and smectite rich clay soils.

6.3 Results and discussion

6.3.1 Effect of mixing ratio

Figure 6.1 presents the results in terms of percentage F^- removal of the batch experiments conducted to evaluate the effect of clay mixing ratio.

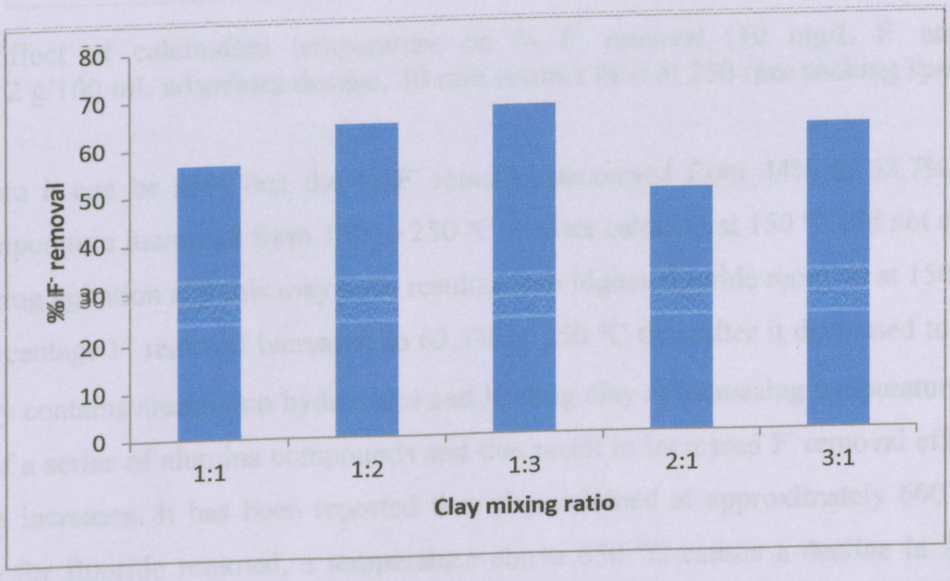

Figure 6.1: Effect of clay mixing ratio on % F^- removal (5 mg/L F^-, 0.3 g/100 mL adsorbent dosage, 30 min contact time at 250 rpm shaking speed, and 6.03±0.5 pH).

Figure 6.1 shows the effect of clay mixing ratio on fluoride removal efficiency, the results shows that clay mixed at ratio of 1:3 (MnO_2 coated Na-bentonite/ Smectite rich clay soils) achieved the

© University of Venda

University of Venda
Creating Future Leaders

highest % F^- removal, it was subsequently adopted as the optimum clay mixing ratio for subsequent experiments.

6.3.2 Effect of calcination temperature

Figure 6.2 present the results of the experiment conducted to find the optimum calcination temperature in terms of % F^- removal.

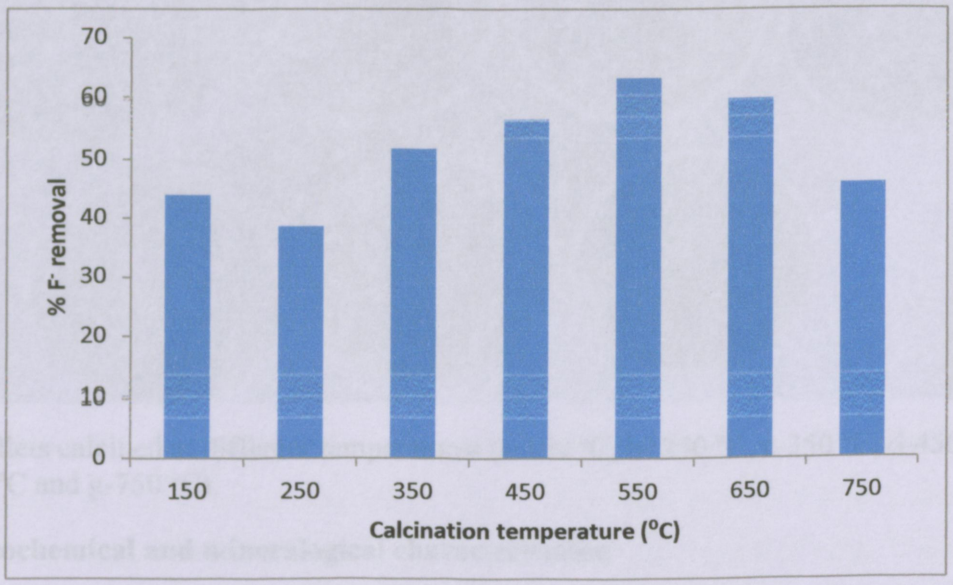

Figure 6.2: Effect of calcination temperature on % F^- removal (10 mg/L F^- adsorbate concentration, 2 g/100 mL adsorbent dosage, 30 min contact time at 250 rpm shaking speed, and 6.03±0.5 pH).

From the figure it can be seen that the % F^- removal decreased from 44% to 38.7% as the calcination temperature increased from 150 to 250 °C. Pellets calcined at 150 °C did not stabilise in solution during agitation and this may have resulted into higher fluoride removal at 150 °C. At 250 °C the percentage F^- removal increased to 63.3% at 550 °C thereafter it decreased to 45.9% at 750 °C. Clay contains aluminium hydroxides and heating clay at increasing temperature result in formation of a series of alumina compounds and this result in increased F^- removal efficiency as temperature increases. It has been reported that clay calcined at approximately 600 °C are most effective for fluoride removal, a temperature above 650 °C causes a decline in fluoride adsorption (Hauge *et al.*, 1994; Piddennavar, 2013). Decrease in removal of F^- at temperature above 550 °C may be attributed to loss of surface hydroxyl groups from the adsorbent. Figure 6.3 shows the image of pellets calcined at different temperatures. It can be observed that pellets

© University of Venda

University of Venda
Creating Future Leaders

calcined at higher temperature appear brown in colour and this indicate loss of moisture in the pellets.

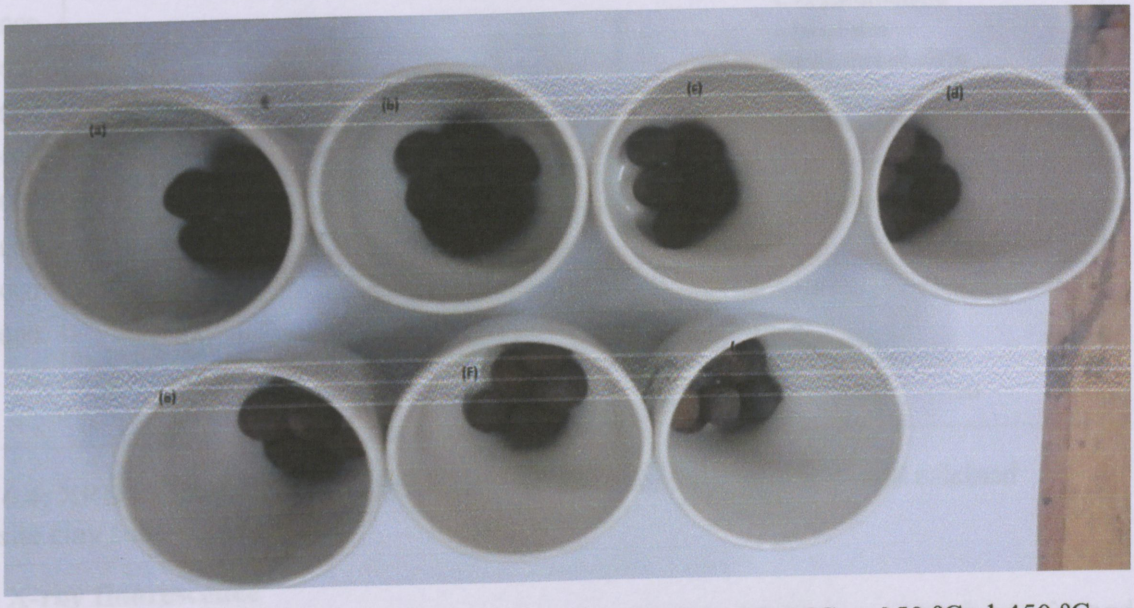

Figure 6.3: Pellets calcined at different temperatures (a-150 ℃, b- 250 ℃, c-350 ℃, d-450 ℃, e-550 ℃, f-650 ℃ and g-750 ℃).

6.3.3 Physicochemical and mineralogical characterisation

6.3.3.1 X-ray diffraction analysis

The XRD spectra of smectite rich clay, MnO_2 coated Na-bentonite and composite prepared at 750℃ calcination temperature is presented in Figure 6.4. The analysis showed that the clay composite is mainly consisted of quartz, albite, cryptomelane and microcline. Montmorillonite mineral was not found in the clay composite.

© University of Venda

University of Venda
Creating Future Leaders

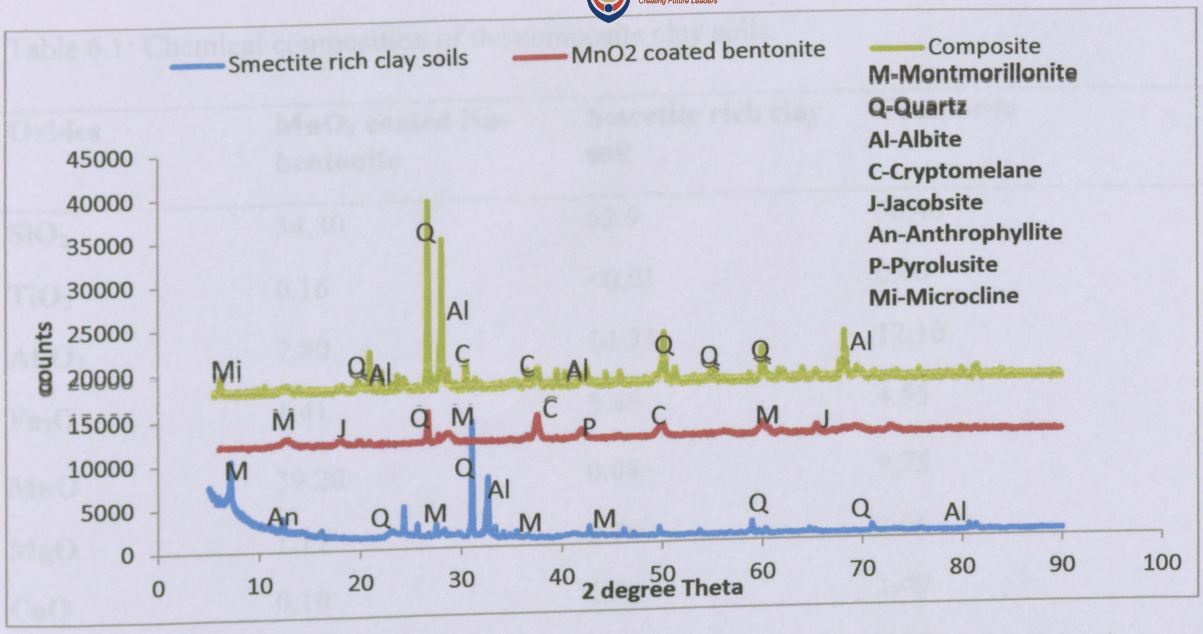

Figure 6.4: XRD Spectra for smectite rich clay, MnO_2 coated Na-bentonite and calcined composite clay soils.

6.3.3.2 X-ray fluorescence

Table 6.1 shows the chemical composition of smectite rich clay, MnO_2 coated Na-bentonite and composite prepared at 750°C calcination temperature. The results showed that clay composite consisted of SiO_2, Al_2O_3, MnO and Fe_2O_3 as the major oxides with traces of MgO, Na_2O, K_2O and CaO. All these oxides were also the major constituents of MnO_2 coated Na-bentonite and smectite rich clay soils. MnO content was found to be low in composite compared to MnO content in MnO_2 coated bentonite. This may be attributed to higher percentage of SiO_2 and other oxides in smectite rich clay which may have diluted the MnO content in MnO_2 coated bentonite.

© University of Venda

University of Venda
Creating Future Leaders

Table 6.1: Chemical composition of the composite clay soils.

Oxides	MnO_2 coated Na-bentonite	Smectite rich clay soil	Composite
SiO_2	34.30	62.9	58.40
TiO_2	0.16	<0.01	0.40
Al_2O_3	7.80	14.35	12.10
Fe_2O_3	1.41	5.45	4.55
MnO	39.20	0.08	9.75
MgO	1.17	2.79	2.06
CaO	0.10	1.79	1.49
Na_2O	0.23	2.52	2.07
K_2O	4.47	0.93	1.89
P_2O_5	<0.01	0.04	<0.01
Cr_2O_3	<0.01	0.02	0.06
SO_3	0.22	<0.01	0.13
Total	**99.96**	**99.15**	**99.88**

6.3.3.3 Scanning Electron Microscopy

Figure 6.5 shows the morphology of smectite rich clay soils, MnO_2 coated Na-bentonite and clay composite. The analysis revealed platy-like features characteristics of smectite clay. The surface is different from that of smectite rich clay soils and MnO_2 coated Na-bentonite clay soils. Smectite clay surface is granular and has irregular pore structure. The surface of MnO_2 coated Na-bentonite is granular and fibrous.

© University of Venda

University of Venda
Creating Future Leaders

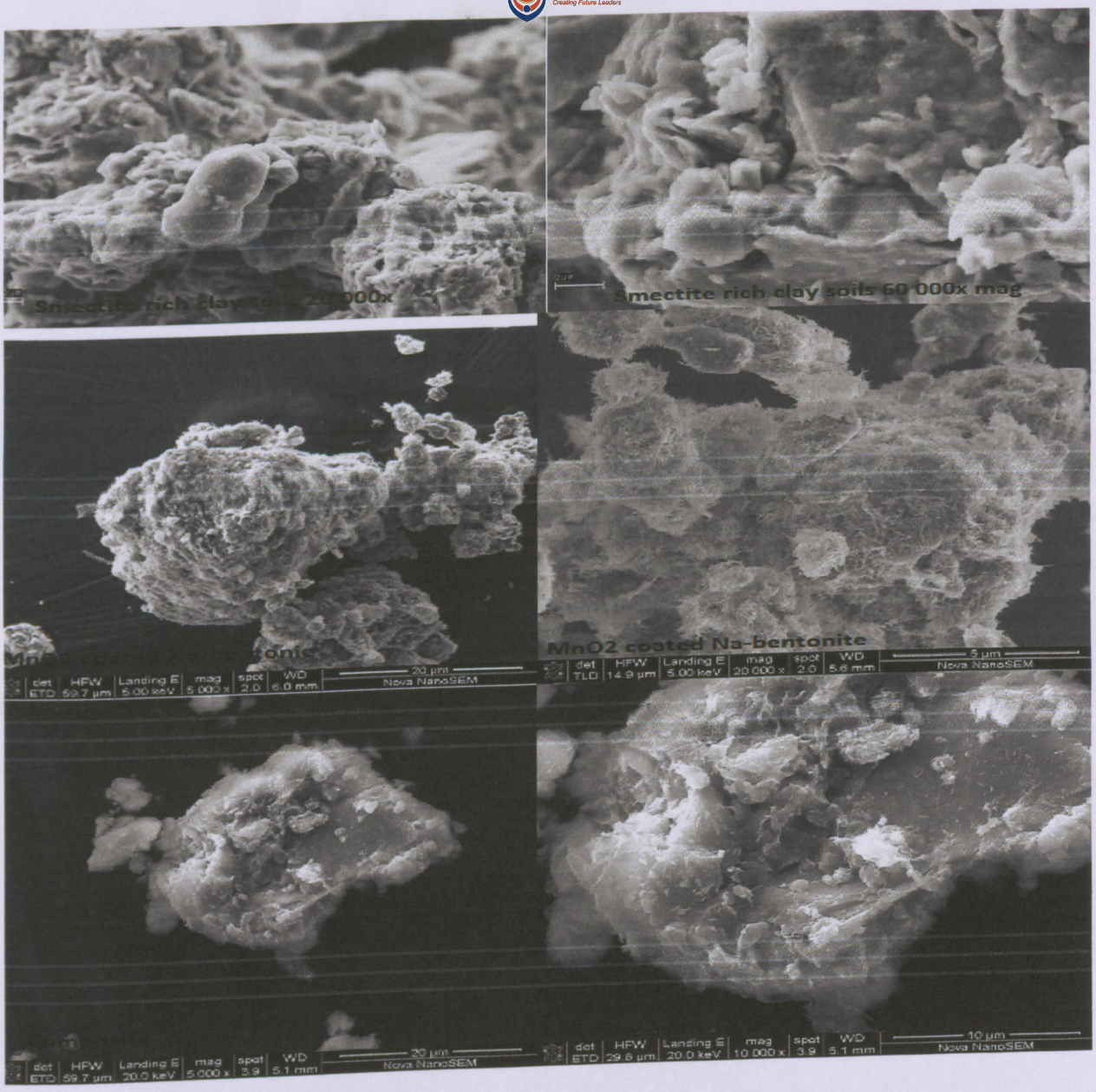

Figure 6.5: Surface morphology of smectite rich clay soils, MnO_2 coated Na-bentonite and clay composite.

6.4 Conclusions

In this study, pellets were successfully fabricated from smectite rich clay soils/MnO_2 coated Na-bentonite clay composite. The optimum mass ratio of MnO_2 coated Na-bentonite clay/smectite rich clay soils for fabricating the composite was found to be 1:3. The optimum temperature for calcination of pellets was found to be 550 °C. The pellets prepared were able to remove ≈63.3% F^- from an initial adsorbate concentration of 10 mg/L. Mineralogical characterisation showed the

© University of Venda

University of Venda
Creating Future Leaders

presence of quartz, albite, cryptomelane and microcline as the main minerals of the calcined pellets. XRF analysis showed that SiO_2, Al_2O_3, MnO and Fe_2O_3 are the major oxides of the clay composite. SEM analysis showed that the composite has platy-like morphology. This study recommends further studies to evaluate the field applicability of MnO_2 coated Na-bentonite clay/smectite rich clay soils composite in defluoridation of groundwater.

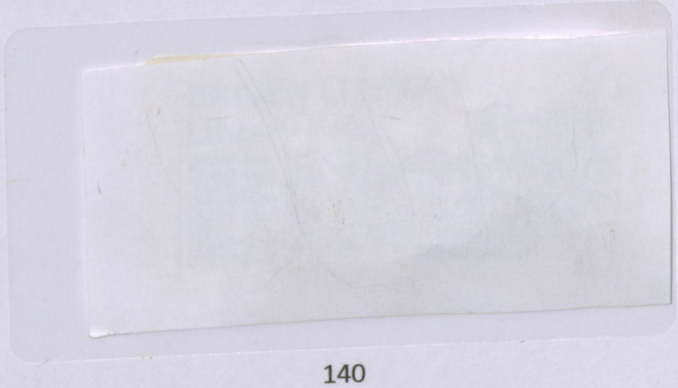

© University of Venda

University of Venda
Creating Future Leaders

References

Department of Water Affairs and Forestry (DWAF). 1996. South African Water Quality Guidelines for Domestic Use, 1st ed., Department of Water Affairs and Forestry, Pretoria. Available at: www.dwaf.gov.za.

Hauge, S., O¨sterberg, R., Bjorvatn, K., Selvig, K. A., 1994. Defluoridation of drinking water with pottery: effect of firing temperature. *Scandinavian journal of dental research,* 102, pp.329–333.

Piddennavar, R. & Krishnappa, P., 2013. Review on defluoridation techniques of water. *The International Journal of Engineering and Science,* 2(3), pp.86-94.

Oladoja, N. A., Liu, Y., Drewes, J. E & Helmreich, B., 2015. Preparation and Characterization of a Reactive Filter for Groundwater Defluoridation. *Chemical Engineering Journal. In press.*

Jia Y., Zhu B. S., Zhang K. S., Jin Z., Luo T., Yu X. Y., Kong., L. T., & Liu J. H., 2015. Porous 2-line ferrihydrite/byerite composite (LFBC): Fluoride removal performance and mechanism. *Chemical Engineering Journal,* 268, pp. 325-336.

Chen, N., Zhang, Z., Feng, C., Li, M., Zhu, D., Chen, R. & Sugiura, N., 2010. An excellent fluoride sorption behavior of ceramic adsorbent. *Journal of Hazardous Materials,* 183, pp.460–465

© University of Venda

University of Venda
Creating Future Leaders

Chapter 7: Conclusions and recommendations

7.1 Conclusions

This study was designed in an attempt to answer the following questions governed by the objectives regarding the synthesis, characterization and performance evaluation of groundwater defluoridation capacity of smectite rich clays soils and Mn-modified bentonite clay composites.

- How to activate bentonite clay with NaOH?
- How to modify activated bentonite clay with MnO_2?
- What are the conditions for fabricating MnO_2 coated Na-bentonite/smectite rich clay soil composite?
- What are the physicochemical properties of smectite rich clay soils and Mn modified bentonite clay?
- What is the F^- removal efficiency of smectite rich clay soils, Mn^{2+} bentonite, MnO_2-modified bentonite clay and its composite from groundwater?
- How to regenerate the adsorbents using alkaline solutions?

The following discussion will attempt to evaluate and elucidate more on the success and drawbacks of the study with regard to each of the above questions and will also give recommendations on the use of the synthesised adsorbent and the future work focus.

7.1.1 Activating raw bentonite using NaOH and Coating Na-bentonite using MnO_2 fabricating MnO_2 Na-bentonite/smectite rich clay soils composite

Optimum conditions for activating bentonite clay with NaOH were evaluated using batch experiments and the established optimum conditions were 15 min contact time and 0.1 M NaOH concentration.

Optimum conditions for coating Na-bentonite using MnO_2 coated bentonite were evaluated using *in-situ* reduction of $KMnO_4$. The following optimum conditions were established: 60 min contact time, 1.5 M $KMnO_4$ and 2.5 g Na-bentonite dose.

The optimum mass ratio of MnO_2 coated Na-bentonite clay/smectite rich clay soils for fabricating the composite was found to be 1:3. The optimum temperature for calcination of pellets was found to be 550 °C.

© University of Venda

7.1.2 Physicochemical and mineralogical characterization of smectite rich clay soils, bentonite and Mn modified bentonite

Elemental composition of the clay soils were evaluated using XRF, mineralogical composition was evaluated using XRD, surface morphology using SEM, surface area using BET, functional groups using FTIR, CEC using ammonium acetate method and pHpzc using titration method. The following conclusions were drawn on the physicochemical and mineralogical properties of the clay soils.

- Smectite rich clay soils mainly consist of SiO_2 Al_2O_3 as major elements; minor components include CaO, Na_2O, MgO and traces of K_2O TiO_2 and MnO. Mineralogical analysis revealed that the clay soils consist of montmorillonite, quartz, albite and anthophyllite. The Quantitative results further confirms the presence of smectite (60.34%) as the major mineral and the presence of quartz (20.21%) and plagioclase (20.39%) as minor minerals. Morphological analysis of smectite rich clay soils showed irregular porous structure at lower magnifications and images at higher magnifications reveals that smectite rich clay soil has smooth surface and platy-like features of the clay. BET showed that smectite rich clay contains significant amount of small pores ranging from microporous to mesoporous with the total surface area of 20.34 m^2/g and average pore diameter of 7.04 nm. FTIR confirmed the presents of Si–OH, Al-OH and Si-O-Al bonds in the smectite rich clay soils. The CEC for smectite rich clay soils was found to be 74.23 (meq/100 g) at pH 5.4 and it increased to 79.93 (meq/100 g) at pH 7.4. pH_{pzc} of the smectite rich clay soils evaluated in this study was found to be 5.8.

- Physicochemical and mineralogical composition of raw bentonite were evaluated and it was found that the clay contains silica (SiO_2) is the main component of bentonite clay while Al_2O_3 is the main minor component. High concentration of SiO_2 and Al_2O_3 indicates that bentonite clay is an alumino-silicate material. Mineralogical analysis confirms the presence of montmorillonite and quartz as the major minerals and muscovite as one of the trace minerals of bentonite clay. The morphological analysis revealed that raw bentonite has granular and spongy like material. FTIR showed the presence of Si-OH and Al-OH as well as Al-O-Si bonds in the bentonite clay. N_2 adsorption-desorption isotherms exhibited type IV isotherm with hysteresis loop indicating the mesoporous nature of the bentonite. Total surface area and pore size were found to be 43.48 m^2/g and

© University of Venda

University of Venda
Creating Future Leaders

7.99 nm respectively. CEC of raw bentonite clay was found to be 288.32 and 293.92 meq/100 g at pH 5.4 and 7.4 respectively. pH_{pzc} was found to be 8.4. After the intercalation of Mn^{2+} ions onto bentonite clay no significant change in mineralogy observed. Modification increased MnO content from 0.09% in raw bentonite to 0.29% in Mn^{2+} modified bentonite clay and further decreased content of Na_2O, CaO and MgO as well as K_2O. Modification with Mn^{2+} increased the surface area of bentonite clay from 43.48 to 66.41 m^2/g and decreased the pore size from 7.99 to 5.55 nm. pH_{pzc} increased from 8.4 to 8.8 after modification with Mn^{2+} ions. The CEC decreased from 288.32 and 293.92 meq/100 g at pH 5.4 and pH7.5 to 110.74 and 114.66 meq/100 g respectively after modification. Modification of bentonite clay with Mn^{2+} ion lead to the formation of new bonds such as Mn-O, Mn-OH and Mn-H_2O in the bentonite clay surface, this was confirmed using FTIR. Surface morphology analysis revealed the formation of larger agglomerate and specs on the surface on the surface of clay platelets.

- Activating bentonite clay with NaOH did not have any significant change in the mineralogy of bentonite clay. XRF confirmed increase Na_2O oxides from 2.12 to 4.22% after activation. The morphology of Na-bentonite was found to be largely granular with irregular structures. pH_{pzc} was found to be 8.4. Surface area was found to be 29.03 m^2/g and the pore distribution was found to be monomodal meaning pore are almost of the same size with the average of 12.83 nm. Coating Na-bentonite with MnO_2 lead to the formation of new minerals such as cryptomelane (KMn_8O_{16}) jacobsite $(Mn_6Fe_4)O_4$ and pyrolusite (MnO_2) which are both the oxides of manganese. Coating increased the percentage composition of Mn in the Na-bentonite and this diluted the percentage of other oxides such as SiO_2, Al_2O_3, MgO and Fe_2O_3. pH_{pzc} of the MnO_2 coated bentonite was found to be 3. Surface morphology of the MnO_2 coated Na-bentonite appeared largely fibrous coatings on the granules which indicate precipitates of manganese oxides on the surface of the clay. Surface area increased to 52.51 m^2/g and the pore size decreased to 5.91 nm. N_2 adsorption-desorption curves displayed type IV isotherm which means pores of MnO_2 coated Na-bentonite ranges from micro to mesoporous.

- Mineralogical characterisation of the clay composite showed the presence of quartz, albite, cryptomelane and microcline as the main minerals of the calcined pellets. XRF

© University of Venda

analysis showed that SiO_2, Al_2O_3, MnO and Fe_2O_3 are the major oxides of the clay composite. SEM analysis showed that the composite has platy-like morphology.

7.1.3 Adsorption efficiency, regeneration, isotherms, kinetics and the adsorption mechanisms

Smectite rich clay soils

- Optimum conditions were evaluated and found to be 30 min contact time at 250 rpm shaking speed on a table shaker, adsorbent dosage of 0.8 g/100 mL, 3 mg/L adsorbate concentration and pH of 2. Fluoride removal at optimum conditions was ≈91.89% for 3 mg/L initial concentration. Regeneration study revealed that smectite rich clay soils can be successfully regenerated using 0.1 M NaOH. Adsorption isotherms showed that the data fits well to Langmuir isotherm than to Freundlich isotherm suggesting that adsorption of fluoride occurred on a monolayer surface. Adsorption kinetic study showed that the data fits well to pseudo second order than to pseudo second order suggesting that the adsorption occurs via chemisorption. The data did not fit well to intra-particle diffusion model of Weber-Morris and showed bilinear plot which showed that the adsorption of fluoride onto smectite rich clay soils is a complex process. Ligands exchange and ion exchange mechanism of F^- adsorption was suggested to be the main mechanism taking place during the adsorption process

Mn^{2+} modified bentonite clay

- Optimum conditions for adsorption of F^- were established to be 30 min contact time, 1.0 g/100 mL adsorbent dosage, 3 mg/L adsorbate concentration and pH of 2. A maximum F-removal of 84.0% was achieved at the optimized batch conditions. Co-existing ions decreased the percentage fluoride removal. Regeneration study revealed that Mn^{2+} bentonite can be successfully regenerated with 0.1 M NaOH. Leaching assessment showed that there is minimal release of chemical species from the adsorbent at various pH levels. The adsorption isotherm data fitted well to Langmuir model suggestion a monolayer adsorption. Kinetic modelling suggested chemisorption as the main mechanism of F^- adsorption. Adsorption of F^- was observed to be a complex process involving external and internal particle diffusion. Fluoride adsorption onto Mn^{2+} bentonite occurred via ligand exchange at lower pH and ion exchange at higher pH.

© University of Venda

MnO_2 coated Na-bentonite clay

- Maximum percentage F^- removal above 91.0% was achieved at all evaluated pH levels (2-12), 5 mg/L F^- initial concentration, optimum dosage of 1.5 mg/L and contact time of 30 min and shaking speed of 250 rpm. Regeneration study showed that MnO_2 coated Na-bentonite can be successfully regenerated with 0.1 M NaOH. Chemical stability test revealed that Mn ions were leached at concentrations above the South African drinking standards Mn in drinking water. Data fitted well to Langmuir isotherm model indicating that adsorption occurred on a mono layered surface. Adsorption kinetics data fitted well to pseudo second order reaction kinetics indicating that the adsorption occurred through chemisorption. The data did not fit to Weber-Morris intra-particle diffusion model it gave multilinear plot showing intra-particle diffusion is not the only rate limiting step. Ligands exchange was established to be F^- uptake mechanism at pH below 3 and at ion exchange was established to be the mechanism of F^- uptake at pH above 3.

MnO_2 coated Na-bentonite/smectite rich clay composite pellets

- The pellets prepared were able to remove ≈63.3% F^- from an initial adsorbate concentration of 10 mg/L at initial pH of 6.03±0.5, adsorbate dosage of 2.0 g and contact time of 30 min.

© University of Venda

7.2 Recommendations

Based on the finding of the study smectite rich clay soils, Mn^{2+} bentonite, MnO_2 coated Na-bentonite and MnO_2 coated Na-bentonite/smectite rich clay can be used for defluoridation of groundwater in rural areas of South Africa and the following aspects were recommended to be evaluated further:

- Evaluation of chemical modification of black smectite rich clay soils to improve its fluoride binding capacity
- Black smectite rich clay soils and Mn^{2+} bentonite showed higher adsorption capacity at acidic pH, therefore it is recommended that future work should work on improving their adsorption capacity at wider range of pH.
- MnO_2 coated Na-bentonite showed higher adsorption capacity at wider range of pH however the stability test showed that the material is not stable since it released secondary contaminants into the treated water, therefore it is recommended that future work should focus on improving the stability of the material
- The study also recommend that future study should evaluate the use of MnO_2 coated Na-bentonite/smectite rich clay soils composite pellets for fluoride removal in a dynamic flow set-up.

© University of Venda